reprinted from
Pressure Vessels and Piping: Design Technology – 1982
A Decade of Progress
Edited by S.Y. Zamrik, and D. Dietrich
(Book No. G00213)

published by
THE AMERICAN SOCIETY OF MECHANICAL ENGINEERS
345 East 47th Street, New York, N.Y. 10017
Printed in U.S.A.

BOSORS

2.4 PLASTIC BUCKLING

DAVID BUSHNELL
Lockheed Palo Alto Research Laboratory
Palo Alto, California

Lockheed
David Bushnell
Consulting Scientist, Computational Mechanics
Mechanics & Materials Engineering Laboratory
O/93-30 B251
3251 Hanover Street, Palo Alto, CA 94304-1191
(415) 424-3237

ABSTRACT

The phenomenon of plastic buckling is first illustrated by the behavior of a fairly thick cylindrical shell, which under axial compression deforms at first axisymmetrically and later nonaxisymmetrically. Thus, plastic buckling encompasses two modes of behavior, nonlinear collapse at the maximum point in in a load vs deflection curve and bifurcation buckling. Accurate prediction of critical loads corresponding to either mode in the plastic range requires a simultaneous accounting for moderately large deflections and nonlinear, irreversible, path-dependent material behavior. A survey is given of plastic buckling which spans three areas: asymptotic analysis of post-bifurcation behavior of perfect and imperfect simple structures, general nonlinear analysis of arbitrary structures, and nonlinear analysis for limit load collapse and bifurcation buckling of shells and bodies of revolution. A discussion is included of certain conceptual difficulties encountered in plastic buckling models, in particular those having to do with material loading rate at bifurcation and the apparent paradox that use of deformation theory often leads to better agreement with tests on structures with very simple prebuckling equilibrium states than does use of the more rigorous incremental flow theory. In the survey of general nonlinear structural analysis emphasis is given to formulation of the basic equations, various elastic-plastic material models, and strategies for solving the nonlinear equations incrementally. In the section on buckling of axisymmetric structures, numerous examples including comparisons of test and theory reveal that critical loads are not particularly sensitive to initial imperfections when the material is stressed beyond the proportional limit. A final summary includes suggestions for future work.

INTRODUCTION

WHAT IS PLASTIC BUCKLING?

To most engineers the word "buckling" evokes an image of failure of a structure which has been compressed in some way. Pictures and perhaps sounds come to mind of sudden, castastrophic collapse involving very large deformations. From a scientific and engineering point of view, the interesting phases of buckling phenomena generally occur before the deformations are very large, when to the unaided eye, the structure appears to be undeformed or only slightly deformed.

In static analysis of perfect structures, there are two phenomena loosely termed "buckling": collapse at the maximum point in a load vs deflection curve and bifurcation buckling. These are illustrated in Figs. 1 and 2. The axially compressed cylinder shown in Fig. 1 deforms approximately axisymmetrically along the path OA until a maximum or limit load λ_L is reached at point A. If the axial load λ is not sufficiently relieved by the reduction in axial stiffness, the perfect cylinder will fail at this limit load, following either the path ABC along which it continues to deform axisymmetrically, or some other path ABD along which it first deforms axisymmetrically from A to B and then nonaxisymmetrically from B to D. Limit point buckling, or "snap-through", occurs at point A and bifurcation buckling at point B. The equilibrium path OABC corresponding to the axisymmetrical mode of deformation is called the fundamental path and the post-bifurcation equilibrium path BD, corresponding to the nonaxisymmetrical mode of deformation, is called the secondary path. The significance of the word "plastic" in the title is that buckling of either type occurs at loads for which some or all of the structural material has

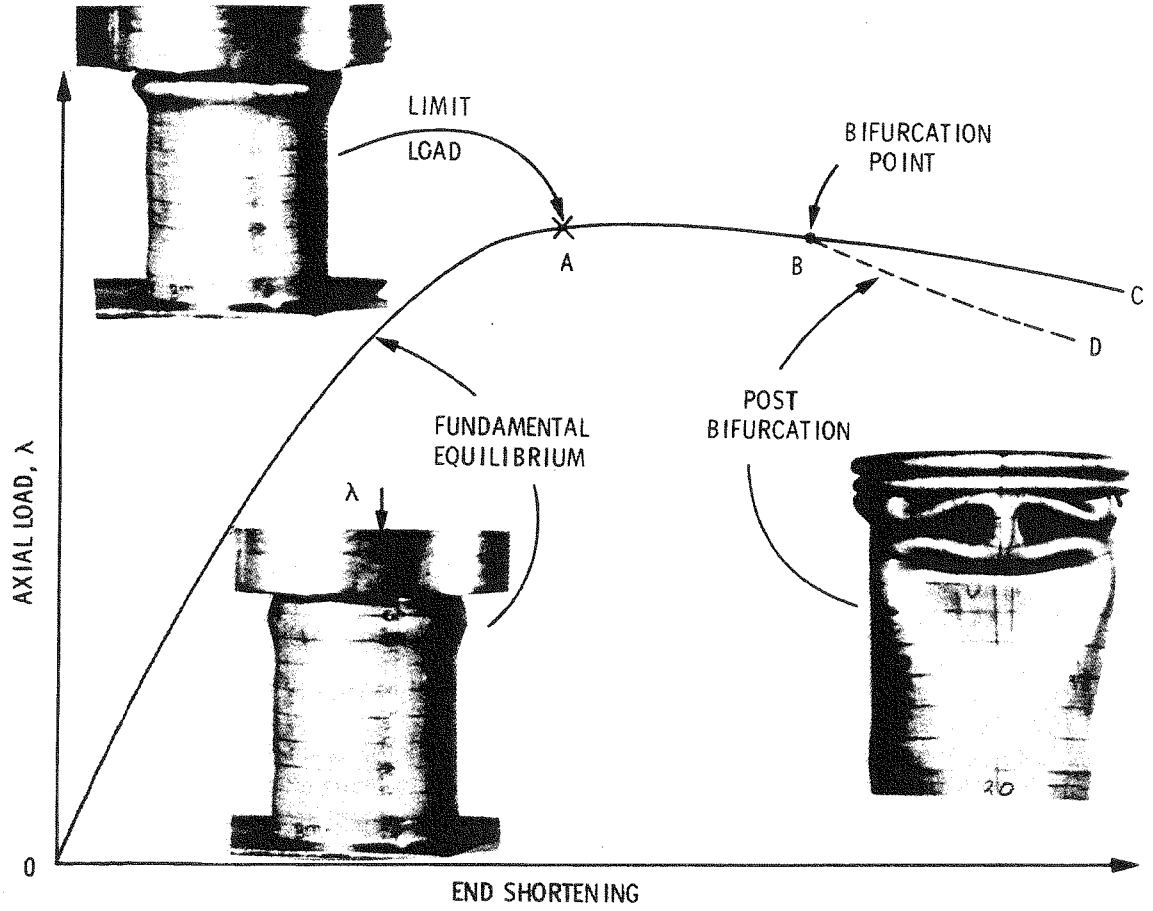

FIG. 1 LOAD-END SHORTENING CURVE WITH LIMIT POINT A, BIFURCATION POINT B, AND POST-BIFURCATION EQUILIBRIUM PATH, BD. (PHOTOGRAPHS COURTESY SOBEL AND NEWMAN [237]).

been stressed beyond its proportional limit. The example in Fig. 1 is somewhat unusual in that the bifurcation point B is shown (correctly) to occur after the collapse point has been reached. In this particular case, therefore, bifurcation buckling is of less engineering significance than axisymmetric collapse.

A more commonly occurring situation is illustrated in Fig. 2(a). The bifurcation point B is between O and A. If the fundamental path OAC corresponds to axisymmetrical deformation and BD to nonaxisymmetrical deformation, then initial failure of the structure would generally be characterized by rapidly growing nonaxisymmetrical deformations. In this case the collapse load of the perfect structure λ_L is of less engineering significance than the bifurcation point, λ_C.

In the case of real structures which contain unavoidable imperfections, there is no such thing as bifurcation buckling. The actual structure will follow a fundamental path OEF, with the failure corresponding to "snap-through" at point E at the collapse load λ_s. However, the bifurcation buckling analytical model is valid in that it is convenient and often leads to a good approximation of the actual failure load and mode. For more general background on buckling of perfect and imperfect structures, see Ref. [1].

CAPSULE OF PROGRESS IN THE 1970'S IN PLASTIC BUCKLING ANALYSIS

Recent progress in our capability to predict plastic buckling failure can be categorized into four main areas, three of them dealing primarily with structural modeling, and the fourth dealing primarily with material characterization.

The three areas dealing with structural modeling are:

1. Development of asymptotic postbuckling theories and applications of these theories to specific classes of structures, such as simple plates, shells and panels (Refs. [2-18]).

2. Development of general-purpose computer programs for calculation of static and dynamic behavior of structures includ-

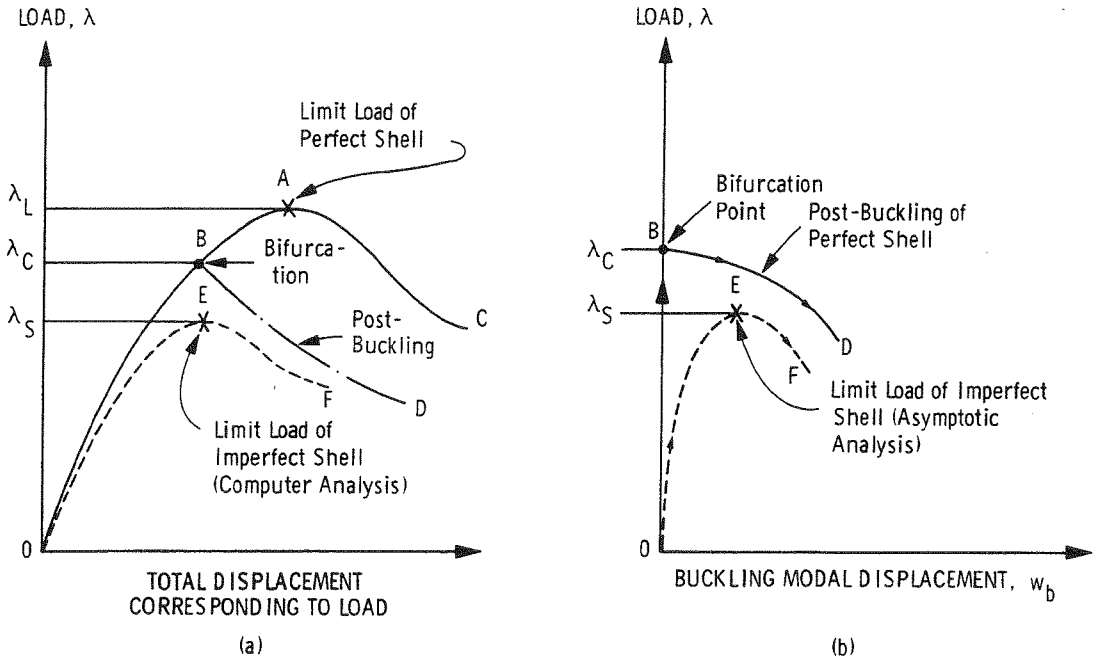

FIG. 2 LOAD-DEFLECTION CURVES SHOWING LIMIT AND BIFURCATION POINTS. (A) GENERAL NONLINEAR ANALYSIS. (B) ASYMPTOTIC ANALYSIS.

ing large deflections, large strains, and nonlinear material effects (Refs. [19-21]).

3. Development of special purpose computer programs for limit point axisymmetrical buckling and non-axisymmetrical bifurcation buckling of axisymmetric structures (Refs. [22-23]).

Asymptotic Analysis

The elastic-plastic bifurcation and asymptotic post-buckling analyses [2-18] rest on the theoretical foundations established by Hill [24-27], whose formulation of the bifurcation problem applies to solids with smooth or piecewise smooth yield surfaces and small or large strains, and Koiter [28-29], whose general elastic post-bifurcation theory leads to an expansion for the load parameter λ in terms of the buckling modal amplitude w_b which is valid in the neighborhood of the critical bifurcation point in (λ, w_b) space. Hill proved that in order for bifurcation of equilibrium paths to occur at stresses beyond the proportional limit, the initial post-buckling path must in general have a positive slope; plastic bifurcation buckling occurs under increasing load. Therefore, it is crucial to determine the post-bifurcation path until it reaches a limt load. The primary aims of the asymptotic analyses of Refs. [2-18] are to calculate limit loads for perfect and imperfect structures. These analyses have contributed vital physical insights into the plastic buckling process and the effect of structural or loading imperfections on this process.

General Nonlinear Analysis

The general-purpose computer programs in widespread use since the early 1970's and presently being written are based on principles of continuum mechanics established for the most part by the late 1950's and set forth in several texts [30-35]. The structural continuum is discretized into finite elements as described in the texts [36-40] and various strategies are employed to solve the resulting nonlinear problem [41-71]. The nonlinearity is due to moderately large or very large deflections and nonlinear material behavior. Various plasticity models are described in texts [72-76], conference proceedings [77-78], and survey articles [79-82]. Additional papers on the formulation, discretization, and solution of nonlinear structural problems appear in the symposia proceedings [83-87]. The primary aim of this vast body of work, most of which was done in the 1970's, has been to produce reliable analysis methods and computer programs for use by engineers and designers. Thus, the emphasis in the literature just cited is not on acquiring new physical insight into buckling and post-bifurcation phenomena, but on creating tools that can determine the equilibrium path OEF in Fig. 2 for an arbitrary structure and on proving that these tools work by use of demonstration problems, the solution of which is known. In most cases no formal distinction is made between prebifurcation and post-bifurcation regimes; in fact, simple structures are modeled with imperfections so that potential bifurcation

points are converted into limit points. The plastic buckling problem loses its special qualities as illuminated so skillfully in Refs. [2-18] and becomes just another nonlinear analysis, requiring perhaps special physical insight on the part of the computer program user because of potential numerical traps such as bifurcation points and limit points usually (and sometimes spuriously!) revealed by changes in the sign of the determinant of a stiffness matrix.

Figures 2(a) and (b) illustrate the two very different approaches to the plastic buckling problem described in the last two paragraphs. In the general nonlinear approach the computations involve essentially a "prebuckling" analysis, or a determination of the unique equilibrium states along the fundamental path OEF in Fig. 2(a). In the asymptotic approach (Fig. 2b) the prebuckling state is usually statically determinate. The secondary path BD of the perfect structure and (in the elastic case) the limit point E on the fundamental path of the imperfect structure are determined by expansion of the solution in a power series of the bifurcation modal amplitude which is asymptotically exact at the bifurcation point B.

Axisymmetric Structures

The third approach to the plastic buckling problem, development of special-purpose programs for the analysis of axisymmetric structures, forms a sort of middle ground between the asymptotic analysis and the general-purpose nonlinear analysis. The approach is similar to the asymptotic treatment because in applications it is restricted to a special class of structures and the distinction between prebuckling equilibrium and bifurcation buckling is retained. It is similar to the general nonlinear approach in that the continuum is discretized and the nonlinear prebuckling equilibrium problem is solved "by brute force." The emphasis is on the calculation of the prebuckling fundamental path, OB in Fig. 2(a), and determination of the bifurcation point B and its associated buckling mode, not on calculation of post-bifurcation behavior BD or of the load-deflection path of the imperfect structure. The goals of this third approach are to create an analysis tool for use by engineers and designers and to use this tool in extensive comparisons with tests both to varify it and to obtain physical insight into the plastic buckling process.

SUMMARY OF THIS SURVEY ON PLASTIC BUCKLING

Certain difficulties associated with plastic bifurcation buckling theory are discussed in the next section. Following this, the asymptotic methods of Hutchinson, Tvergaard, and Needleman [2-18] are described and examples shown. The general nonlinear approach is then summarized with emphasis on the Total Lagrangian vs Updated Lagrangian formulations, strategies for solving nonlinear equations, and characterization of elastic-plastic material behavior. Next, a strategy for axisymmetric nonlinear snap-through and nonaxisymmetric bifurcation buckling of elastic-plastic axisymmetric shells is described, followed by numerous examples in which experimental and theoretical results are compared. The chapter closes with some recommendations for future work.

WHERE PLASTIC BUCKLING FITS INTO THE BIG PICTURE

Since most plastic buckling analyses are probably performed with use of general-purpose computer programs, and since

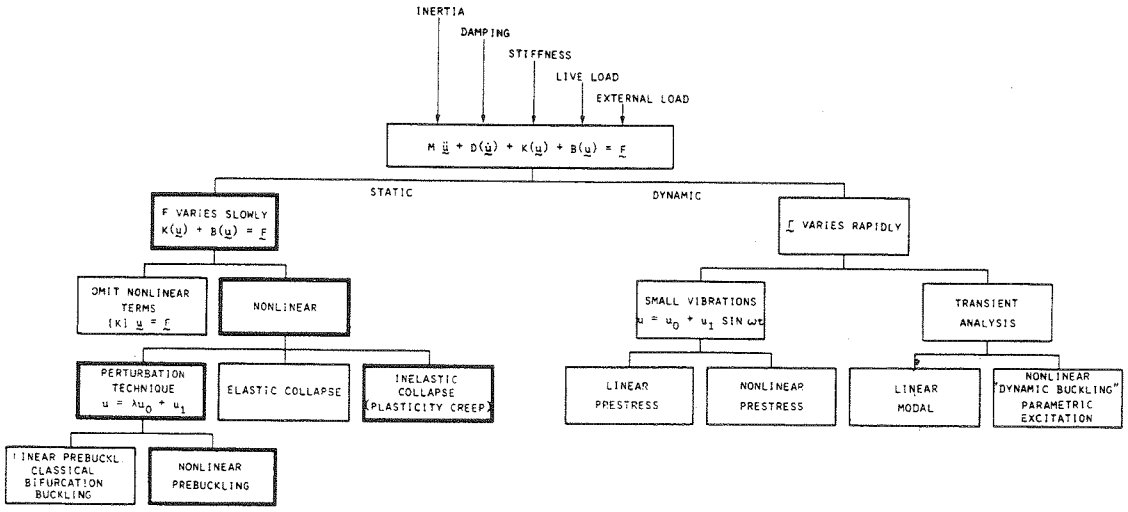

FIG. 3 GENERAL NONLINEAR STATIC AND DYNAMIC ANALYSIS AND WHERE PLASTIC BUCKLING FITS INTO THE BIG PICTURE. BOXES WITH HEAVY OUTLINES ARE DISCUSSED HERE

these programs solve a very broad class of problems, it helps to focus the discussion by showing graphically where the discipline called "plastic buckling" fits into the general field of structural analysis. The chart shown in Fig. 3 starts with a general equation for the dynamic response, u, of a structure to time-dependent loading, F. The operators D, K, and B may be nonlinear. In this chapter we are concerned with the physics and methods enclosed in the emphasized boxes. There has been much work done on dynamic, large-deflection elastic-plastic failure of structures neglecting and including the effects of interaction with a surrounding fluid medium. This significant research will not be surveyed here. In particular, the box labeled "Dynamic Buckling," although an important part of the general discipline of plastic buckling, will not be covered because of lack of space.

CONCEPTUAL DIFFICULTIES IN BIFURCATION BUCKLING IN THE PLASTIC RANGE

SUMMARY

Before the 1970's bifurcation buckling analyses involving plasticity were applied to simple structures with uniform prestress. Sewell [4] gives an extensive survey and a bibliography with more than 600 papers. Basic conceptual difficulties were cleared up and paradoxes resolved. It is now understood that the nonconservative nature of plastic flow does not prevent the use of bifurcation buckling analysis to predict instability failure of practical structures; the concept of consistent loading of the material in the transition from the prebifurcation state to an adjacent post-bifurcation state permits the use of instantaneous prebifurcation material properties in the stability equations; and an investigation of the effect of very small initial imperfections on the collapse loads of cruciform columns indicates that the reduced shear modulus $\overline{G}$ obtained from deformation theory should be used in the stability equations even if there is no history of shear along the prebifurcation path.

With the high speed electronic computer, it is now feasible to calculate the elastic-plastic bifurcation buckling loads of rather complex structures, including large prebuckling deflections and elastic-plastic effects.

THE PROBLEM OF NONCONSERVATIVENESS

Systems involving plastic flow are nonconservative. The energy required to bring a structure from its prebifurcation state to an adjacent buckled state depends upon the path of transition if any of the material is loading into the plastic region. Hill [25, 26] has shown, however, that as long as the infinitesimal path is reasonably direct, the variation in infinitesimal energy dissipation from one path to another consists of higher order terms only.

THE PROBLEM OF LOADING RATE DURING BUCKLING

Analysis of the bifurcation buckling of elastic-plastic structures dates back to 1889 when Engesser [88] presented his tangent modulus theory for columns and Considére [89] set forth the "effective" or "double" modulus theory based on the assumption that the column unloads elastically on the concave side during incipient buckling at a given load. In 1895 Engesser, who had assumed that the total load on the column remains constant during buckling, acknowledged error in his original theory and determined the general expression for the reduced modulus. In 1910, von Kármán [90] presented the Considère Engesser theory again, with actual evaluation of the reduced modulus for rectangular and idealized H-sections and comparisons with tests. Until Shanley's paper appeared in 1947 [91] the reduced modulus or "double modulus" model was accepted as the exact theory of column action, even though the tangent modulus model gave better agreement with tests. Shanley [91] resolved the paradox in 1947, when he stated:

> "... in the derivation of the reduced-modulus theory a questionable assumption was made. It was assumed, by implication at least, that the column remains straight while the axial load is increased to the predicted critical value, after which the column bends or tries to bend. Actually, the column is free to 'try to bend' at any time. There is nothing to prevent it from bending simultaneously with increasing axial load. Under such a condition it is possible to obtain a nonuniform strain distribution without any strain reversal taking place."

In a discussion appended to Shanley's paper, von Kármán further clarified the theory stating,

> "Both Engesser's and my own analyses of the problem were based on the assumption that the equilibrium of the straight column becomes unstable when there are equilibrium positions infinitesimally near to the straight equilibrium position under the same axial load. .
>
> ... Mr. Shanley's analysis represents a generalization of the question ... What is the smallest value of the axial load at which a bifurcation of the equilibrium positions can occur, regardless of whether or not the transition to the bent position requires an increase of the axial load?"

In 1950 Duberg and Wilder [92] provided further insight into the problem by showing that for small, finite imperfections bending will take place immediately as the load is applied but that local unloading of the material will not occur until the column has been subjected to a relatively large bending moment. For vanishingly small initial imperfections, finite bending of the column will start at the bifurcation load predicted by the tangent modulus theory. Elastic unloading will not occur, however, until a higher load at which the column has deformed a finite amount along the post-bifurcation load-deflection curve. Duberg and Wilder show that for practical engineering materials, the maximum load carrying capability of the column is only slightly above the tangent modulus bifurcation point.

It is physically reasonable to extend the concept of "tangent modulus bifurcation" to buckling of two-dimensional

plate and shell structures. Experiments and analyses have been conducted for simple plates and shells in which the prebuckling state is characterized by uniform compressive stress (See, e.g., [93-102]). The analyses just cited are based on the tangent modulus method. Sewell [4] gives a more extensive bibliography.

In 1972 Hutchinson [7] calculated axisymmetric collapse pressures of an elastic-plastic spherical shell with various axisymmetric imperfections. As the imperfection amplitude approaches zero the collapse load approaches a value very slightly above the tangent modulus bifurcation load calculated from J_2 flow theory for a perfect shell. In justifying the use of the tangent modulus approach to bifurcation problems in general, Hutchinson [3] in 1974 wrote:

> "The bifurcation solution is a linear sum of the fundamental solution increment and the eigenmode. We can always include a sufficiently large amount of the fundamental solution increment relative to the eigenmode such that the bifurcation mode satisfies the total loading restriction.
>
> . . . The confusion in bifurcation applications apparently stems from the misconception that when bifurcation occurs total loading will be violated. On the contrary, it is the total loading condition itself which supplies the constraint on the combination of fundamental solution increment and eigenmode which must pertain."

The "total loading" condition cited above justifies the use of the "tangent modulus" approach to bifurcation buckling problems of elastic-plastic shells. The fact that the collapse load is only slightly above the bifurcation load for vanishingly small imperfections makes an elastic-plastic bifurcation stability analysis in principle just as suitable for design purposes as an elastic bifurcation stability analysis. For bifurcation buckling of general shells under combined loading, in which the stresses are nonuniform and in which the prebuckling solution may be characterized by regions which are elastic or unloading and other regions which are loading into the plastic range, the "total loading" condition enunciated by Hutchinson may be generalized by the statement that the rate of change of material properties or "tangent properties" in the prebifurcation analysis govern the eigenvalue analysis also.

The following heuristic argument should further clarify the "total" loading or "consistent" loading concept. Let us hypothesize that the eigenvalue obtained from the consistent loading model is physically meaningless because a *finite* amount of material which has been loading into the plastic region suddenly unloads in the *infinitesimal* transition from the unbuckled state q to the buckled configuration $q + \delta q$. The effect would be to produce a stiffer structure and hence, in the presence of a given prebuckling state, a higher eigenvalue than would result from the consistent loading model. Suppose also that an eigenvalue and corresponding kinematically admissible mode have been determined from the consistent loading model. Now assume that a new nonlinear equilibrium analysis is performed for the shell with an infinitesimal imperfection of the same shape as this buckling mode. Since the imperfection is infinitesimal, the load-deflection behavior will differ from that of the perfect shell only infinitesimally for loads smaller than the lowest eigenvalue obtained from the consistent loading model. If, as hypothesized, this eigenvalue were physically meaningless and the true bifurcation point lies a finite load increment above it, then the material of the infinitesimally imperfect shell would continue to load consistently right through the neighborhood of the bifurcation load calculated by means of the consistent loading model. A contradiction therefore exists: It has just been hypothesized that the eigenvalue from the consistent loading model is physically meaningless because *infinitesimal* perturbations of the form of the buckling mode cause a *finite* amount of the material to unload suddenly. However, the material of an actual shell containing such a perturbation in geometry loads consistently at the eigenvalue calculated from the consistent loading model. Therefore, this eigenvalue must be physically meaningful and must correspond to a bifurcation point on the load-deflection curve of the perfect shell.

THE FLOW THEORY VS DEFORMATION THEORY PARADOX

During the years when plastic buckling of uniformly stressed plates and shells was first being investigated, a perplexing paradox became apparent: Theoretical considerations and direct experimental evidence indicates that for general load paths flow theory is correct while deformation theory is not. However, bifurcation buckling analyses based on deformation theory conform better to experimentally determined buckling loads than do such analyses based on flow theory. The discrepancy may have to do with whether or not the instantaneous yield surface has corners. Experimental evidence on this point is contradictory. About half of the experiments indicate that corners develop on yield surfaces and half do not. Experiments by Smith and Almroth [103] indicate that the yield surface may develop a region of very high curvature which "smooths" out with time. Recent surveys of yield surface experimentation are given by Michno and Findley [104] and Hecker [105].

The discrepancy in the prediction of bifurcation buckling loads is most pronounced in the case of an axially compressed cruciform column, discussed by Stowell [94], Drucker [106], Cicala [107], Bijlaard [108], Gerard and Becker [102], and Onat and Drucker [97]. If the column is not too long, it buckles in a torsional mode. The prebifurcation stress state is uniform compression while the bifurcation mode involves pure shear. In a flow theory involving a smooth yield surface the shear modulus remains elastic as the material of the column is uniformly compressed into the plastic range. Use of deformation theory gives the instantaneous shear modulus

$$\bar{G} = \frac{G}{1 + 3G\left(\frac{1}{E_s} - \frac{1}{E}\right)} \qquad (1)$$

where E_s is the secant modulus. Since the predicted torsional buckling stress is proportional to the effective shear modulus, the discrepancy in predicted bifurcation loads is governed by the difference between G and $\bar{G}$. Figure 4, taken from Gerard and Becker [102], shows that tests definitely indicate that $\bar{G}$ rather than G should be used in the bifurcation buckling analysis. Onat and Drucker [97] and Hutchinson and Budiansky [17] resolved the paradox by showing that cruciform columns with very small initial twist distributions and modeled with use of J_2 flow theory are predicted to collapse at loads only slightly above the bifurcation loads predicted with deformation theory. Apparently a very small amount of shearing strain in the prebifurcation solution suffices to reduce the effective shear modulus from the elastic value G to a value near that predicted by deformation theory.

Because of this extreme sensitivity of the shear modulus to small, imperfection-related shearing forces applied while the material is being stressed, nominally without shear, into the plastic range, the value of G_{eff} predicted by deformation theory should be used in bifurcation buckling analyses. The purpose of this strategy is to eliminate much of the flow theory vs deformation theory discrepancy in buckling predictions.

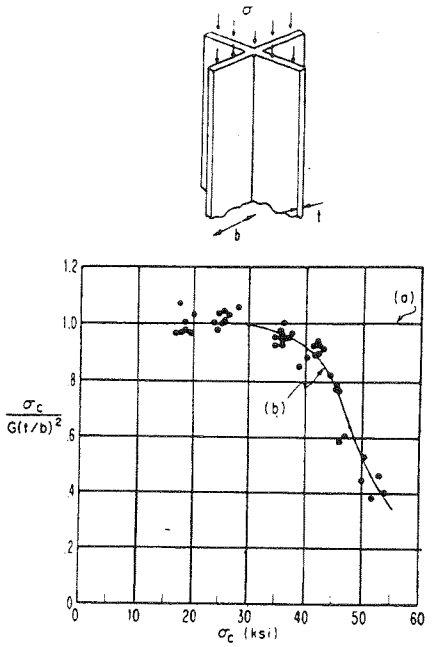

FIG. 4 THEORETICAL AND EXPERIMENTAL RESULTS FOR THE PLASTIC BUCKLING OF A CRUCIFORM COLUMN. CURVE (A), PREDICTION OF INCREMENTAL THEORY WITH SMOOTH YIELD SURFACE; CURVE (B), PREDICTION OF ANY DEFORMATION THEORY WITH $\nu = \frac{1}{2}$; TEST DATA FROM 2024-T4 CRUCIFORM SECTION
(FROM GERARD AND BECKER (1957) [102]).

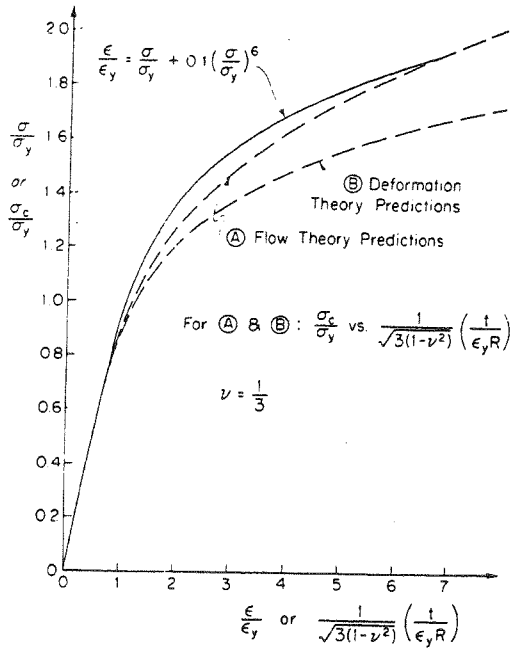

FIG. 5 TENSILE STRESS-STRAIN CURVE AND BIFURCATION STRESSES FOR A PERFECT SPHERICAL SHELL UNDER EXTERNAL PRESSURE
(FROM HUTCHINSON [7])

In cases involving no in-plane shear either in the prebuckling phase or in the buckling process, J_2 deformation theory still predicts lower bifurcation buckling loads than does J_2 flow theory. The axisymmetric buckling analysis of a spherical shell presented by Hutchinson [7] and shown here in Fig. 5 is a good example. Since J_2 deformation theory has given better agreement with test results than has J_2 flow theory, and since the discrepancy is not entirely related to the difference in effective shear modulus, it is prudent to perform stability analyses using both theories in order to establish the sensitivity of the predictions to the two models.

ASYMPTOTIC ANALYSIS: POST-BIFURCATION AND IMPERFECTION SENSITIVITY IN THE PLASTIC RANGE

Practically all of the work in this area has been done in the last decade by Hutchinson, Tvergaard, Needleman and their coworkers [2-18]. Hutchinson gives a summary in [3] and Tvergaard in [5] and [6]. The theory represents extensions to

the general theory of uniqueness and bifurcation in elastic-plastic solids derived by Hill in 1958-1959 [26-27] and the general post-buckling theory developed by Koiter for elastic structures in 1945 [28].

ELASTIC POST-BIFURCATION ANALYSIS

At a bifurcation point where the buckling mode is unique, Koiter's general elastic post-buckling theory leads to an asymptotically exact expansion for the load parameter λ in terms of the bifurcation buckling modal amplitude, w_b:

$$\lambda/\lambda_c = 1 + a\, w_b + b\, w_b^2 + \ldots \qquad (2)$$

Three types of elastic initial post-buckling behavior are shown in Fig. 6. Solid curves show the behavior of perfect structures and dotted curves the behavior of imperfect structures with imperfections in the form of the critical bifurcation buckling mode. The ultimate load carrying capabilities of the structures represented by Figs. 6(a) and (b) are sensitive to initial imperfections while that represented by Fig. 6(c) is not. For the case 6(a), which is asymmetric with respect to the sign of the buckling modal amplitude w_b, a negative imperfection amplitude w_{imp} converts bifurcation buckling into limit-point or "snap" buckling at a reduced load λ_s given by Koiter's general theory as

$$\lambda_s/\lambda_c \simeq 1\text{-}2\,(-\rho\, a\, w_{imp})^{1/2} \qquad (3)$$

in which ρ is a constant that depends on the imperfection shape. For the symmetric case 6(b) the limit load of the imperfect structure is

$$\lambda_s/\lambda_c \simeq 1\text{-}3\,(-b/4)^{1/3}\,(\rho\, w_{imp})^{2/3} \qquad (4)$$

Tvergaard [5] and the authors he references give similar formulas for initial post-buckling in cases where there are

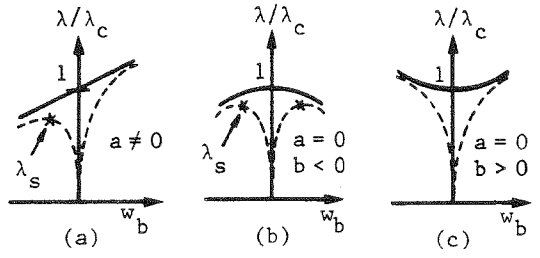

FIG. 6 INITIAL POST-BUCKLING BEHAVIOR IN CASES WHERE THE BIFURCATION MODE IS UNIQUE. DASHED CURVES SHOW EFFECT OF SMALL INITIAL IMPERFECTIONS (FROM TVERGAARD [5]).

several buckling modes associated with the critical bifurcation point.

PLASTIC POST-BIFURCATION ANALYSIS

Figures 7(a) and (b) are analagous to Figs. 6(a) and (b). Note that bifurcation in the plastic range occurs under increasing load, so that unlike the elastic cases, the maximum load-carrying capability of perfect structures is slightly above the bifurcation load λ_c and occurs at amplitudes w_b for which a finite amount of material has experienced strain reversal.

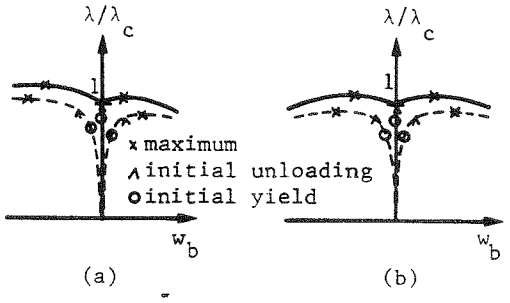

FIG. 7 INITIAL POST-BUCKLING BEHAVIOR IN THE PLASTIC RANGE IN CASES WHERE THE BIFURCATION MODE IS UNIQUE. DASHED CURVES SHOW EFFECT OF SMALL INITIAL IMPERFECTIONS (FROM TVERGAARD [5]).

Perfect Structures

For the plastic range an asymptotic theory of initial post-bifurcation behavior of perfect structures was developed by Hutchinson [3, 8]. An asymptotic expansion is obtained for the initial post-bifurcation load in terms of the bifurcation modal amplitude, w_b, as in Koiter's elastic post-buckling theory. In the plastic range, the treatment is complicated by the phenomenon of the elastic unloading, which starts at bifurcation and spreads into the material as the buckling modal amplitude increases. When the buckling mode is unique the asymptotically exact expression for the load parameter λ in terms of the buckling modal amplitude w_b is

$$\lambda/\lambda_c = 1 + \lambda_1\, w_b + \lambda_2\, w_b^{1+\beta} \qquad (5)$$

with $0 < \beta < 1$. The value of β depends on the shape of the unloading regions [3]. The constant λ_1 is positive since bifurcation takes place under increasing load. Its value is determined by the requirement that plastic loading takes place. The coefficient λ_2 is negative, so that the truncated expansion [5] can be used to estimate the maximum support load of the perfect structure, which is slightly above the critical bifurcation load. An extension of the asymptotic expansion [5] to cases of

several coincident buckling modes has not been carried out. The asymptotic theory for plastic post-bifurcation of perfect structures has been applied by Tvergaard and Needleman to study the behavior of structures with symmetric [16] and asymmetric post-bifurcation behavior [11-13].

Imperfect Structures

In 1972 Hutchinson [7] reported the results of a numerical axisymmetric plastic buckling analysis of perfect and imperfect spherical shells loaded by uniform external pressure. The shell material is characterized by a Ramberg-Osgood stress-strain relation

$$\epsilon/\epsilon_y = \sigma/\sigma_y + \alpha\,(\sigma/\sigma_y)^n \qquad (6)$$

with $\alpha = 0.1$ and $n = 6$. The geometrical parameter of the sphere is

$$[3\,(1-\nu^2)]^{-1/2}\; t/(\epsilon_y\, R) = 3 \qquad (7)$$

From Fig. 5 it is seen that the bifurcation stress of the perfect shell is 1.5 times the effective yield stress σ_y and is about 7 percent above the prediction of J_2 deformation theory. Figures 8 and 9 show the results of an analysis including imperfections of various amplitudes taken in the shape of the bifurcation buckling mode. Figure 8 (a) reveals that even though the initial post-bifurcation slope is positive, the buckling load is sensitive to initial imperfections. The onset of elastic unloading occurs at practically the same load as the collapse load. Figure 8(b) shows that the difference in predicted failure between the J_2 flow theory and J_2 deformation theory models disappears for imperfection amplitudes greater than about one-tenth the wall

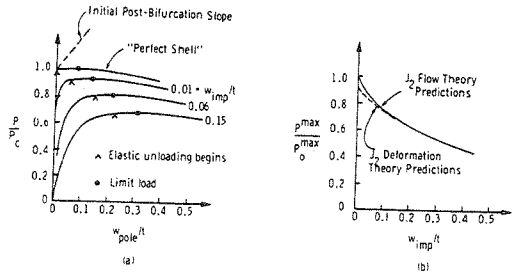

FIG. 8 (A) PLASTIC POST-BIFURCATION BEHAVIOR AND IMPERFECTION SENSITIVITY OF A SPHERICAL SHELL UNDER EXTERNAL PRESSURE.
(B) IMPERFECTION SENSITIVITY OF SPHERICAL SHELL SHOWING DIFFERENCE BETWEEN FLOW AND DEFORMATION THEORIES ONLY FOR SMALL IMPERFECTION AMPLITUDES.
(FROM HUTCHINSON [7])

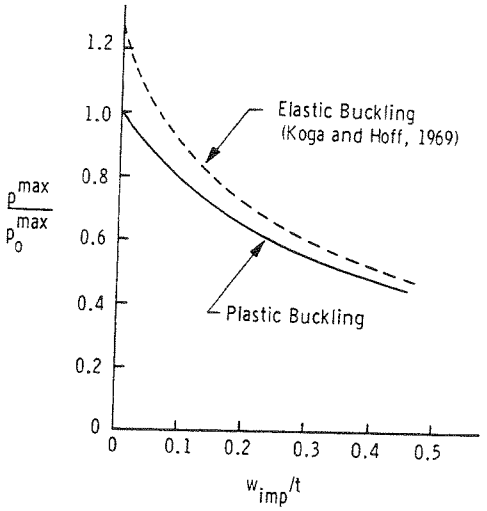

FIG. 9 BUCKLING PRESSURES FOR SPHERICAL SHELLS WITH FLAT SPOT IMPERFECTIONS. FOR BOTH CURVES, p_o^{max} IS THE MAXIMUM SUPPORT PRESSURE OF THE PERFECT SHELL AS PREDICTED BY J_2 FLOW THEORY (FROM HUTCHINSON [7]).

thickness. Figure 9 shows that for very small imperfections the plastic buckling load is not as sensitive to imperfections as is the the elastic buckling load. Also, as Hutchinson [7] points out, imperfection sensitivity is not as severe a problem for plastic as it is for elastic structures because plastic buckling requires relatively high thickness-to-radius ratios for which it is much less difficult to manufacture "reasonably perfect" shells. This conclusion is borne out by the comparisons between test and theory for a great variety of axisymmetric shells shown in a following section.

Hutchinson further discusses the effect of small imperfections on plastic buckling loads in [9]. There he provides an asymptotic estimate of the load at which elastic unloading begins. For many unstable structures this load is only slightly below the limit load. An asymptotic expression for the limit load, such as given by Koiter's general theory [28] for elastic shells [Eqs. (3) and (4)] is not yet available. The main problem is that the limit load of the structure with an infinitesimal imperfection in the form of the critical bifurcation buckling mode is not infinitesimally close to the bifurcation point, as is true in the elastic range, but lies a finite distance away. Consequently, elastic unloading usually occurs before the limit point is reached. An asymptotic expansion of the initial part of the equilibrium solution for the imperfect structure is valid only to the point at which elastic unloading begins. Representation of the remaining part requires a second asymptotic expansion that accounts for the growing elastic unloading region.

Hutchinson and Budiansky [17], Needleman and Tvergaard [14], and Tvergaard [15] have devised asymptotic theories for

the plastic limit loads λ_s of imperfect structures using hypoelastic theories (J_2 flow theory without elastic unloading). Even though these asymptotic analyses ignore elastic unloading, they yield accurate predictions of the limit loads. Figures 10-12 apply to elastic-plastic imperfect cylindrical panels under axial compression. A Ramberg-Osgood-type material stress-strain law was used for the analysis:

$$\epsilon = \frac{\sigma_y}{E}\left[\frac{1}{n}\left(\frac{\sigma}{\sigma_y}\right)^n - \frac{1}{n} + 1\right] \qquad (8)$$

The figures show the effects of panel depth θ and material hardening parameter n on the equilibrium paths and limit loads of imperfect panels. (In each case the imperfection is in the form of the critical bifurcation mode of the perfect panel.) Figures 10 and 11 show the results of an elastic-plastic finite element analysis and Fig. 12 shows a comparison between this numerical approach with the more approximate hypoelastic approach.

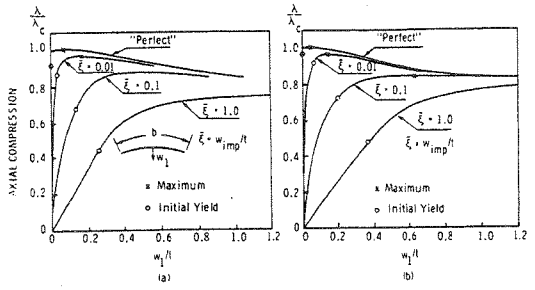

FIG. 10 LOAD VS MODAL DEFLECTION FOR CYLINDRICAL PANEL THAT BIFURCATES IN THE PLASTIC RANGE: $t/b = 0.025$; $n = 10$; $\nu = 0.3$
(a) $\theta = 0.5$, $\sigma_y/E = 0.002$
(b) $\theta = 0.75$, $\sigma_y/E = 0.0028$ (θ given in Fig. 11)
(FROM TVERGAARD [15])

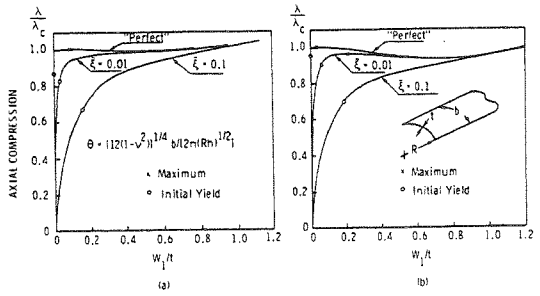

FIG. 11 LOAD VS MODAL DEFLECTION FOR CYLINDRICAL PANEL THAT BIFURCATES IN THE PLASTIC RANGE: $t/b = 0.025$; $n = 3$; $\nu = 0.3$.
(a) $\theta = 0.5$, $\sigma_y/E = 0.002$; (b) $\theta = 0.75$, $\sigma_y/E = 0.0028$
(FROM TVERGAARD [15])

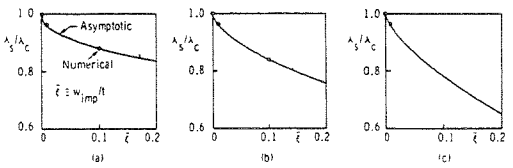

FIG. 12 COMPARISON OF NUMERICAL RESULTS AND ASYMPTOTIC HYPOELASTIC PREDICTIONS FOR THE IMPERFECTION SENSITIVITY OF ELASTIC-PLASTIC CYLINDRICAL PANELS.
(a) $\theta = 0.5$, $\sigma_y/E = 0.002$, $n = 10$
(b) $\theta = 0.75$, $\sigma_y/E = 0.0028$, $n = 10$
(c) $\theta = 0.75$, $\sigma_y/E = 0.0028$, $n = 3$
(FROM TVERGAARD [15])

A SURVEY OF WORK DONE ON GENERAL NONLINEAR ANALYSIS

Most engineering analyses involving plastic buckling are performed with general purpose computer programs that are based on the displacement method with finite element discretization. The vast potential of the finite element method was recognized after Turner, Clough, Martin and Topp published their classic paper in 1956 [110]. Use of the finite element method for the solution of nonlinear structural problems began in the early 1960's.

NONLINEAR FINITE ELEMENT ANALYSIS PRIOR TO AND INCLUDING 1973

Table 1 presents some of the important papers [111-152] and [52-54] published in the early years of nonlinear static finite element analysis. The references in the table have been divided into three sections, those that deal with geometric nonlinearity only, those that deal with material nonlinearity only, and those that deal with both types of nonlinear behavior. Each section ends with reference to survey articles pertinent to that section. The list of papers is far from exhaustive. A more complete list of references appears in the survey article by Tillerson, Stricklin and Haisler [54]. Tillerson, *et al.* [54] include a review of direct minimization procedures based on search methods as well as formulations based on finite difference discretization of the energy functional used in the principle of virtual displacements. The papers listed in Table 1 might be thought of as forming a theoretical foundation upon which rest the current general purpose finite element computer programs for nonlinear structural analysis. Other works on nonlinear structural analysis prior to 1973 are included in the symposia proceedings [83-86].

For formulations with combined geometric and material nonlinearities, the tangent stiffness method is favored because

TABLE 1 SOME FINITE ELEMENT FORMULATIONS AND SOLUTION STRATEGIES PRIOR TO AND INCLUDING 1973

Type of Nonlinearity	Ref. No.	Author	Year	Formulation*	Solution Strategy
Geometric Only	[111]	Turner *et al.*	(1960)	UL, TM	No Equilibrium Check
	[114]	Argyris *et al.*	(1964)	TM	No Equilibrium Check
	[116]	Martin	(1966)	UL, TM	
	[117]	Gallagher *et al.*	(1967)	TM	
	[118]	Mallet & Marcal	(1968)	TL, TM	Newton-Raphson
	[119]	Murray & Wilson	(1969)	UL, TM	Modified Newton
	[120]	Oden	(1967)	TM	Newton-Raphson
	[121]	Oden & Key	(1970)	TM	Newton-Raphson
	[122]	Stricklin *et al.*	(1971)	TM	Self-Correcting
	[123]	Martin	(1969)	Survey	Survey
	[124]	Oden	(1969)	TL, TM	Modified Newton
	[125]	Haisler *et al.*	(1972)	Survey	Survey
Material Only	[126]	Gallagher *et al.*	(1962)	R	
	[127]	Argyris	(1965)	R	
	[128]	Swedlow & Yang	(1965)	TM	
	[129]	Pope	(1966)	TM	
	[130]	Marcal	(1965)	R, TM	
	[132]	Marcal & King	(1967)	TM	
	[134]	Witmer *et al.*	(1969)	R	Successive Substitution
	[135]	Zienkiewicz *et al.*	(1969)	R	Successive Substitution
	[136]	Yamada *et al.*	(1969)	TM	No Equilibrium Check
	[137]	Khojasteh-Bakht	(1970)	R, TM	
	[138]	Marcal	(1972)	Survey	Survey
	[139]	Yamada	(1970)	Survey	Survey
Combined Geometric and Material	[140]	Felippa	(1966)	UL, TM	No Equilibrium Check
	[141]	Armen *et al.*	(1968)	R, TM	No Equilibrium Check
	[143]	Hibbitt *et al.*	(1970)	TL, TM	
	[144]	Marcal	(1970)	TL, TM	No Equilibrium Check
	[148]	Yagmai & Popov	(1971)	UL, TM	No Equilibrium Check
	[149]	Hofmeister *et al.*	(1971)	UL, TM	Modified Newton
	[150]	Zienkiewicz *et al.*	(1971)	Various	Various
	[151]	Nayak *et al.*	(1972)	Various	Various
	[152]	Levine *et al.*	(1973)	UL, R, TM	
	[52]	Stricklin *et al.*	(1973)	Survey	Survey
	[53]	Stricklin *et al.*	(1972)	Survey	Survey
	[54]	Tillerson *et al.*	(1973)	Survey	Survey

*UL = Updated Lagrangian
TL = Total Lagrangian
R = Nonlinearities included in a pseudo force vector (Right-hand-side)
TM = Tangent modulus (tangent stiffness) method

it is required anyway for convergence in cases involving significant geometric nonlinearities. Currently the Total Lagrangian formulation seems to be favored over the Updated Langrangian formulation for applications involving large rotations and small strains (strains less than about 4 percent). The "TL" is conceptually a bit more straightforward than the "UL" and it is easier to generate program code for the tangent stiffness constitutive law in cases involving small strains [50]. The favored solution strategy is a modified Newton method because it provides a reliable equilibrium check without the use of an inordinate amount of computer time.

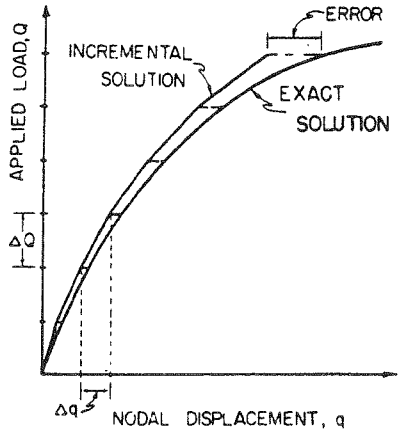

FIG. 13 DRIFTING TENDENCY IN INCREMENTAL STIFFNESS PROCEDURE (FROM TILLERSON *et al.* [54])

Figures 13-15 demonstrate the meaning and numerical behavior of the incremental method with no iterative check on equilibrium (Fig. 13), the method of successive substitutions (Fig. 14) and two Newton-like methods (Fig. 15). The slopes of the straight solid line segments at each load step or in each iteration represent schematically the stiffness matrix; a change in slope indicates calculation of a new stiffness matrix. The modified Newton-Raphson method is a combination of the full Newton-Raphson method and the method of successive substitutions: At a certain load, Q, a new tangent stiffness matrix is calculated and the method of successive substitutions is used to determine the state at the load $Q + \Delta Q$. The stiffness matrix is recalculated at any load level for which the number of iterations of successive substitutions required for convergence to some specified accuracy is greater than a specified amount. More will be said about formulation and solution strategy in the following sections.

During this same period (1965-1973), many papers were published introducing new elements for the analysis of thin and thick shells. Perhaps the most important of these is the article by Ahmad, *et al.* [154], who developed an isopara-

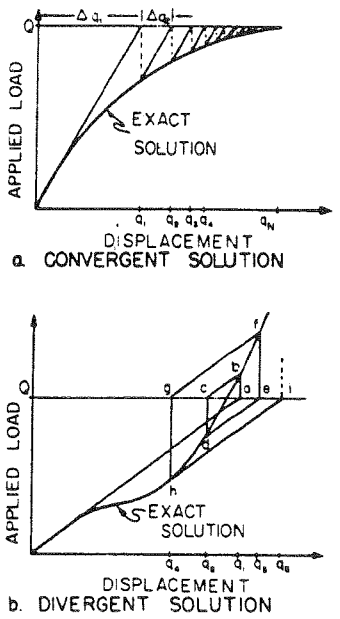

FIGURE 14 CHARACTERISTICS OF SUCCESSIVE APPROXIMATIONS PROCEDURE (FROM TILLERSON *et al.* [54])

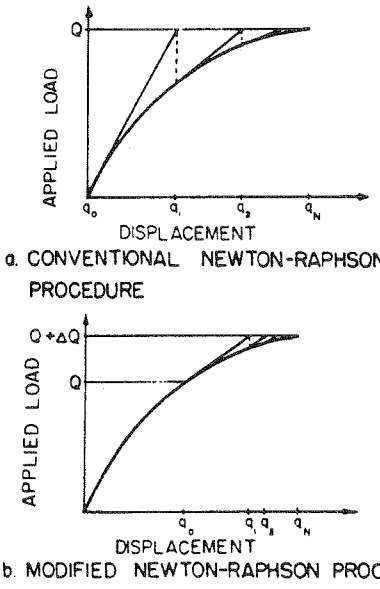

FIG. 15 CONVERGENCE CHARACTERISTICS OF NEWTON-RAPHSON METHOD (FROM TILLERSON *et al.* [54])

metric curved shell element through systematic degeneration from an isoparametric solid element. The convergence with increasing mesh refinement of results obtained with use of this "Ahmad" element is greatly improved by reduced Gaus-

sian integration schemes introduced by Zienkiewicz, *et al.* [155], and Pawsey and Clough [156].

In all of these analyses cited above which include elastic-plastic material behavior, the constitutive law is based on either isotropic or kinematic [157, 158] strain hardening. Other hardening models, such as the multiple subvolume models of White and Besseling [159] and Mroz [160], the two-surface theory of Eisenberg and Phillips [161], and the discontinuous models of Batdorf and Budiansky [162] and Hodge and Berman [163] had been formulated by 1971 but had not yet been implemented into general-purpose computer programs. In 1972 Pugh, Corum, Liu, and Greenstreet [164] specified certain hardening models for plasticity and creep to be used in analyses of nuclear reactor structures. The hardening models cited above are described in a survey article by Armen [165]. The isotropic, kinematic, and multiple subvolume models are compared with tests involving various nonproportional loading paths in a paper by Hunsaker, Vaughan and Stricklin [79].

The large body of work cited above forms the basis for a number of general and special-purpose computer programs for nonlinear analysis in widespread use since the early 1970's. These programs are described in the symposium proceedings [19]. Bushnell [20] created an information retrieval system for the symposium [19] based on data from questionnaires sent to computer program developers and users. His paper contains a great deal of detailed information on the major structural analysis computer programs being used by the

TABLE 2 COMPARISON AND RATING OF AVAILABLE FEATURES OF PROGRAMS AS OF 1973

Ref. No.	Program	Element Library (1)	Material Treatment (2)	Ease of Use/ Documentation (3)	Special Features (4)							
					a	b	c	d	e	f	g	h
[166]	ANSYS	3	3	3	1	1	1	1	0	X	1	X
[167]	ASAS	3	1	2	1	1	1	1	1	X	1	X
[168]	ASKA	3	2	3	1	1	0	1	1	X	1	X
[169]	BERSAFE	2	X	X	0	0	1	1	1	X	1	X
[170]	EPACA	2	3	3	1	0	0	1	1	0	0	0
[171]	MARC-CDC	3	3	3	1	0	1	1	1	1	1	1
[172]	NEPSAP	3	3	2	1	0	1	1	1	1	1	1
[173]	PAFEC 70+	3	1	X	1	1	1	1	0	X	1	X
[174]	PLANS	3	3	2	0	0	1	1	1	0	1	1

The code used in the above table is as follows:

In column (1): Element Library
- 1 = Limited to a special class of problems
- 2 = Moderately general
- 3 = General

In column (2): Material Treatment
- 1 = Limited
- 2 = Moderately general
- 3 = General

In column (3): Ease of Use/Documentation

This rating is based on either of the above items and includes some user reaction.
- 1 = Difficult/no documentation
- 2 = Moderate/limited documentation
- 3 = Easy/extensive documentation

In column (4): Special Features

Subcolumn
- (a) Restart
- (b) Substructuring
- (c) Multipoint constraints (tying nodes)
- (d) Pre- and postprocessors
- (e) Equilibrium checks
- (f) Assumption checks
- (g) Selective I/O
- (h) Taking advantage of linear range

The rating for the special features is based on the following code.
- X = No information
- 0 = Not available
- 1 = Available

TABLE 3 ANALYSIS FEATURES OF PROGRAMS AS OF 1973

Program	Plasticity Theory (1)	Material Property (2)	Linearization Technique (3)	Linear Equation Solver (4)
ANSYS	I, K	P, L, ML, RO	R	W
ASAS	I	P, L, ML, RO	R	F, PT, W
ASKA	I, K	P, L	R	PT
BERSAFE	X	P, L, ML	X	W
EPACA	I, K	P, L, RO	TM	G
MARC-CDC	I, K	P, L, ML, RO	TM	G
NEPSAP	I, K	P, L, ML	TM	S
PAFEC 70+	I	P, RO	R	F, B, W
PLANS	K	P, L, RO	R	PT

The code used in the above table is as follows:

General: X = No information

In column (1): Plasticity Theory
I = Isotropic hardening
K = Kinematic hardening

In column (2): Material Property
P = Elastic-perfectly plastic
L = Elastic-linear hardening
ML = Elastic-multilinear segments
RO = Ramberg-Osgood or any other power-law representation

In column (3): Linearization Technique
R = Right-hand side (initial strain, or stress)
TM = Tangent modulus

In column (4): Linear Equation Solver
W = Wavefront
F = Full matrix
PT = Partitioning
IT = Iterative
G = Gaussian elimination
S = Skyline
B = Constant bandwidth

engineering community as of 1973, including opinions by users. Armen [165] also surveyed computer programs, placing special emphasis on modeling of elastic-plastic material havior. Tables 2 and 3 are from Ref. [165]. The computer programs listed in these tables are documented in Refs. [166-174].

LARGE STRAIN FORMULATIONS AND TENSILE BIFURCATION

To the engineer the phrase "plastic buckling" usually connotes failure of a structure composed of thin or slender parts subjected to compressive loading. As mentioned previously, buckling can occur at a limit point or at a bifurcation point, as illustrated in Figs. 1 and 2. For most structures, buckling occurs when the strains are very small. Such phenomena pose problems for the designers of columns, domes, and thin-walled vessels for use with internal or external pressure.

However, there is another class of problems for which both limit point and bifurcation plastic "buckling" occur. These involve elastic-plastic continua under tensile loading. At certain values of the tensile load, local necking initiates in cylindrical rods, stretched sheets, spinning disks, and internally pressurized vessels, and voids open up in continua. Although the term "buckling" is not applied to such problems, they belong to the same mathematical class as the "classical" buckling problems, the only difference being that formulations of these problems must allow for finite strains. A survey of plastic buckling phenomena should briefly summarize this closely related field in which so much has been accomplished in the 1970's.

Finite strain formulations in continuum mechanics are included in the texts [31-35] and [76] and in papers by Green and Naghdi [175], Budiansky [176-177], Lee [178], Willis [179], Sewell [4], and Hutchinson [3,180]. Finite strains are coupled with finite element discretization in the formulations of Hibbitt, *et al.* [143], Hofmeister, *et al.* [149], Zienkiewicz and Nayak [150], Bathe, *et al.* [49], Bathe and Ozdemir [50], and McMeeking and Rice [181]. Tvergaard [6] gives a survey on applications of tensile bifurcation theory to necking in bars, plates and shells. There are numerous works

on large strain tensile bifurcation, including application to cylindrical bars by Miles [182], Chen [183], Needleman [184], and Hutchinson and Miles [185]; application to growth and coalescence of voids by Needleman [186]; and applications to plates and shells by Hill and Hutchinson [187], Needleman [188], Stören and Rice [189], Tvergaard [190], Needleman and Tvergaard [191], and Tvergaard [192]. Sewell [4] lists many additional references.

Sewell [4] and Hutchinson [180] present a lucid formulation of the problem. Hutchinson uses the Total Lagrangian formulation in incremental (rate) form, presents a generalization of J_2 flow theory to the finite strain case [177], and writes the equations for application to thin plates and shells. He indicates that the two conditions required for the small strain relation to provide an accurate approximation to the exact finite strain formulation are:

1. The distinction between the metric tensors of the undeformed and deformed configurations should be small.
2. The stresses should be small compared to the instantaneous moduli.

NONLINEAR ANALYSIS SINCE 1973

Important recent developments in nonlinear structural analysis include the formulation and solution of static and dynamic problems in which creep, plasticity and large deformation occur simultaneously; the development of unified theories for the prediction of creep and plastic flow; the invention of new, more accurate models for cyclic elastic-plastic phenomena; and the evolution of better strategies for the solution of nonlinear equations. Several new computer programs have appeared for the analysis of two and three dimensional continua. Most of the programs are based on the Total Lagrangian formulation and include dynamic effects (inertial body forces). In many of them, temperature-dependent material properties, finite strains, and arbitrarily large displacements are permitted. Plates and shells are modeled most frequently with use of the Ahmad-Pawsey isoparametric element [154-156]. The simultaneous nonlinear equations that result from discretization of a continuum are solved by various strategies, but in contrast to the state-of-the-art a few years ago (Table 1), an iterative equilibrium check is now almost always provided.

Combined Plasticity and Creep; Viscoplasticity

Cyr and Teter [193] derived a computer program for two-dimensional structures with temperature-dependent material properties. Strains are assumed to be small and the tangent stiffness method is used, with creep effects included in the tangent modulus rather than as pseudo-load terms. Sharifi and Yates [172] use a similar approach in their derivation of a program applicable to three dimensional continua. Bushnell [22, 23, 194-196] developed computer programs for axisymmetric shells and solids including calculation of bifurcation points corresponding to nonaxisymmetric equilibrium states adjacent to the fundamental states, which are derived including the effects of moderately large axisymmetric deflections, elastic-plastic material properties, and primary or secondary creep. In his small strain formulation he uses a double iteration strategy for solving the nonlinear equations and a subincremental technique for accurately determining plastic flow and creep. More details on his formulation will be given in a following section. Zienkiewicz and Cormeau [197], Nagarajan and Popov [198], and Kanchi, Zienkiewicz and Owen [199] use a viscoplastic model to obtain inviscid plasticity predictions either by extrapolating results for very large viscosity coefficients or by introducing time steps at each load level to produce a quasi-static relaxation to the true nonlinear elastic-plastic solution.

Krieg [200] gives a survey of theories in which inelastic strain is treated as a unified quantity, not separated into time-dependent and time-independent parts. Such unified formulations are capable of representing primary and secondary creep, cyclic hardening, conventional plastic behavior and creep-induced, strain-rate-dependent Bauchinger effects. Difficulties in implementing these theories into computer programs for use by engineers include the design of material tests for determination of constants and functions in the models and the possibility of numerical instability in the integration of the constitutive equations. Krieg [200] proposes various strategies depending on whether accuracy or stability are limiting conditions. Hughes and Taylor [201] propose a one-parameter family of implicit algorithms for viscoplastic finite element analysis that is unconditionally stable. Rashid and Tang [202] unify creep and plasticity by treating the yield surface as strain rate dependent with a single associated flow rule for both plastic and creep strains. Classical plasticity theory applies at high strain rates and creep holds for low strain rates. The numerical implementation is difficult because an unfavorable relationship between yield surface growth and contraction and the stress rate can lead to oscillatory solution behavior.

New Computer Programs

New general-purpose computer programs that handle simultaneously large deflections, creep and plasticity include ADINA [203], AGGIE I [204], TRICO [205], and programs generated at the Institut für Statik und Dynamik (ISD) in West Germany [206]. General-purpose programs that handle large deflections and elastic-plastic effects include STAGSC1 [207], ANSR [208], and GNATS [209]. A special-purpose program for application to problems with large deflections, plasticity and creep of axisymmetric pressure vessels is BOSOR5 [22], which calculates the nonlinear fundamental path (OA in Fig. 1) and bifurcation points (B in Fig. 2a) on this path corresponding to nonaxisymmetric buckling modes. A set of benchmark problems has been established. Clinard, Corum and

Sartory [210] show comparisons of benchmark test results with results obtained by various general-purpose programs.

New Elastic-Plastic Material Models

New analytical models for elastic-plastic material behavior include the "two-surface" theories of Krieg [211], Dafalias and Popov [212] and Petersson and Popov [213]. These models are especially designed to predict accurately the behavior of a material subjected to repeated reversed loadings into the plastic range. Although they show great promise, they have not yet been incorporated into general-purpose programs. Krieg and Key [214] discuss implementation of a finite strain plasticity theory into a finite element computer program. This model includes a combined kinematic-isotropic hardening rule.

New Strategies for Traversing Limit Points

Obtaining solutions in the neighborhood of a limit point such as E in Fig. 2(a) presents a difficulty if the load is prescribed because the stiffness matrix is singular at E and ill conditioned close to E. Haisler, Stricklin and Key [60] briefly survey numerical methods for tracking the load-deflection curve over the limit point and suggest a self-correcting approach based on displacement incrementation in the neighborhood of the limit point. As an illustration they choose an arch with a concentrated load, for which it is obvious which displacement component to specify. Gallagher [215, 215a], gives surveys for nonlinear elastic systems. Yokoo, *et al.* [216], present a perturbation method which they claim is especially designed for numerical investigation of limit points and postbuckling equilibrium. They distinguish between an incremental constitutive relation

$$\Delta \sigma_{ij} = C_{ijk\ell}\ \Delta\epsilon_{k\ell} \tag{9}$$

and the instantaneous rate relation

$$\dot{\sigma}_{ij} = C_{ijk\ell}\ \dot{\epsilon}_{k\ell} \tag{10}$$

by expanding all variables in Taylor series of the load parameter about the known state corresponding to the last converged solution.

The method of Riks [65, 66] appears more promising. In a paper which very clearly sets forth the difference between limit point collapse ("snapping") and bifurcation buckling [65], he suggests a method for traversing limit point collapse loads by introducing an auxiliary equation such that the normalized determinant of the Jacobean of the augmented equation system is maximized at each load step. Physically Riks' method corresponds to use of the arc length of the equilibrium path as a loading parameter. The use of such a loading parameter eliminates numerical difficulties associated with ill conditioned stiffness matrices for loads near the limit point and the singularity at the limit point. Riks extends the method for application to bifurcation buckling problems in Ref. [66].

In Ref. [67] Haftka, Mallett, and Nachbar propose a method whereby discretized nonlinear snap-through buckling problems are transformed into linear bifurcation problems: The nonlinear prebuckling behavior of a real structure is represented by an "imperfection" in a hypothetical "modified structure," and a form of Koiter's analysis [28] is used to predict the behavior in the neighborhood of the snap-through buckling point. The aim is to avoid lengthy computations associated with a direct nonlinear analysis. However, in Ref. [68] Cohen and Haftka find that the method does not appear to be practical for shells of revolution because in many cases the prebuckling nonlinearity may be too large to be treated accurately as a small imperfection.

The methods developed by Bergan and Søreide [61] and Bergan, *et al.* [62], also appear promising. Bergan and Søreide [61] construct an algorithm for automatic computation of variable load increments and decrements. The magnitude of the load increment or decrement is based on a maximum allowable difference between a linear and quadratic extrapolation of the equilibrium path in $(p, \|\mathbf{r}\|)$ space, where p is the scalar load amplitude, $\mathbf{r}$ is the solution vector, and $\|\mathbf{r}\|$ is a suitably chosen norm of the solution vector. (For example, for a shallow spherical cap subjected to uniform external pressure, p is the pressure and $\|\mathbf{r}\|$ might be the volume enclosed between the undeformed and deformed cap.) This procedure leads to a nearly constant number of iterations required for convergence at each load level. Bergan, *et al.* [62] extend the strategy of [61] by introducing a scalar quantity called the "current stiffness parameter", S_p:

$$S_p = \dot{\mathbf{r}}_o^T \cdot \mathbf{R} / (\dot{\mathbf{r}}^T \cdot \mathbf{R}) \tag{11}$$

in which $\mathbf{R}$ is the reference load vector normally held constant, $\dot{\mathbf{r}}_o$ is the initial rate of change of the solution vector with respect to the loading parameter p, and $\dot{\mathbf{r}}$ is the current rate of change of the solution vector. The "current stiffness parameter" S_p is unity for linear systems, less than unity for softening systems, greater than unity for stiffening systems, and negative for unstable systems. The size of the load increment is determined by the strategy of Bergan, *et al.*, [62], and the sign of the load increment is determined by the sign of S_p. In examples Bergan, *et al.*, [62], have determined that it is advantageous to take two load steps without equilibrium iterations just after any reversal in the sign of Δp and to prescribe an upper bound for the norm of the solution vector in the neighborhoods of limit points.

Figures 16-18 are taken from Ref. [62]. Figure 16 shows how the current stiffness parameter S_p varies with the solution norm $\|\mathbf{r}\|$ and with the load parameter p for a system which

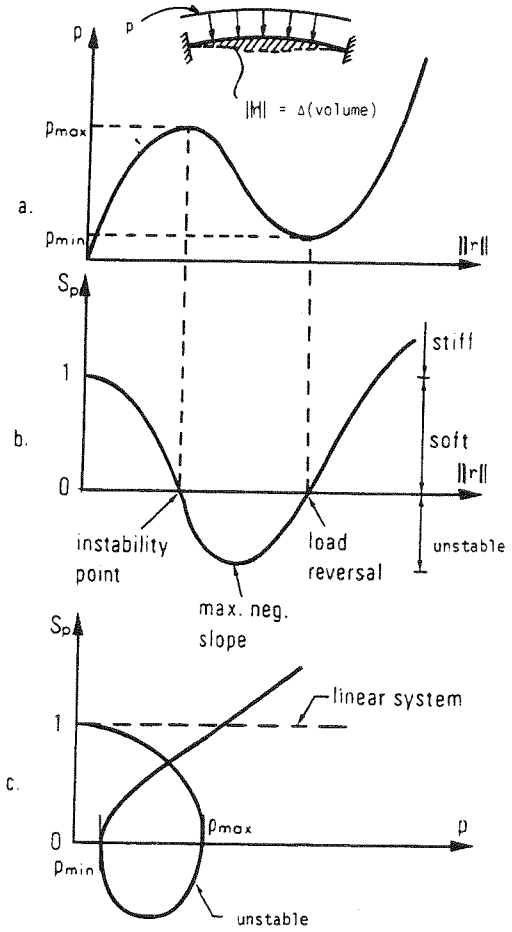

FIG. 16 BEHAVIOR OF CURRENT STIFFNESS PARAMETER FOR INSTABILITY PROBLEM (FROM BERGAN *et al.* [62])

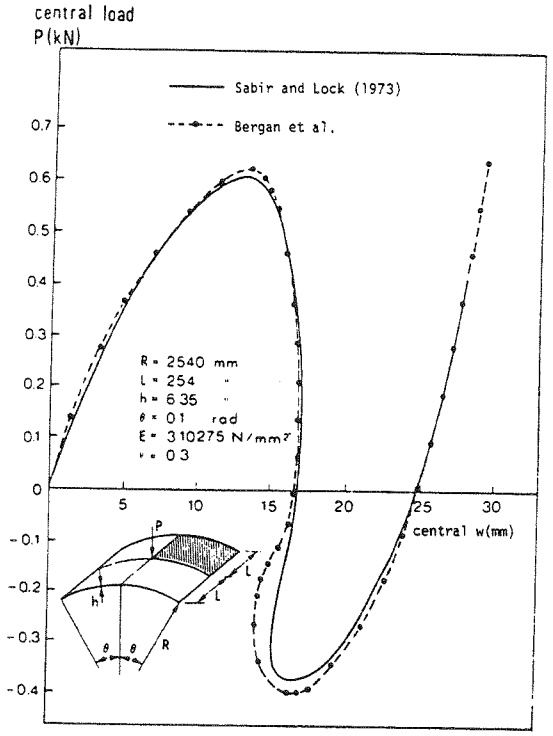

FIG. 17 LOAD-DEFLECTION CURVES FOR HINGED CYLINDRICAL SHELL (FROM BERGAN *et al.* [62])

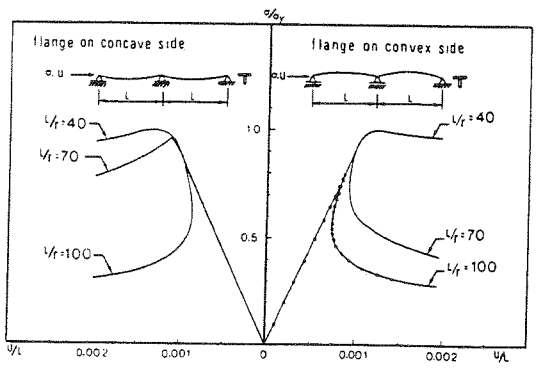

FIG. 18 LOAD-DISPLACEMENT CURVES FOR TWO-SPAN BEAM-COLUMNS (FROM BERGAN *et al.* [62])

initially softens, snaps through, and then stiffens. Figures 17 and 18 demonstrate that the strategies described in [62] work for problems with rapidly and abruptly changing stiffness and stability characteristics. Both examples were completed in only one computer run per case. Load incrementation was used throughout. Bergan, *et al.* [63] introduce a "bifurcation index" I_p defined as

$$I_p = S_p^- \cdot S_p^+ / (S_p^- - S_p^+) \qquad (11a)$$

in which S_p^- is the value of S_p just before bifurcation and S_p^+ is that just after bifurcation. In Ref. [63] is given a table in which values of I_p in the range $+\infty > I_p > -\infty$ are associated with various types of bifurcation buckling behavior: $I_p \to \infty$ means no bifurcation; I_p positive and of moderate size means bifurcation to an initially stable branch; $I_p = 0$ means bifurcation to a neutrally stable branch; $0 > I_p > -0.5$ means bifurcation to an unstable branch with moderate sensitivity to initial imperfections; $-0.5 > I_p > -\infty$ indicates highly imperfection-sensitive bifurcation.

FORMULATION AND SOLUTION OF NONLINEAR STRUCTURAL PROBLEMS

Two areas will be emphasized in this section: the formulation of the governing equations starting from the principle of virtual displacements and various methods for solving the resulting nonlinear equations and their advantages and disadvantages. The discussion of formulations follows articles by Bathe, Ramm, and Wilson [49] and Bathe and Ozdemir [50]. That on solution techniques follows Almroth and Felippa [218].

FORMULATION

The motion of a general body is shown in Fig. 19, which is taken from Refs. [49] and [50]. The configuration is known at times 0 and t and the objective is to determine it at time $t + \Delta t$. In the following derivation a left superscript indicates the time when the quantity occurs and a left subscript indicates the configuration with respect to which the quantity is measured. In the case of derivatives, a left subscript indicates the time of the coordinate with respect to which the quantity is differentiated. Thus,

$$ {}_{t+\Delta t}u_{i,j} \equiv \frac{\partial u_i}{\partial ({}^{t+\Delta t}x_j)} \tag{12} $$

All tensors are referred to Cartesian reference frames. The principle of virtual displacements, written for the current configuration (time = $t + \Delta t$) is

$$ \int_{({}^{t+\Delta t}V)} ({}^{t+\Delta t}\tau_{ij})\,\delta\,({}_{t+\Delta t}e_{ij})\,({}^{t+\Delta t}dV) = {}^{t+\Delta t}R \tag{13} $$

where

$$ {}^{t+\Delta t}R = \int_{{}^{o}A} ({}^{t+\Delta t}_{o}t_k)\,\delta u_k\,({}^{o}dA) + \int_{{}^{o}V} {}^{o}\rho\,({}^{t+\Delta t}_{o}f_k)\,\delta u_k\,({}^{o}dV) \tag{14} $$

The quantities $({}^{t+\Delta t}\tau_{ij})$ are the Cartesian components of the Cauchy (true) stress tensor at time $t + \Delta t$, and $({}^{t+\Delta t}_{o}f_k)$ are surface tractions and body force components at time $t+\Delta t$

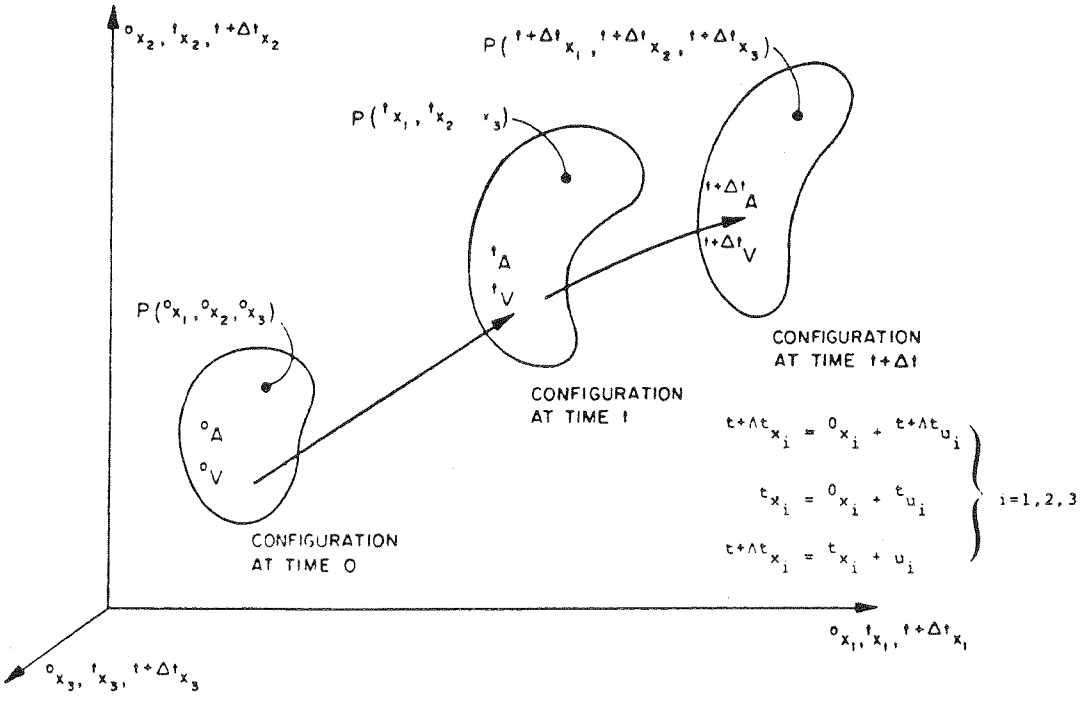

FIG. 19 MOTION OF BODY IN CARTESIAN COORDINATE SYSTEM (FROM BATHE, RAMM AND WILSON [49])

but measured with respect to the configuration at time = 0. The variation δu_k is an infinitesimal variation in the current displacement component $(t + \Delta t_{u_k})$. The summation convention for repeated indices is used here. The variation in true strain corresponding to the infinitesimal variation in the displacement field is

$$\delta\,({}^{t+\Delta t}e_{ij}) = \delta\,\frac{1}{2}\,({}^{t+\Delta t}u_{i,j} + {}^{t+\Delta t}u_{j,i}) \tag{15}$$

In dynamic analysis the body force components include inertial effects.

Since the configuration at the current time $t + \Delta t$ is unknown, the principle of virtual displacements, Eq. (13), must be expressed in a form in which all variables are referred to a known state. Then the integration will be performed over known volumes and areas. If the static and kinematic variables are referred to the initial state (time = 0), the formulation is known as Total Lagrangian (TL). If they referred to the previous known state (time = t), the formulation is known as the Updated Lagrangian (UL). The remainder of this derivation will follow the total Lagrangian formulation. Bathe, *et al.* [49], and Bathe and Ozdemir [50] present details of both the TL and UL formulations.

In the TL formulation the principle of virtual displacements becomes [31, 34, 35]:

$$\int_{{}_oV} ({}^{t+\Delta t}_{\ o}S_{ij})\ \delta\ ({}^{t+\Delta t}_{\ o}\epsilon_{ij})\ {}^{o}dV = {}^{t+\Delta t}R \tag{16}$$

in which ${}^{t+\Delta t}_{\ o}S_{ij}$ are the components of the 2nd (symmetric) Piola-Kirchoff stress tensor and ${}^{t+\Delta t}_{\ o}\epsilon_{ij}$ are the components of the Green-Lagrange strain tensor which is written in terms of the current displacements ${}^{t+\Delta t}u_k$:

$$\begin{aligned}\delta\ ({}^{t+\Delta t}_{\ o}\epsilon_{ij}) = \delta\,\frac{1}{2}\,({}^{t+\Delta t}_{\ o}u_{i,j} + {}^{t+\Delta t}_{\ o}u_{j,i} \\ + {}^{t+\Delta t}_{\ o}u_{k,i}\ {}^{t+\Delta t}_{\ o}u_{k,j})\end{aligned} \tag{17}$$

If *incremental* static and kinematic quantities are defined as

$$\begin{aligned}{}_oS_{ij} &\equiv {}^{t+\Delta t}S_{ij} - {}^{t}_{o}S_{ij} \\ {}_o\epsilon_{ij} &\equiv {}^{t+\Delta t}_{o}\epsilon_{ij} - {}^{t}_{o}\epsilon_{ij} \\ u_i &\equiv {}^{t+\Delta t}u_i - {}^{t}u_i\end{aligned} \tag{18}$$

the total Green-Lagrange strain increment can be decomposed into linear and nonlinear parts

$${}_o\epsilon_{ij} = {}_oe_{ij} + {}_o\eta_{ij} \tag{19}$$

with

$$\begin{aligned}{}_oe_{ij} &= \frac{1}{2}\,[\,{}_ou_{i,j} + {}_ou_{j,i} + ({}^{t}_{o}u_{k,i})\,({}_ou_{k,j}) \\ &\quad + ({}_ou_{k,i})\,({}^{t}_{o}u_{k,j})] \\ {}_o\eta_{ij} &= \frac{1}{2}\,({}_ou_{k,i})\,({}_ou_{k,j})\end{aligned} \tag{20}$$

In addition, the *increments* of 2nd Piola-Kirchoff stress tensor components can be related to the *increments* of Green-Lagrange strain tensor components by the linear constitutive law

$${}_oS_{ij} = {}_oC_{ijrs}\,({}_o\epsilon_{rs}) \tag{21}$$

which is an approximation, since ${}_oC_{ijrs}$ changes along the path in the finite increment Δt. Furthermore, the variation in the total strain $\delta\,({}^{t+\Delta t}_{\ o}\epsilon_{ij})$ is equal to the variation in the total strain increment $\delta\,({}_o\epsilon_{ij})$. This equivalence and the relations (18), (19), and (21) can be used to express Eq. (16) in the form

$$\begin{aligned}\int_{{}_oV} {}_oC_{ijrs}\,({}_o\epsilon_{rs})\ \delta\ ({}_o\epsilon_{ij})\,{}^{o}dV + \int_{{}_oV} {}^{t}_{o}S_{ij}\ \delta\ ({}_o\eta_{ij})\,{}^{o}dV \\ = {}^{t+\Delta t}R - \int_{{}_oV} {}^{t}_{o}S_{ij}\ \delta\ ({}_o\epsilon_{ij})\,{}^{o}dV\end{aligned} \tag{22}$$

This variational principle represents a nonlinear equation for the incremental displacements u_i. The Updated Lagrangian formulation leads to a completely analogous expression in which the subscripts and superscripts (o) are replaced by (t) and the equivalence of the 2nd Piola-Kirchoff stress tensor ${}^{t}_{t}S_{ij}$ to the Cauchy (true) stress tensor ${}^{t}\tau_{ij}$ is noted. Of course, the constitutive tensor for the U.L. formulation is now ${}_tC_{ijrs}$, which takes on different values from ${}_oC_{ijrs}$. The relationship between the two constitutive tensors is given by

$${}_oC_{mnpq} = \frac{{}_o\rho}{{}_t\rho}\,({}^{o}_{t}x_{m,i})\,({}^{o}_{t}x_{n,j})\,({}_tC_{ijrs})\,({}^{o}_{t}x_{p,r})\,({}^{o}_{t}x_{q,s}) \tag{23}$$

$${}_tC_{mnpq} = \frac{{}_t\rho}{{}_o\rho}\,({}^{t}_{o}x_{m,i})\,({}^{t}_{o}x_{n,j})\,({}_oC_{ijrs})\,({}^{t}_{o}x_{p,r})\,({}^{t}_{o}x_{q,s}) \tag{24}$$

in which the derivatives $({}^{o}_{t}x_{m,i})$, etc. are defined as in Eq. (12). Bathe and Ozdemir [50] note that the TL formulation for large displacements but small strain analysis is programmed more easily because

> "In this case large displacement analysis is a simple extension of small displacement analysis in that the same subroutine which calculates the material matrix in small displacement analysis can be used without modification for large displacement conditions. It is only necessary to work with 2nd Piola-Kirchoff stresses and

Green-Lagrange strains instead of conventional small displacement stresses and strains."

Equation (22) can be transformed into a system of simultaneous nonlinear algebraic equations by division of the volume ${}^{o}V$ into an assemblage of finite elements and use of isoparametric interpolation

$$ {}^{o}x_i = \sum_{k=1}^{N} h_k \, ({}^{o}x_i^k) \quad ; \quad u_i = \sum_{k=1}^{N} h_k \, (u_i^k) \qquad (25) $$

in each element, where N is the number of nodal points in the isoparametric element and h_k are appropriate interpolation polynomials. Integration is carried out numerically, usually by Gaussian quadrature. For nonlinear elastic-plastic analysis of shells the Ahmad-Pawsey isoparametric element [154-156] is very popular. Bathe and Ozdemir [50] first linearize Eq. (22) by replacing ${}_{o}\epsilon_{rs}$ by ${}_{o}e_{rs}$ and $\delta\,({}_{o}\epsilon_{ij})$ by $\delta\,({}_{o}e_{ij})$ and then perform modified Newton iterations, setting

$$ {}^{t+\Delta t}u_i^{(k)} = {}^{t+\Delta t}u_i^{(k-1)} + \Delta u_i^{(k)} \qquad (26) $$

in which k is the iteration number and ${}^{t+\Delta t}u_i^{(0)} \equiv {}^{t}u_i$. More details, including the formulation for follower loads such as pressure, are given in Refs. [49] and [50].

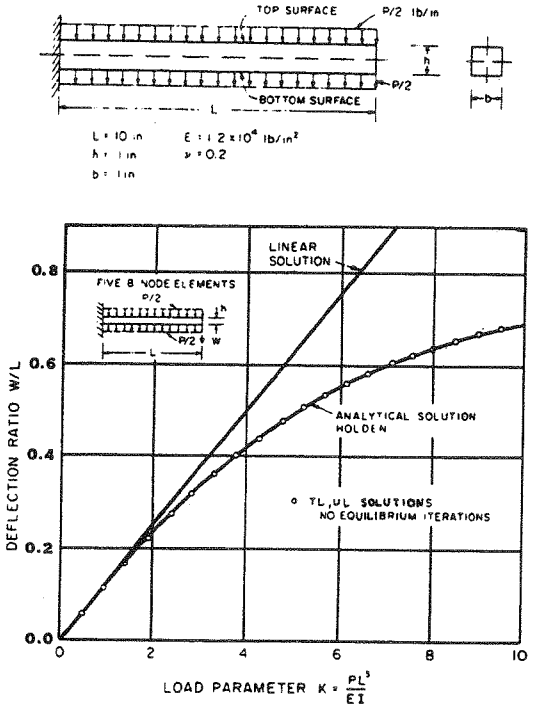

FIG. 20 LARGE DISPLACEMENT ANALYSIS OF A CANTILEVER UNDER UNIFORMLY DISTRIBUTED LOAD (FROM BATHE AND OZDEMIR [50])

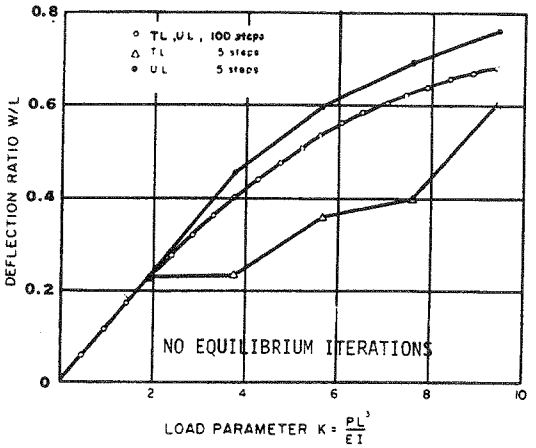

FIG. 21 LARGE DISPLACEMENT ANALYSIS OF A CANTILEVER, COMPARISON OF NONLINEAR FORMULATIONS (FROM BATHE AND OZDEMIR [50])

Figures 20 and 21 show the large deflection static response of an elastic cantilever with a distributed dead load. Five 8-node plane stress isoparametric elements were used in the discretized model. The solutions were obtained from equations linearized as just described for the TL formulation, with no iterations for equilibrium refinement. It is seen that the differences in results from the UL and TL formulations are due only to the increment size, those for a large number of increments agreeing with each other and with Holden's solution [220]. Presumably the large discrepancies shown in Fig. 21 would have vanished if iterations had been performed at each of the five load steps, since the state of the elastic material is independent of the load path and Eq. (21) is therefore exact in this case.

Other examples are given in Refs. [49] and [50], including the dynamic response of an elastic-plastic spherical cap with an external uniform pressure applied as a step load.

METHODS OF SOLVING NONLINEAR EQUATIONS

Formulation and discretization of nonlinear structural analysis problems lead to a set of nonlinear algebraic equations of the form

$$ F(q, \lambda) = 0 \qquad (27) $$

where λ is a load parameter and q is a solution vector. Table 4, taken from Ref. [218], lists the various strategies for solving nonlinear equations, the names given these strategies in the mathematical literature, and the names given in the engineering literature. Three of the four groups are pictured graphically in Figs. 13-15.

TABLE 4 ALGORITHMS FOR NUMERICAL SOLUTION OF NONLINEAR ALGEBRAIC EQUATIONS

Major Groups	Algorithms	Identifiers Often Used in Engineering Literature
Newton-like	Standard Newton Modified Newton Damped Newton Quasi-Newton Steffensen	Newton-Raphson
Successive substitution	Picard iteration Perturbation Contraction	Initial stress Initial Strain Pseudoload
Initial value (continuation, imbedding, parameter differentiation)	Uncorrected integration, Corrected integration, Infinite interval	Incremental Step-by-step Self-correcting Dynamic relaxation
Minimization	Random search Sequential search Steepest descent Conjugate gradient Variable metric Gauss-Newton	Energy search

Newton-Like Methods

These are based on Taylor series linearization in the neighborhood of a solution (q, λ). A sufficiently close initial estimate q^o is required to start the iteration process. The iteration sequence is

$$K(q^k, \lambda)\ \Delta q^k = F(q^k, \lambda)$$
$$q^{k+1} = q^k + \Delta q^k,\ k = 0,1,\ldots \tag{28}$$

in which the elements of the K-matrix are

$$K_{ij} = \partial F_i / \partial q_j \tag{29}$$

The primary advantage of the method is its characteristic of quadratic convergence near the solution. The primary disadvantage is the need to generate and factor a new stiffness matrix for every iteration. Most general-purpose programs contain an option for performing a Newton iteration or iterations at intervals of several load steps, say every fourth to every tenth load step, depending on the rapidity of convergence of the computationally less expensive but more weakly convergent method of successive substitutions, which is used for the intervening load steps. The strategy used in this modified Newton method depends on the bandwidth of K. For the analysis of shells of revolution it is feasible to perform Newton iterations at every load step, whereas for the analysis of general shells a single Newton iteration every fourth to tenth load step, depending on the nonlinear behavior, is reasonable. The other Newton-like methods listed in Table 4 have been little used in structural analysis.

Successive Substitution Method

In this iterative method all nonlinear terms are transferred to the right-hand side as pseudoloads. A typical iteration is

$$K_o\ \Delta q^k = \lambda F_L + F_{NL}(q^k, \lambda)$$
$$q^{k+1} = q^k + \Delta q^k \tag{30}$$

in which K_o is constant stiffness matrix (the tangent stiffness at some earlier load step), and the nonlinear terms are contained in F_{NL}. The primary advantage of this method is that the stiffness matrix K_o is formed infrequently compared to the number of iterations. Therefore, it is economical in mildly nonlinear problems or when used in conjunction with a modified Newton method, in which K_o is updated whenever a prespecified number of iterations has been exceeded [207]. The primary disadvantage is that the method is only linearly convergent at best and is divergent in severely nonlinear problems, as shown in Fig. 14. In addition, the stability determinant is not available.

Initial Value Method

Equation (27) is converted into an initial value problem by differentiating it with respect to the load parameter λ,

$$\dot{F} = \frac{\partial F}{\partial q}\,\dot{q} + \frac{\partial F}{\partial \lambda} = 0 \qquad (31)$$

in which the initial condition is $q(0) = 0$ if $\lambda = 0$ corresponds to the undeformed configuration. Equation (31) may be solved by any standard forward integration scheme, such as Euler, Runge-Kutta or predicter-corrector linear multi-step methods. The primary disadvantage of the so-called "uncorrected" or "forward marching" scheme represented by Eq. (31) is the tendency of the solution $q(\lambda)$ to drift from the true equilibrium path as shown in Fig. 13. This drifting tendency is corrected by formation of a linear combination of Eq. (27) and Eq. (31), thus

$$\dot{F} + \alpha F = 0 \qquad (32)$$

or by solution of the second order system

$$\ddot{F} + \alpha \dot{F} + \beta F = 0 \qquad (33)$$

Use of Eq. (32) yields a solution that approaches the true equilibrium path exponentially and use of Eq. (33) yields a solution that approaches the true equilibrium path in damped oscillations. Tillerson, *et al.* [54], present a thorough discussion with many examples of these first order and second order "self-correcting" schemes.

One of the most popular strategies in the $\dot{F} = 0$ class is a scheme in which the "force imbalance" terms from the previous load step are used to modify the right-hard-side in the current load step. This is relatively inexpensive to do on the computer, since it does not involve the formation and factoring of a stiffness matrix, and it permits the use of larger load steps than would otherwise be possible. Without iterations at a given load step, however, the drifting tendency shown in Fig. 13 would still be present.

The primary advantages of the initial value methods are that implementation in existing linear codes is straightforward, the stability determinant is available at every load step, and much of the numerical integration software can be applied to nonlinear dynamic analysis. The primary disadvantage of the uncorrected or noniterative $\dot{F} = 0$ scheme is its tendency to drift from the true equilibrium path.

Direct Minimization Methods

In these methods the nonlinear equation system (27) is not solved at all, but a minimum is sought of the energy function from which Eq. (27) is derived. This method has been extensively applied in situations involving relatively few degrees of freedom, such as optimization problems, but has not been found to be competitive for the solution of nonlinear problems with large numbers of degrees of freedom.

For a more complete discussion of nonlinear equation solving strategies the reader is referred to Tillerson, *et al.* [54], and Felippa [55].

Reduction by Introduction of Global (Rayleigh-Ritz) Functions

A promising technique for solving a large system of nonlinear equations is to reduce the number of unknowns by introduction of generalized degrees of freedom q such that $X = Tq$, where X is a "Rayleigh-Ritz" approximation to the true unknown nonlinear solution vector X' of the discretized (large) model with N nodal point degrees of freedom, and T is an (N, M) matrix, the M columns of which represent suitably chosen discretized Rayleigh-Ritz modes. (Note that $M \ll N$.) The nonlinear equations (27) in the reduced form are solved by the Newton-Raphson method for several load steps with a continuing check on the residual force vector R, which is calculated by insertion of the approximate solution X instead of q in Eq. (27): $F(X, \lambda) = R$. If the norm of the residual force vector R exceeds a certain percentage of the load vector, the set of M Rayleigh-Ritz basis vectors T is updated in some way.

Nickel [68a] uses vibration modes as basis vectors in nonlinear dynamic response; Nagy [68b] chooses buckling modes; Almroth, Stern and Brogan [69] accumulate new basis vectors X' as the load is increased by solving the full nonlinear system $F(X', \lambda) = 0$ whenever the norm of the residual force vector $R = F(X, \lambda)$ exceeds a pre-specified tolerance; Noor and Peters' [70] basis vectors are the nonlinear solution X' and a number of its derivatives with respect to the equilibrium path (loading) parameter λ; Hajela and Sobieski [71] choose eigenmodes of the stiffness matrix as basis vectors.

These promising methods require extensive testing and have yet to be applied to problems involving both large deflections and elastic-plastic material behavior.

ELASTIC-PLASTIC MATERIAL MODELS

This section contains a brief outline of classical plasticity theory, a derivation of the incremental constitutive tensor ${}_oC_{ijrs}$ that appears in Eqs. (21) and (22), descriptions of various hardening theories, and a summary of work done on integrated constitutive laws for use with analysis of elastic-plastic plates and shells. Some of the discussion on classical plasticity theory follows Almroth [82]; the derivation of ${}_oC_{ijrs}$ follows Bathe and Ozdemir [50]; the descriptions of various hardening theories follow surveys by Armen [80], Almroth [82], and Hunsaker, Vaughan and Stricklin [79]; and the summary on integrated constitutive laws for use with analyses of elastic-plastic plates and shells follows Bieniek and Funaro [219].

Classical Plasticity Theory

Classical plasticity theory requires definition of the following:

1. An initial yield surface and subsequent loading surfaces

which bound the region in stress space within which deformation is elastic.

2. A flow law which provides the ratios between the increments of plastic strain components.

3. A hardening rule which specifies the modification of the yield (loading) surface as plastic flow occurs.

4. A plastic or "hardening" modulus which provides a ratio between the increment of an effective stress quantity to the increment of an effective plastic strain quantity.

In addition, classical plasticity theory is based on the following assumptions:

1. Materials are isotropic with respect to initial yielding.

2. Plastic deformation occurs with no change in volume. There is negligible plastic flow under pure hydrostatic pressure.

3. Yielding and subsequent response are insensitive to the rate of deformation.

4. The material exhibits no hysteresis. That is, unloading from points A to B in stress space occurs such that the elastic modulus of the virgin material governs the ratio between stress and strain increments. Reloading from B to A occurs without plastic flow, and continued loading further into the plastic range takes place as if there had been no unloading.

5. The total strain may be decomposed into elastic and plastic components. This assumption is generally valid if the strains are small.

6. The relationship between stress and strain determined from a uniaxial test holds for multi-axial loading, in which "stress" is replaced by an "effective stress" quantity and "strain" is replaced by an "effective strain" quantity.

By far the most popular yield criterion in use today for nonlinear computerized analysis of metallic structures is due to von Mises (1913). He realized that since negligible plastic flow occurs under hydrostatic pressure, the yield condition should be expressed in terms of deviatoric stress components and that this condition should not depend on coordinate transformations. Thus, the yield limit is defined in terms of the second invariant of these deviatoric components. Mises' further observation that increments in the components of plastic strain are proportional to the components of deviatoric stress constitutes a flow rule that is identical to the criterion that a small increment in plastic strain be normal to the yield surface in stress space. This "normality condition" was later justified by Drucker (1954) on the basis of conservation of energy. The "effective stress" referred to in assumption 6 above is implicitly defined by the yield condition because it is a quantity which must be constant over the entire initial yield surface.

Most applications of plastic analysis have been restricted to isothermal conditions. Non-isothermal plasticity forms the basis for the general-purpose computer programs described in Refs. [171, 172, 203, 204, 206] and formulations are presented in Refs. [203] and [204]. The discussion here will be limited to isothermal plasticity.

Incremental Constitutive Tensor ${}_oC_{ijrs}$ [see Eqs. (21) and (22)]

Almost all plastic buckling analysis has been carried out with use of the von Mises yield criterion, its associated flow rule, and hardening rules based on either isotropic or kinematic strain hardening. Bathe and Ozdemir [50] present an isothermal Total Lagrangian formulation which is valid for either of these two hardening models. The aim of this formulation, which is repeated here, is to obtain the incremental constitutive tensor ${}_oC_{ijrs}$ through which the incremental components of the 2nd Piola-Kirchoff stress tensor, d_oS_{ij}, are related to the incremental components of the Green-Lagrange strain tensor, $d_o\epsilon_{rs}$:

$$d_oS_{ij} = {}_oC_{ijrs}\, d_o\epsilon_{rs} \tag{34}$$

The initial yield surface and subsequent loading surfaces are expressed by

$$F({}^t_oS_{ij},\ {}^t\kappa) = F({}^t_oS_{ij},\ {}^t_o\epsilon^p_{ij}) = 0 \tag{35}$$

in which ${}^t\kappa$ is a hardening parameter that depends on the total plastic strains ${}^t_o\epsilon^p_{ij}$. The total strain increments are the sums of the elastic and plastic strain increments,

$$d_o\epsilon_{ij} = d_o\epsilon^e_{ij} + d_o\epsilon^p_{ij} \tag{36}$$

The components of plastic strain increments are given by the associated flow rule

$$d_o\epsilon^p_{ij} = {}^t\lambda\ \frac{\partial F}{\partial({}^t_oS_{ij})} \tag{37}$$

During plastic flow the change in F is zero, since the state of the material point is always on the loading surface. Therefore,

$$dF = \frac{\partial F}{\partial({}^t_oS_{ij})}\ d_oS_{ij} + \frac{\partial F}{\partial({}^t_o\epsilon^p_{ij})}\ d_o\epsilon^p_{ij} = 0 \tag{38}$$

The increment in stress results from an increment in elastic strain

$$d_oS_{ij} = {}_oC^e_{ijrs}\, d_o\epsilon^e_{rs} \tag{39}$$

where ${}_oC^e_{ijrs}$ is a component of the elasticity tensor. The components of the "tangent stiffness" constitutive tensor ${}_oC_{ijrs}$ can be derived from Eqs. (34-39) (see [31]):

$$
{}_oC_{ijrs} = {}_oC^e_{ijrs}
$$

$$
- \frac{{}_oC_{ijmn} \dfrac{\partial F}{\partial ({}^t_o S_{mn})} \; {}_oC^e_{rspq} \dfrac{\partial F}{\partial ({}^t_o S_{pq})}}{\dfrac{\partial F}{\partial ({}^t_o \epsilon^p_{mn})} \dfrac{\partial F}{\partial ({}^t_o S_{mn})} + {}_oC^e_{k\ell pq} \dfrac{\partial F}{\partial ({}^t_o S_{k\ell})} \dfrac{\partial F}{\partial ({}^t_o S_{pq})}} \tag{40}
$$

This tensor relates the increments of 2nd Piola-Kirchoff stress to the increments of Green-Lagrange strain at a material point. It is calculated at all of the Gaussian integration points in each finite element at each time or load increment.

VARIOUS HARDENING THEORIES

In computerized nonlinear analysis of metallic structures there is general agreement about the validity of the von Mises initial yield criterion and its associated flow law. However, this is not the case for hardening laws. There are many models for the subsequent changing of shape and location of the loading surface as plastic flow proceeds. These models are formulated in papers such as [157-163] and [211- 213] and reviewed by Armen [80, 165], Knets [81], Almroth [82], Hunsaker, Vaughan and Stricklin [79], Michno and Findley [104], and Hecker [105]. The brief review given here follows those given in Refs. [79], [80], and [82].

Isotropic Hardening

This theory is the simplest to apply in computerized analysis, requires the least amount of storage of data, and hence is the most popular. The loading surface is assumed to expand uniformly about the origin in stress space, maintaining the same center, shape, and orientation as the initial yield surface. Figure 22 shows in two-dimensional stress space the yield and loading surfaces for a case in which the stress state moves from point 1 to point 2. Unloading and subsequent reloading in the reverse direction will result in yielding at point 3. The isotropic hardening law was formulated based on experimental evidence that a material, loaded in tension into the plastic range and then unloaded and reloaded into compression far enough into the plastic range, will follow the same effective stress-effective strain curve as if it had been continuously loaded in tension. This behavior is demonstrated in Fig. 23. However, the isotropic model violates the observation initially made by Bauschinger (1886) that upon reloading in compression, the material yields at a lower stress than it would have if it had been loaded in compression initially.

Kinematic Hardening

This theory grew out of observations by Bauschinger (1886), who noticed that after cold-work in tension the compressive yield stress appears to be reduced by an amount

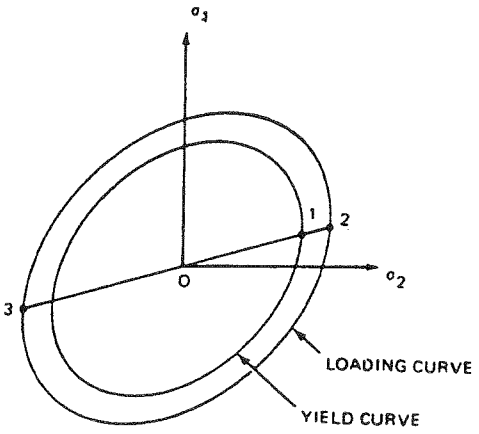

FIG. 22 ISOTROPIC HARDENING (FROM ARMEN [80])

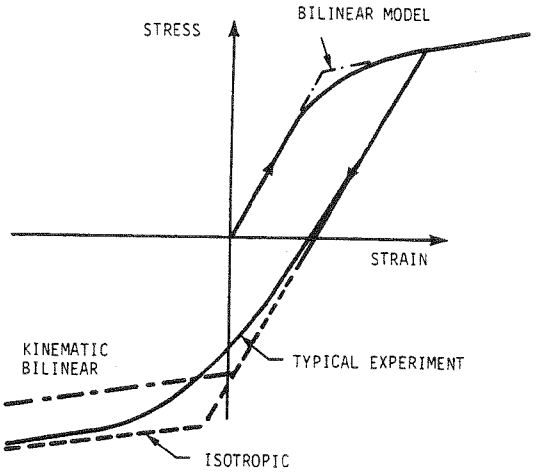

FIG. 23 STRESS-STRAIN CURVES WITH STRESS REVERSAL

approximately equal to the increase in the yield strength (strain hardening) caused by the initial loading in tension. Therefore, the kinematic hardening model, originally formulated by Prager [157] and modified by Ziegler [158], is based on the assumption that during plastic deformation the loading surface translates as a rigid body in stress space. The size, shape, and orientation of the initial yield surface is maintained, as illustrated in Fig. 24. The yield surface and loading surface are shown for an initial shift of the stress state from point 1 to point 2. The center of the yield locus translates to a new point, α_{ij}. Upon reloading in compression the material yields at a smaller stress at point 3 than it would have if it had been initially compressed along the path 0-3. The kinematic model is illustrated in stress-strain space in Fig. 23 for a case in which

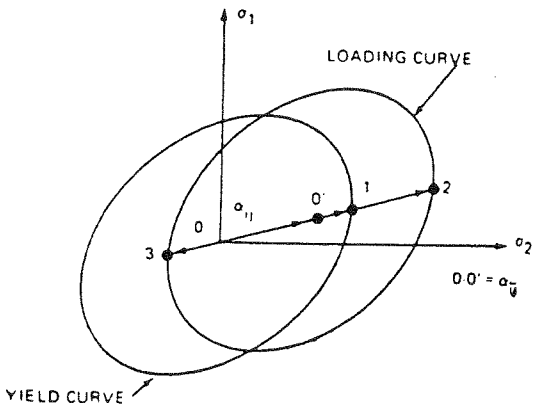

FIG. 24 KINEMATIC HARDENING (FROM ARMEN [80])

the actual stress-strain curve is modeled in a bilinear fashion. It is seen that the kinematic model reflects the initial yield in compression better than does the isotropic model, but that the hardening modulus after yield is too small, resulting in an underestimation of the absolute value of the stress as the material is further strained in compression. Models of combined kinematic and isotropic hardening in which the loading surface translates and expands simultaneously have been formulated by Krieg and Key [214] and Hodge [221].

Multiple Subvolume Models

The failure of both isotropic and kinematic models to predict what happens in the "near plastic" range for reversed and nonproportional loading has led to the implementation of more elaborate material models in nonlinear structural analysis computer programs. The STAGSC1 program for the static and dynamic analysis of general shells [207] includes a model in which the material is assumed to consist of a mixture of separate components which all undergo the same strain history. All components have the same elastic modulus and exhibit perfectly plastic behavior. Each component has a unique yield stress and occupies a certain fraction of the total volume. Use of only one component results in an elastic-perfectly plastic material; use of two components leads to a model which is identical to kinematic strain hardening with a bilinear stress-strain curve; use of many components constitutes a model in which the stress-strain curve is approximated by a series of line segments. This idea of treating strain hardening material as an amalgam of separate elastic-perfectly plastic components was originated by Brandzaeg in 1927 [222], Duwez in 1935 and White in 1950 and later refined by Besseling [159]. The model is known by various names, including White-Besseling, mechanical sublayer, and subvolume. (The name "sublayer" is unfortunate because it implies that each component in the amalgam occupies a distinct volume or layer, which is not the case. The various components are assumed to be mixed homogeneously).

Figure 25 shows the behavior exhibited by the White-Besseling model for a simple one-dimensional case. Since the components are all subjected to the same strain, the proportional limit of the composite will be the same as that of the weakest of the components. However, since the other components can take additional load, the composite will exhibit strain hardening with a piecewise linear stress-strain curve. If the stress is reversed after loading beyond the yield limit for one or more components, yield will occur in the reversed direction when the average stress in the composite reaches the value $\sigma = \sigma_1 - 2\sigma_y$, where σ_1 is the maximum stress during initial loading and σ_y is the yield limit for the weakest

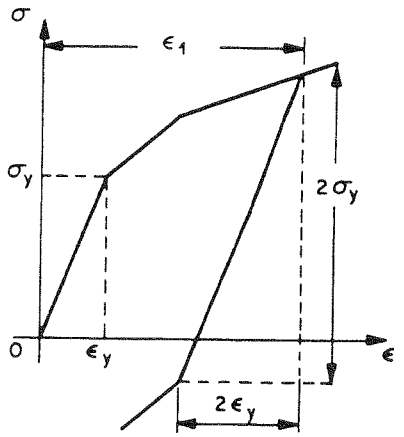

FIG. 25 STRESS-STRAIN RELATIONS ACCORDING TO WHITE-BESSELING THEORY (FROM ALMROTH [82])

component. In contrast to the kinematic theory, the White-Besseling theory gives a hardening modulus at the outset of reversed yield which equals the hardening modulus at initial yield, hence agreeing much better with material behavior observed in tests. The material behavior in the White-Besseling model is completely defined by a segmented approximation of the tensile stress-strain curve. This segmented approximation provides the required specification of the number of material components, the volume fraction of each component, and the yield strength of each component.

Mroz (160) introduced a similar model called "a field of work-hardening moduli." The Mroz model contains a number of different yield surfaces which lie within one another and translate in stress space according to the rules of kinematic hardening. The hardening modulus depends on how many of the moduli are currently active. Results obtained with the Mroz model are almost identical to those obtained with use of the White-Besseling model.

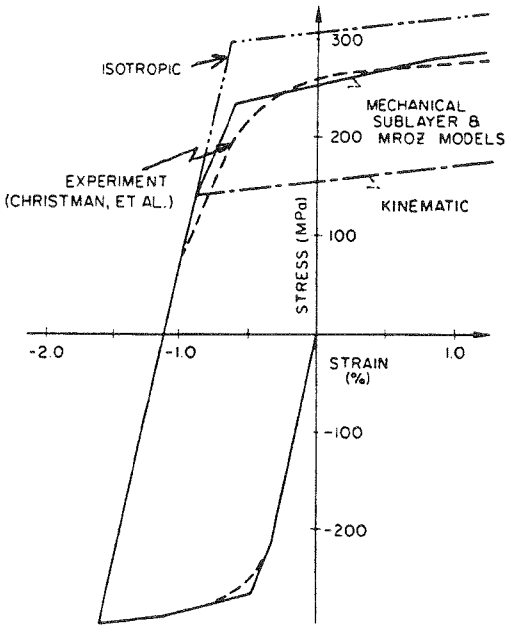

FIG. 26 COMPARISON OF HARDENING RULE PREDICTIONS WITH EXPERIMENT FOR REVERSE LOADING OF ALPHA TITANIUM (FROM HUNSAKER *et al.* [79])

The main advantage of the White-Besseling and Mroz models is the better representation of the material behavior upon reversed loading into the plastic range. Figure 26 shows a comparison with an experiment of Christman, *et al.* [223]. The multiple-material models are obviously superior to the isotropic and kinematic models. The main disadvantage of the White-Besseling and Mroz models is that they require about N times more computer storage than do the isotropic or kinematic models, where N is the number of material components. Hunsaker, *et al.* [79], elaborate on computer storage requirements for all of the hardening models discussed so far.

Hunsaker, Vaughan and Stricklin [79] present comparisons of test and theory for the isotropic, kinematic, White-Besseling, and Mroz hardening models in cases involving uniaxial cyclic loading (Fig. 26) and proportional and nonproportional biaxial loading. Figures 27a and 27b show results for the hoop (tangential) stress component in a commercial cold-drawn tube loaded by combinations of tension and internal pressure which are increased nonproportionally. The four hardening models are compared to tests by Marin and Hu [224]. Contrary to the opinion expressed in [80], the simple isotropic model is superior in this and in the other nonproportional loading case studied by Hunsaker, *et al.* [79]. The White-Besseling and Mroz models behave in a similar way. The kinematic model, as programmed by Hunsaker, *et al.* [79], gives the worst predictions.

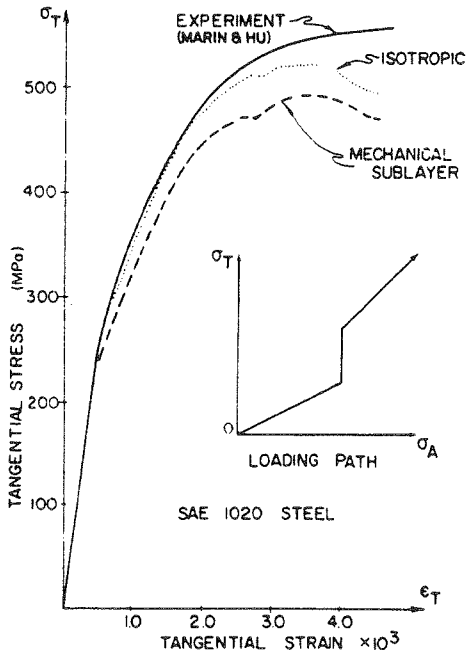

(a)

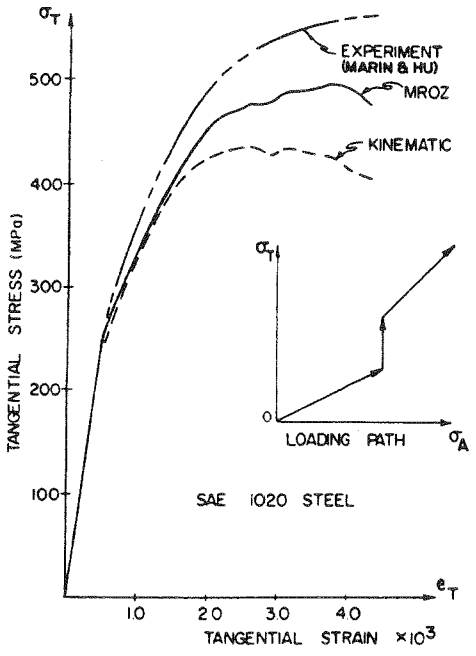

(b)

FIG. 27 FIRST BIAXIAL TEST, TANGENTIAL COMPONENTS: (A) ISOTROPIC HARDENING AND MECHANICAL SUBLAYER; (B) KINEMATIC HARDENING AND MROZ MODEL (FROM HUNSAKER, VAUGHAN, AND STRICKLIN [79])

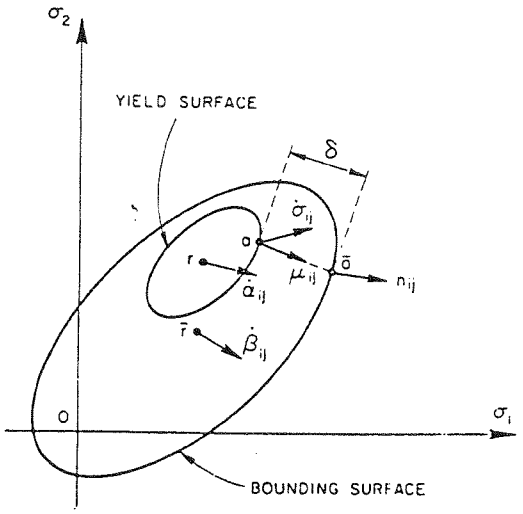

FIG. 28 SCHEMATIC REPRESENTATION OF THE YIELD AND BOUNDING SURFACES AND ILLUSTRATION OF THEIR MOTIONS (FROM DAFALIAS AND POPOV [212])

Two-Surface Theories

Eisenberg and Phillips [161] define two distinct surfaces in order to account for noncoincident yield and reloading stress states. Krieg [211] and Dafalias and Popov [212] presented independently and almost simultaneously very similar models of this type which improve the representation of material behavior for reversed plastic loading. The yield surface is always contained inside a limit or bounding surface, as shown in Fig. 28, which is taken from Ref. [212]. Both yield and bounding surfaces change with plastic loading. The hardening modulus is expressed as a function of the distance in stress space from the point of loading to the limit surface along the normal to the yield surface. Figure 29 shows some parameters and the behavior of the Dafalias-Popov model in a uniaxial loading model. The general formulas derived in [212] can be specialized to reproduce purely kinematic hardening or combined isotropic-kinematic hardening. Figure 30 shows a comparison between test and theory for random cyclic loading of a steel specimen. Two curves were made to match by a curve-fitting procedure, the upper curve of the loop labeled ① and the lower curve of the loop labeled ②. The initial plateau was

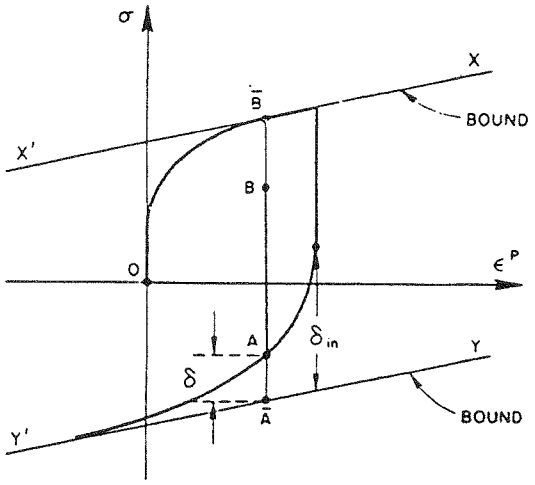

FIG. 29 ELEMENTS OF THE DAFALIAS-POPOV HARDENING MODEL FOR UNIAXIAL LOADING (FROM DAFALIAS AND POPOV [212])

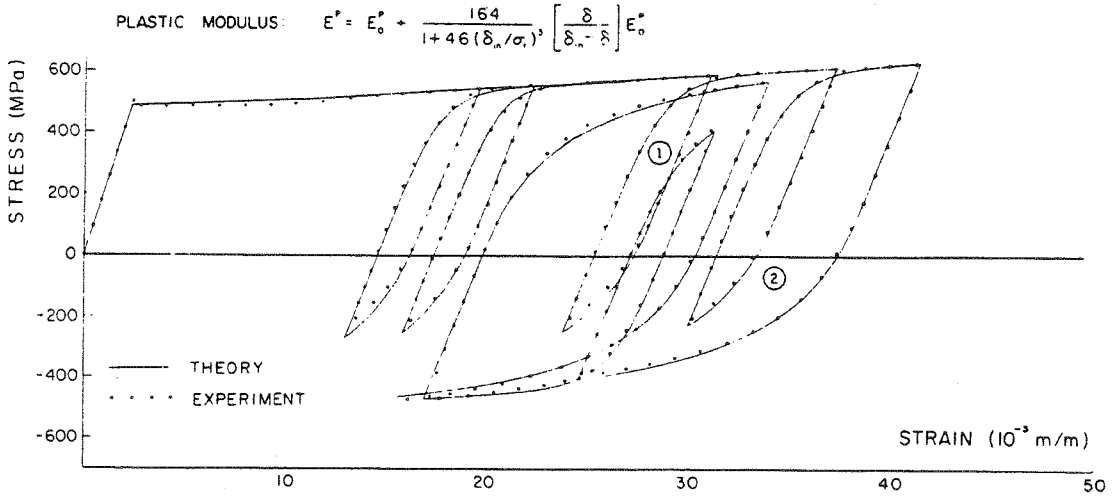

FIG. 30 RANDOM CYCLIC LOADING ON GRADE 60 STEEL SPECIMEN (FROM DAFALIAS AND POPOV [212])

treated separately. Agreement between test and theory for the rest of the stress-strain plot is excellent. The approach to multiaxial loading as presented by Dafalias and Popov is not tied to any hardening law and appears to be sufficiently general and sound to warrant further investigation and incorporation into computer programs for nonlinear structural analysis.

Yield and Loading Surfaces with Corners

The hardening theories described so far are all associated with smooth yield and loading surfaces. Therefore, such theories will not change the discrepancies between flow and deformation theories noted previously in connection with the prediction of bifurcation buckling of cruciform columns, spherical shells, and flat plates. As emphasized by Sewell [225], this discrepancy is diminished by a hardening model in which the loading surface develops corners. Batdorf and Budiansky [162] developed such a model based on the concept of slip. Figure 31 shows the growth of the loading function as the stress state moves from point 0 to point 3. The unshaded region is the initial yield surface. Since the stress state is generally at a corner, the resulting constitutive equation is complex. The complicated material manipulations required for implementation of this model have led to its neglect in computerized structural analysis. However, it does give better results than the classical theories for the case of tension-torsion loading of simple test specimens. The slip theory does not account for the Bauschinger effect. Koiter [29] showed that the slip theory corresponds to a loading surface which has a vertex at the stress point. In three-dimensional stress space this vertex is the tip of a cone the generators of which are tangents to the initial yield surface.

Hodge and Berman [163] review piecewise linear yielding and hardening. The oldest and most widely used piecewise linear yield surface is the Tresca criterion. Figure 32 shows a hardening rule of interdependent loading planes proposed by Hodge [226] in which the Bauschinger effect is accounted for.

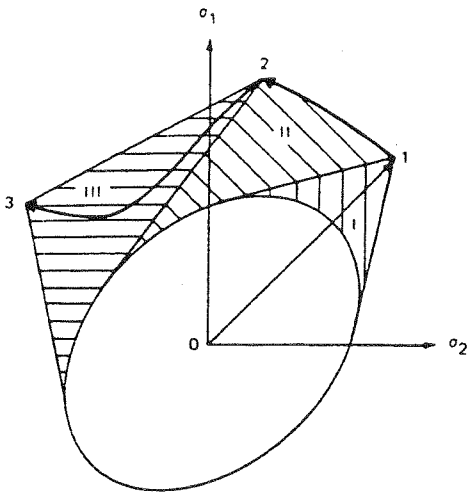

FIG. 31 SLIP THEORY HARDENING (FROM ARMEN [80])

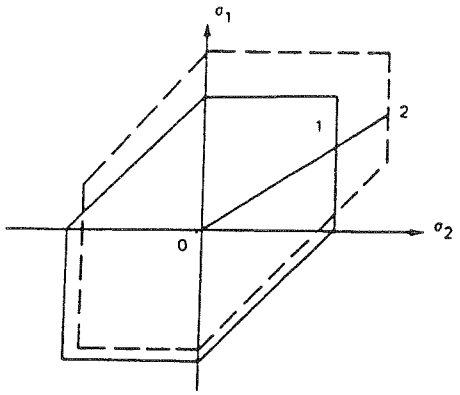

FIG. 32 PIECEWISE LINEAR HARDENING WITH INTERDEPENDENT LOADING PLANES (FROM ARMEN [80])

Other Models

Armen [80] briefly reviews other nonlinear material models, including models for initially anisotropic metals, models with hydrostatic stress dependence, rate sensitive models, nonisothermal models, and models without a yield surface. The reader is referred to Armen's paper and the papers referenced there for further details.

INTEGRATED CONSTITUTIVE LAW FOR ELASTIC-PLASTIC PLATE AND SHELL ANALYSIS

The constitutive laws discussed in the previous section apply to incremental stress and strain at a point. In the analysis of plates and shells the variation of total strain through the thickness is generally assumed to be linear. A three dimensional problem is thereby reduced to a two dimensional problem.

In discrete models of plates and shells an arbitrarily chosen reference surface is divided into finite elements. The stiffness matrix of each element, whether it be an initial stiffness matrix of the undeformed structure of a "tangent" stiffness matrix including geometric and material nonlinearities, has the form

$$K = (B^T C B)\, dA \qquad (41)$$

in which dA is the element area, B is a matrix relating nodal point degrees of freedom to incremental strains and changes of curvature of the reference surface, and C is the constitutive matrix relating incremental strains and changes in curvature of the reference surface to incremental stress resultants and

moments. For example, in shell analysis in which transverse shear deformations are neglected

$$\dot{S} = C\dot{e} \tag{42}$$

where the transpose of $\dot{S}$ and the transpose of $\dot{e}$ are

$$\dot{S}^T \equiv (\dot{N}_1, \dot{N}_2, \dot{N}_{12}, \dot{M}_1, \dot{M}_2, \dot{M}_{12}) \tag{43}$$

$$\dot{e}^T \equiv (\dot{e}_1, \dot{e}_2, \dot{e}_{12}, \dot{\kappa}_1, \dot{\kappa}_2, 2\dot{\kappa}_{12}) \tag{44}$$

and C is a 6 x 6 symmetric matrix containing elements such as

$$C_{11} = \int_{z_1}^{z_2} E_{11}\, dz \; ; \; C_{44} = \int_{z_1}^{z_2} E_{11}\, z^2\, dz$$
$$C_{14} = -\int_{z_1}^{z_2} E_{11}\, z dz \tag{45}$$

In Eq. (43) N_1, M_1, N_2, M_2 are the stress and moment resultants in the "1" and "2" coordinate directions and N_{12}, M_{12} are the inplane shear resultant and torsion resultant. Equation (44) lists the corresponding reference surface strains, changes in curvature and twist. In Eq. (45), z_1 and z_2, the limits of integration over the shell wall thickness coordinate z, depend on the location of the reference surface, and E_{11} is a component of the constitutive tensor analogous to ${}_oC_{ijrs}$ in Eqs. (21) and (22). Equations (45) are valid if the shell is thin enough so that the ratio of thickness to a typical radius of curvature can be neglected compared to unity.

There are two ways of formulating the constitutive law for elastic-plastic plates and shells. The most frequently used and most generally applicable way is to find the tangent stiffness components E_{11}, etc. at a number of points through the wall thickness and perform the integrations indicated in Eq. (45) numerically. This requires calculations such as indicated in Eq. (40) and storage of data such as total plastic strain components corresponding to every integration point through the thickness and over the surface of the structure. The advantage of this method is its broad applicability. The shell wall can consist of layers of different materials which can be loaded and cycled in an arbitrary way. The disadvantages are the requirement of computations and storage of data corresponding to a large number of control stations.

The less frequently and less generally applicable way of formulating the constitutive law is to express it initially in terms of stress *resultant* rates $\dot{S}$ and *reference surface* strain rates $\dot{e}$ at a point on the two dimensional reference surface, rather than in terms of stress rates σ_{ij} and strain rates $\dot{e}_{ij}$ at an arbitrary point in the three-dimensional shell wall continuum. The yield criterion, flow law, and hardening law must now be expressed in terms of resultant rates $\dot{S}$ and reference surface strain and change in curvature rates $\dot{e}$. The advantages of this method are the diminished requirements of computations and data storage. The tangent stiffness is calculated and associated data stored only at control stations on the reference surface. The disadvantage is its limited applicability. It is useful only for shells with one kind of material through the wall thickness and there is almost no experience with application to strain hardening materials. This second method of formulating the constitutive law is described in detail in Ref. [219].

PLASTIC BUCKLING OF RING-STIFFENED SHELLS OF REVOLUTION: PREBUCKLING AND BIFURCATION BUCKLING STRATEGIES

INTRODUCTION

As mentioned previously, the plastic buckling analysis of axisymmetrically loaded axisymmetric shells is a sort of halfway house between the asymptotic analyses of Hutchinson, Tvergaard, and Needleman (Refs. [2-18]) and the general nonlinear analyses of Swanson [166], Schrem [168], Hellen [169], Zudans [170], Marcal [171], Henshell [173], Pifko [174], Bathe [203], Argyris [206], Almroth [207], Mondkar [208], their coworkers, and other developers of general-purpose computer programs. The nonlinear prebuckling behavior can easily be modeled including moderately large deflections and nonlinear material behavior. Limit points on load-deflection equilibrium curves such as point A in Fig. 1 and bifurcation points such as point B in Fig. 2a can be calculated with relatively small amounts of computer time because the discretization is one-dimensional. Only the meridian needs to be discretized because displacements are axisymmetric in the prebuckling analysis and vary harmonically in the circumferential direction in the bifurcation buckling analysis. One-dimensional discretization leads to stiffness matrices with very small average bandwidths that can be calculated, stored, and factored efficiently. Therefore, complex shells with discontinuities, branches, ring stiffeners, and layered wall construction can be analyzed inexpensively. It is feasible to use a rigorous strategy to solve the nonlinear axisymmetric prebuckling problem, including at each load level nested iteration loops: an inner loop for nonlinear behavior due to moderately large displacements and an outer loop for elastic-plastic-creep material property updating. The strongly convergent and therefore very reliable Newton-Raphson method can be used in the inner loop and a subincremental strategy can be used in the outer loop. The relative efficiency and economy with which such one-dimensional numerical problems can be solved on the computer permits parameter studies that are not feasible with more general multi-dimensionally discretized configurations.

The axisymmetric shell problem deserves emphasis also because it is of special significance to the pressure vessel and piping industry. Most tests are on simplified models of actual

structures, and one of the first simplifications is to neglect structural elements that destroy axisymmetry. Over the last twenty years there have, therefore, been many tests involving plastic buckling of axisymmetric shells. Greater understanding of the plastic buckling process is gained by numerous comparisons between test and theory. In this way the significance of imperfections, post-yield strain hardening, and nonproportional material loading can be evaluated.

This section and the next are both devoted to shells of revolution. In this section a strategy for solving problems with both material and geometric nonlinear behavior is described, both for prebuckling and bifurcation buckling analyses. The following section contains numerous examples with comparisons between test and theory. Most of these examples are taken from Refs. [22, 23, and 227-233]. The theoretical results were obtained with use of the BOSOR5 computer program [22], which is applicable to segmented, branched, ring-stiffened shells of revolution with or without discontinuities between segments and branches. Figure 33 shows an example of an axisymmetric branched shell structure with nodal points indicating discretization. Discrete rings are modeled as segmented substructures attached to the shell reference surface as shown in Fig. 34. The cross-sections of the dicrete rings do not deform but are free to rotate and translate with the portion of the shell to which they are considered to be attached. The type of input data required by BOSOR5 is indicated in Fig. 35 (with the thickness of the input data deck greatly exaggerated!). Details of the derivation of equations are given in [195, 196, 228, and 22].

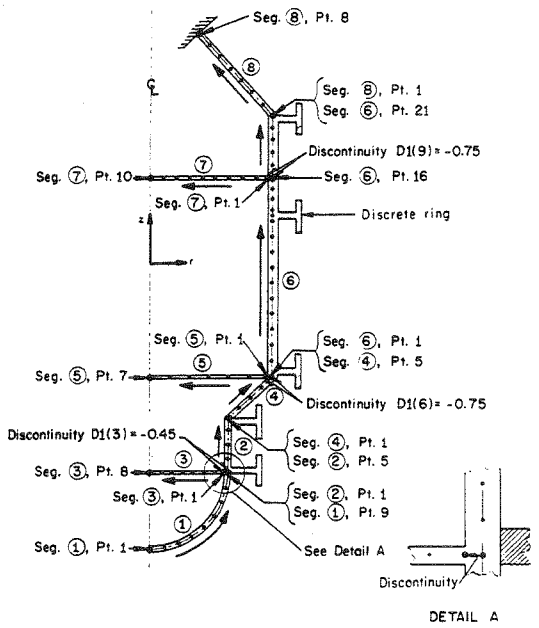

FIG. 33 BRANCHED RING-STIFFENED SHELL OF REVOLUTION WITH NODAL POINT DISCRETIZATION

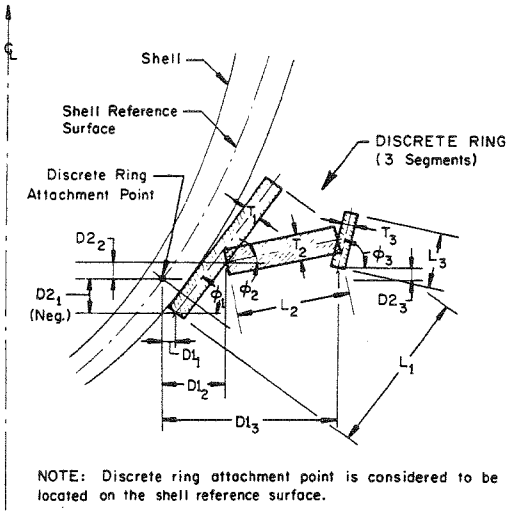

FIG. 34 DISCRETE RING AS MODELED IN THE BOSOR5 COMPUTER PROGRAM (FROM BUSHNELL [22])

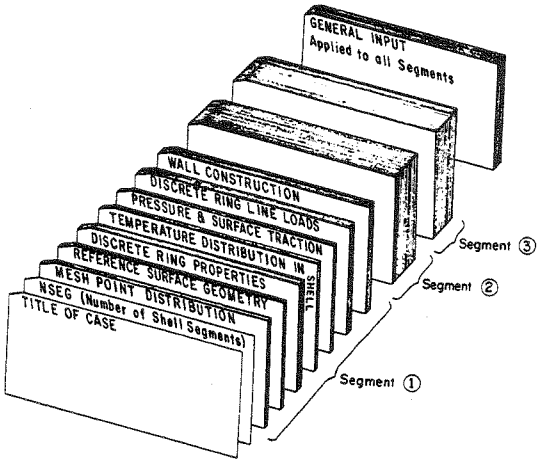

FIG. 35 BOSOR5 INPUT DECK (FROM BUSHNELL [22])

BASIS ASSUMPTIONS

The analysis summarized here and the results presented in the next section are based on the following assumptions and approximations:

1. Thin-shell theory holds; i.e., normals to the undeformed surface remain normal and undeformed. Transverse shear deformation is neglected.
2. The structure is axisymmetric and prebuckling deformations are axisymmetric.
3. The axisymmetric prebuckling deflections in the nonlinear theory, while considered finite, are moderate: The square of the meridional rotation can be neglected compared with unity.

4. A typical cross-section dimension of a discrete ring stiffener is small compared with the radius of the ring.

5. The cross-sections of the discrete rings remain undeformed as the structure deforms, and the rotation about the ring centroid is equal to the rotation of the shell meridian at the attachment point of the ring.

6. If meridional stiffeners are present, they are numerous enough to include in the analysis by an averaging or "smearing" of their properties over any parallel circle of the shell structure.

7. The shell is thin enough to allow neglect of terms of order t/R compared to unity, where t is a typical thickness and R is a typical radius of curvature.

8. In the integrated constitutive law [C in Eq. (42)] coupling between normal stress resultants and shearing and twisting motions is neglected.

TWO ANALYSIS PHASES: AXISYMMETRIC PREBUCKLING AND NONSYMMETRIC BIFURCATION BUCKLING

Shell-of-revolution codes for plastic buckling represent implementation of two distinct analyses:

1. A nonlinear stress analysis for axisymmetric behavior of axisymmetric shell systems (including large deflections, elastic-plastic material behavior, and creep).

2. An eigenvalue analysis in which the eigenvalues represent bifurcation buckling loads of axisymmetric shell systems subjected to axisymmetric loads, and eigenvectors represent axisymmetric or nonsymmetric buckling modes.

The efficiency of computer codes for shells of revolution derives from the fact that for the two types of analysis just listed the independent variables can be separated and an analytically two-dimensional problem thus reduced to a numerically one-dimensional model. Such a model leads to compact, narrowly banded stiffness, load-geometric, and mass matrices.

For example, the independent variables of the BOSOR5 analysis [22] are the arc length s measured along the shell reference surface and the circumferential coordinate θ. The dependent variables are the displacement components u, v and w of the shell wall reference surface, which can be expressed in the form

$$
\begin{aligned}
u(s,\theta) &= u_o(s) + \sum_{n=n_{\min}}^{n_{\max}} u_n(s)\sin n\theta \\
v(s,\theta) &= \sum_n v_n(s)\cos n\theta \\
w(s,\theta) &= w_o(s) + \sum_n w_n(s)\sin n\theta
\end{aligned}
\qquad (46)
$$

Nonlinear Prebuckling Stress Analysis

In the nonlinear prebuckling phase only the axisymmetric displacement components $u_o(s)$ and $w_o(s)$ in Eq. (46) are nonzero. Terms linear through quartic appear in the total prebuckling energy functional. This energy functional, originally an integro-differential form, is converted into an algebraic form by appropriate discretization and numerical integration over the meridional coordinate. The simultaneous nonlinear algebraic equations obtained by minimization of the algebraic form with respect to nodal point displacement components u_{oi} and w_{oi} and Lagrange multipliers λ_i are solved as described later.

Results from the nonlinear axisymmetric stress analysis are used in the eigenvalue analyses for plastic bifurcation buckling. The prebuckling meridional and circumferential stress resultants N_{10} and N_{20} and the meridional rotation β_0 appear as known variable coefficients in the energy expression which governs plastic bifurcation buckling.

Plastic Bifurcation Buckling

In the bifurcation buckling analysis the symmetric and nonsymmetric displacement components contained in the summations indicated in Eq. (46) are considered to be infinitesimal, kinematically admissible variations of displacements from the "prebuckled" state $u_o(s)$, $w_o(s)$ obtained from the nonlinear stress analysis. Since the buckling displacements u_n, v_n, and w_n are infinitesimal, one need only retain linear terms in u_n, v_n, and w_n in the kinematic relations and constraint conditions.

Hence the energy functional governing bifurcation buckling becomes a homogeneous quadratic form in nodal point displacement components u_{ni}, v_{ni}, w_{ni}, and Lagrange multipliers λ_{ni}. The values of the load parameter (eigenvalues) which render the quadratic form stationary with respect to u_{ni}, v_{ni}, w_{ni}, λ_{ni} represent buckling loads, and the normalized eigenvectors represent buckling modes. The minimum critical load as a function of circumferential wave number n is found by means of a strategy to be described later.

Prebuckling Solution Strategy — A Double Iteration Loop

The prebuckling iteration strategy used in BOSOR5 is as follows. At each load level or time step there are two nested iteration loops. In the inner loop the set of simultaneous nonlinear algebraic equilibrium equations with given fixed material properties and plastic creep strains is solved. This is the "Newton-Raphson loop". In the outer loop the strain-dependent material properties, the constitutive matrix (C), the meridional and circumferential plastic strain components ϵ_1^p, ϵ_2^p, and creep strain components ϵ_1^c, ϵ_2^c, are calculated. Double iterations at a given load level continue until the displacements no longer change. In this way the favorable convergence property of the Newton-Raphson procedure is preserved, equilibrium is satisfied within the degree of approximation inherent in a discrete model, and the flow law of the material is satisfied at every point in the structure. This strategy is illustrated in the flow chart shown in Figure 36.

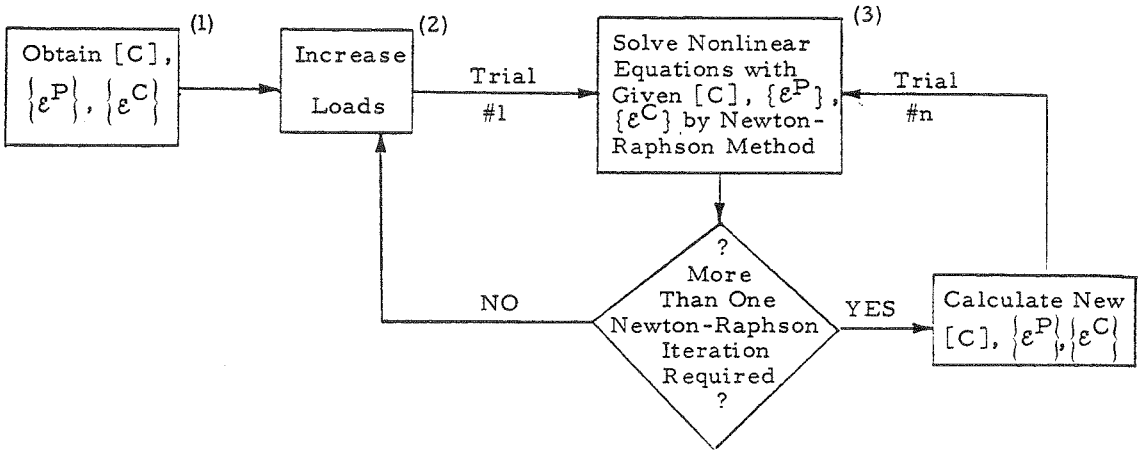

FIG. 36 FLOW CHART OF THE DOUBLE ITERATION LOOP USED IN BOSOR5 FOR PROBLEMS IN WHICH BOTH MATERIAL AND GEOMETRICAL NONLINEARITIES EXIST

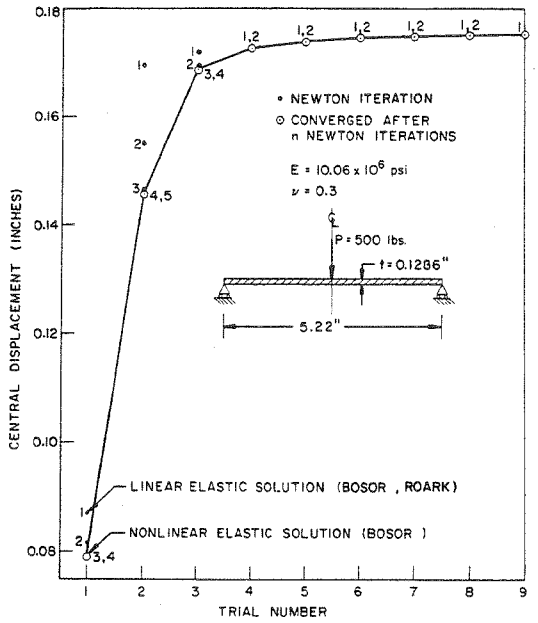

FIG. 37 CONVERGENCE OF MAXIMUM DISPLACEMENT IN THE PLATE FOR A VERY LARGE LOAD INCREMENT, 500 lb (FROM BUSHNELL [196])

Figure 37 shows the convergence with trial number of the central normal displacement of a centrally loaded elastic-plastic flat circular plate. (A "trial" is defined in Fig. 36.) In this case a very large load increment, $\Delta P = 500$ lb, is used in order to better illustrate the double-loop iteration process. Nine trials are required in order to achieve convergence of the displacement distribution within a tolerance of 0.1 percent. The first Newton-Raphson iteration on the first trial yields the linear elastic solution. This BOSOR5 solution (w_{max} = 0.08718 in.) agrees with the formula tabulated in Roark [234] (w_{max} =0.08703 in.). Throughout the first trial the material is treated as elastic, since this is the first load step and thus no previous history of plastic flow exists. Four Newton-Raphson iterations are required in this first trial for convergence to the nonlinear elastic solution. The solution vector thus obtained is used as input for the determination of how much plastic flow occurs, and a new solution is obtained after five Newton-Raphson iterations in Trial #2. Two Newton-Raphson iterations are required for convergence in each of trails four-eight, and a ninth trial is required to ensure that the change in material properties between Trial #8 and Trial #9 is so slight that it affects the displacement vector by less than 0.01 percent. The predicted maximum normal displacement is 0.17532 in.

THE SUBINCREMENTAL METHOD

In practically all nonlinear analyses the load is applied incrementally and the response is determined for each value of the load. Each load level involves the solution of a system of simultaneous algebraic equations, the rank of this system being equal to the number of degrees of freedom in the discretized mathematical model. Let us henceforth refer to this system of simultaneous equations as "System A". In most analyses in which material nonlinearity is included, the iteration loop for the solution of System A contains calculations for determination of the plastic strain components. Usually these quantities are obtained in a one-step process in which the total increments of strain accumulated from one load level

to the next are allocated among elastic, plastic, and possibly creep components. The relative magnitudes of the various components are known, at least as the load step begins, because the analysis contains a flow theory and the position of each material point in stress space is known from the converged results associated with the previous load level. The direction of plastic flow for each material point is generally considered to be constant for the entire load increment. For example, it may be assumed that this direction is parallel to the normal to the yield surface at a location in stress space determined by the converged result at the previous load level. Determination of the plastic strain components requires in the general three-dimensional case solution of a set of six simultaneous equations at each material point and in the case of axisymmetric deformations of thin shells of revolution the solution of two simultaneous equations at each material point. We shall henceforth refer to this small system of simultaneous equations as "System B".

The prebuckling analysis on which BOSOR5 is based differs from many other analyses in two respects. The calculation of the plastic and creep strain components is removed from the iteration loop in which System A is solved, and a subincremental approach is used for calculation of the plastic and creep strain components so that the direction of flow is permitted to change continuously within a single load interval.

The removal of the calculations involving plastic flow from the iteration loop for the solution of System A removes an objection pointed out by Tillerson *et al.* [54], to the use of the Newton-Raphson method for problems involving elastic-plastic material. They found that the "Newton-Raphson" procedure failed to converge if they used the tangent stiffness approach because of indications of alternative loading and unloading from iteration to iteration. Since the coefficients of their System A changed in a discontinuous manner in successive iterations, their strategy could not really be called a Newton method. In the BOSOR5 analysis the Newton-Raphson method is used with success.

In the subincremental process the total increments of strain accumulated from one load level to the next are divided into subincrements of a certain magnitude. For each subincrement the direction of plastic flow is considered to be constant, given by the normal to the yield surface at a location in stress space determined by the result at a previous subincrement. For each strain subincrement the stress subincrements are determined from the flow law and the given relationship between effective stress subincrement and effective plastic strain subincrement (the uniaxial stress-strain curve). Thus, the equation System B is solved for each subincrement and each material point.

The Need for the Subincremental Method

Why is the subincremental method needed? This question can perhaps be best answered with reference to the equations which form the simultaneous System B (creep neglected):

$$\{\Delta\epsilon\} = [D^{-1}]\{\Delta\sigma\} + \Delta\epsilon^{-p}\left\{\frac{\partial\bar{\sigma}}{\partial\sigma}\right\}_0 \qquad (47a)$$

$$= [D^{-1}]\{\Delta\sigma\} + \frac{E-E_T}{EE_T}\,\Delta\bar{\sigma}\left\{\frac{\partial\bar{\sigma}}{\partial\sigma}\right\}_0 \qquad (47b)$$

$$= [D^{-1}]\{\Delta\sigma\} + \frac{E-E_T}{EE_T}\,f(\Delta\sigma_{ij})\left\{\frac{\partial\bar{\sigma}}{\partial\sigma}\right\}_0 \qquad (47c)$$

in Eq. (47a-c) the left-hand side $\Delta\epsilon$ is the known vector of strain component increments; $\Delta\sigma$ is the unknown vector of stress component increments; $\Delta\bar{\epsilon}^p$ is the unknown effective plastic strain increment, which in Eq. (47b) is expressed in terms of the effective stress increment $\Delta\bar{\sigma}$ and in Eq. (47c) in terms of the effective stress component increments through the nonlinear "loading" function $f(\Delta\sigma_{ij})$. The vector $(\partial\bar{\sigma}/\partial\sigma)_0$ represents the components of a unit normal to the yield surface at a point in stress space fixed by the stress components σ_0 calculated at the previous load level at which a converged solution has been obtained. The nonlinear System B can in principle be solved for the stress component increments $\Delta\sigma_{ij}$. However, it often happens, especially at stress concentrations where $\Delta\epsilon_{ij}$ is relatively large, that System B does not have a solution. Figure 38 demonstrates what happens. A sequence of values of $\Delta\bar{\epsilon}^p$ can be tried in Eq. (47a) to generate the solid curve in Fig. 38(a). The dashed curve is the stress-strain curve. Ideally, the value of $\Delta\bar{\epsilon}^p$ which satisfies all of the conditions is computed as one of the intersections of the two curves. Indeed, solutions can be obtained in this manner as long as the effective strain increment is less than about 0.1 percent. For larger strain increments, however, the result shown in Fig. 38(b) is common. The subincremental method prevents this anomaly.

Another problem in calculating $\Delta\sigma_{ij}$ from Eqs. (47) arises from the fact that the tangent modulus E_T is a nonlinear function of $\bar{\epsilon}^p$ or $\bar{\sigma}$. In the BOSOR5 analysis the actual stress-strain curve is replaced by a series of straight line segments. As the load is increased from one level to the next, E_T changes in a discontinuous way that is not possible to express in a simple

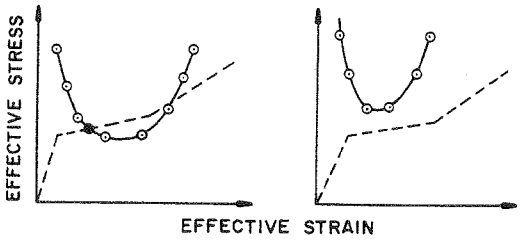

FIG. 38 SCHEMATIC REPRESENTATION OF THE SOLUTION OF EQS. (47) WITHOUT USE OF THE SUBINCREMENTAL METHOD (FROM BUSHNELL [196])

functional form. It is necessary to divide the increment such that at every material point E_T is constant within any subincrement.

Paths in Strain Space and Stress Space

The subincremental method is especially advantageous when applied to problems in which the paths followed by material points have less curvature in strain space than in stress space, which is usually the case for thin shells stressed beyond the proportional limit.

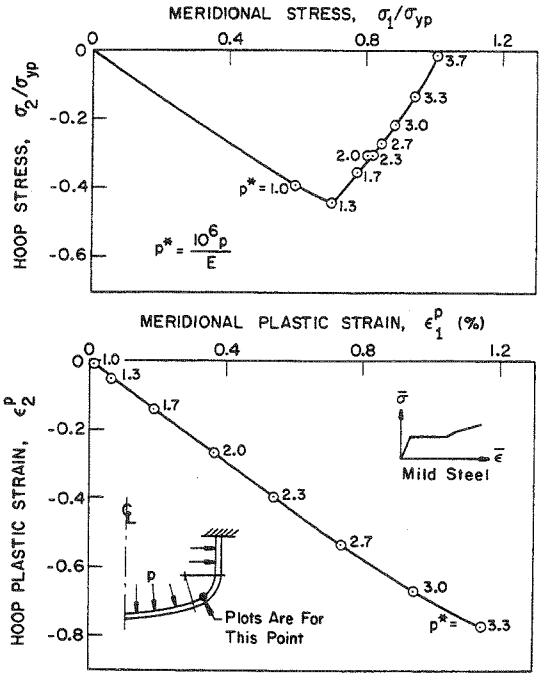

FIG. 39 PATHS FOLLOWED IN STRESS SPACE AND STRAIN SPACE BY A MATERIAL POINT IN AN INTERNALLY PRESSURIZED TORISPHERICAL VESSEL HEAD OF MILD STEEL (FROM BUSHNELL [196])

Figures 39 and 40 illustrate this behavior. Figure 39 shows the paths in strain and stress space followed by the point for which the effective strain is maximum in an internally pressurized mild steel torispherical pressure head. Whereas the straining of the material is nearly proportional throughout the range of pressure, the loading of the material is approximately proportional only until the effective stress reaches the yield stress, after which the path in stress space follows the yield surface in a counterclock-wise direction. A similar phenomenon occurs for a centrally loaded flat plate, results for which are shown in Fig. 40. Here the path in strain space is more curved because of the direction of loading and certain peculiarities of

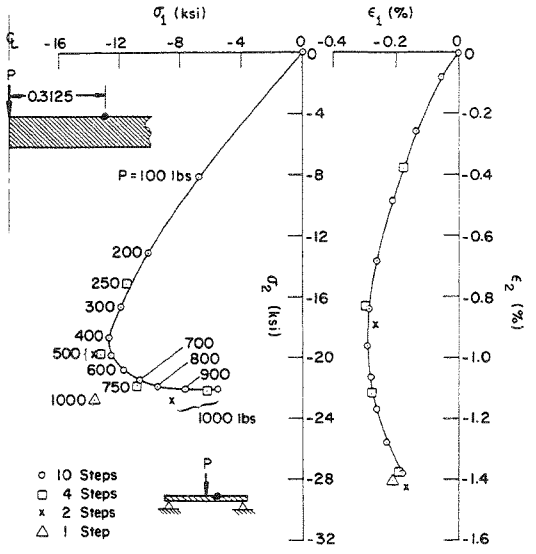

FIG. 40 PATHS FOLLOWED IN STRESS SPACE AND STRAIN SPACE BY A MATERIAL POINT IN A CIRCULAR FLAT PLATE WITH A CONCENTRATED LOAD, P (FROM BUSHNELL [196])

the geometrically nonlinear behavior. Still the curvature of this path is not as great as that of the path in stress space. The subincremental method is especially suitable for problems such as these because of the non-proportional loading of the material. If the subincremental method had not been used, many more load steps would have been required to avoid the aforementioned difficulties associated with the solution of Eqs. (47).

Fewer Load Steps Needed

A basic advantage of the subincremental method, then, is that it allows the use of much larger load increments than would otherwise be possible. The magnitude of the subincrement can be determined such that in Eqs. (47a-c) E_T is constant within a subincrement and the nonlinear function $f(\Delta\sigma_{ij})$, now $f(d\sigma_{ij})$, where "d" indicates "subincrement", can be linearized. Furthermore, if the material creeps, the magnitude of each subincrement can be established such that the change in effective stress during a subincrement is less than a certain preset percentage of the current effective stress. This criterion is important because the creep law used in BOSOR5 is derived from tests in which the stress is held constant.

Trade-Off in Computer Time

There is a trade-off in the use of the subincremental method. Fewer load steps need to be taken to cover a given load range, which generally means that the often large simulta-

neous equation System A must be solved fewer times than would otherwise be the case. On the other hand, incremental stress components and plastic and creep strain components must be calculated for each subincrement. Therefore, relatively more computer time must be used for determination of the behavior of the material. A great advantage of the subincremental method is that it makes the elastic-plastic analysis more reliable. The maximum size of a subincrement is preset. Therefore, more subincrements will automatically be used for material points corresponding to stress concentrations. In this way the errors incurred by linearization of Eqs. (47a-c) and by changes in the direction of plastic flow within an increment are made less severe. Details including creep effects are included in Ref. [196].

STRATEGY USED IN BOSOR5 TO FIND MINIMUM PLASTIC BIFURCATION BUCKLING LOADS

The BOSOR5 user chooses a range of circumferential wave numbers, n_{min} to n_{max}, and a starting wave number n_o which he feels corresponds to the minimum bifurcation load. He also chooses appropriate quasi-static functions of time for the loading. (Distributed loads, line loads, and temperature may all vary differently with time.) The user chooses a time range and time increments such that whatever load range and load increments he is interested in will result. For example, if the user wants to determine the buckling pressure of a shell with some spatial temperature distribution which does not change with time, he provides two time functions for the loading: a constant for the temperature function and a time-linearly-varying pressure coefficient. The actual temperature and pressure are products of the appropriate time functions and spatial distributions. This strategy is essential for problems involving creep and not difficult to get used to in other problems.

Given this input, BOSOR5 calculates the determinant of the global stability matrix. This determinant is calculated for each time increment until it changes sign or until the specified time range is covered. During this phase of the calculations the circumferential wave number is held constant at n_o.

If the determinant changes sign BOSOR5 sets up, for values of n within the specified range n_{min} to n_{max}, eigenvalue problems of the type

$$(K_{1n} + \lambda_n K_{2n}) \quad (q_n) = 0 \tag{48}$$

The quantity (K_{1n}) represents the stiffness matrix corresponding to n circumferential waves for the structure as loaded at the time step just before the determinant corresponding to $n = n_o$ changes sign. (K_{2n}) is the load-geometric matrix, which is derived from the terms

$$(R)^T (N_o) (R) + (U)^T (P) (U) \tag{49}$$

for the shell plus analogous discrete ring terms. In expression (49), N_o and P represent the increments of prebuckling stress resultants and pressure from the time step just before the determinant sign change to the next time step. Quantities R and U represent transformations from shell wall rotation and displacement components to nodal point degrees of freedom.

In solving Eq. (48) for λ_n, one is not as interested in the actual values of the eigenvalues λ_n as in finding the minimum λ_n with varying number of circumferential waves, n. The actual values of λ_n cannot generally be used to obtain the buckling load, that is

$$N_{cr} \neq N_{of} + \lambda_n N_o \tag{50}$$

because the elastic-plastic tangent stiffness often changes precipitously with increasing load in the neighborhood of the bifurcation point.

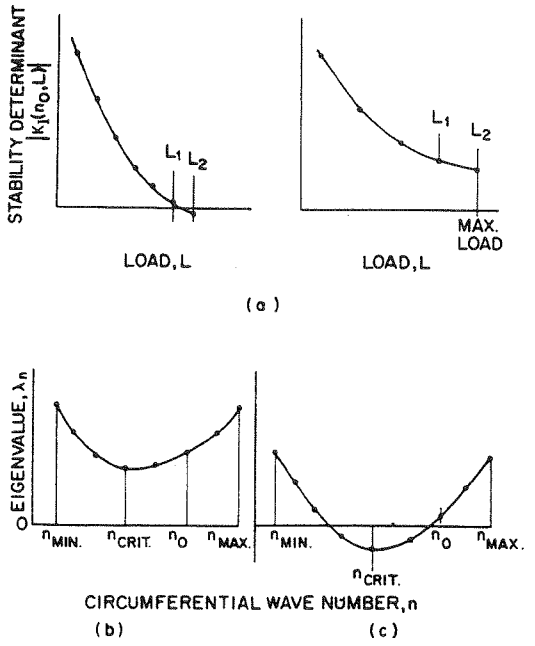

FIG. 41 (A) STABILITY DETERMINANT AT $n = n_o$ AS FUNCTION OF LOAD L; (B), (C) EIGENVALUES AS FUNCTION OF NUMBER OF CIRCUMFERENTIAL WAVES, n (FROM LAGAE AND BUSHNELL [229])

Figure 41 shows graphically the search for a minimum bifurcation buckling load. For the initially chosen wave number n_o the stability determinant $|K_1 (n_o, L)|$ is calculated for each load increment, as shown in Figure 41 (a). The load, L, is increased until one or more eigenvalues are detected between two sequential load steps or until the maximum allowable user-specified load has been reached.

Under normal circumstances, at this point in the calculations a series of eigenvalue problems of the form (48) is set up and solved, where:

$K_1(n)$ = the stiffness matrix corresponding to n circumferential waves of the structure as loaded by L_1 (See following definitions and Fig. 41)

$K_2(n)$ = the load-geometric matrix corresponding to the prestress increment resulting from the load increment $L_2 - L_1$

L_1 = the load state just before the sign change of the stability determinant, or the second-to-last load for which the prebuckling analysis converges

L_2 = the load state just after the sign change of the stability determinant, or the last load for which the prebuckling analysis converges

λ_n = the eigenvalue

q_n = the eigenvector

n = the number of circumferential waves lying in a range $n_{min} \leq n \leq n_{max}$, with n_{min} and n_{max} provided by the program user. Note that the initial guess n_o also lies in the range $n_{min} \leq n_o \leq n_{max}$, and corresponds, in the user's judgment, to the minimum bifurcation load.

BOSOR5 computes the eigenvalues λ_n and eigenvectors q_n for $n_{min} \leq n \leq m_{max}$ in wave number increments of n_{incr} (which is also supplied by the program user). Typical results are shown in Fig 41(b) and 41(c).

If the precritical behavior is nonlinear, the tangential stiffness varies with the load. An eigenvalue analysis will therefore yield a rigorous solution to the bifurcation problem only if the tangential stiffness happens to be evaluated at the bifurcation buckling load, i.e., if the computed eigenvalue is zero. If the material were elastic and if geometric nonlinearity were mild, the buckling load would be very nearly

$$L_{cr} = L_1 + \lambda_{n_{crit}}(L_2 - L_1) \qquad (51)$$

However, especially because of the nonlinearity of the material, the tangent modulus of which often changes very steeply for stresses above the proportional limit, the eigenvalue $\lambda_{n_{crit}}$ cannot be used to calculate L_{cr} as in Eq. (51) if plastic flow occurs before L_2. In problems involving plastic buckling, the purpose of the series of eigenvalue problems is to find the critical circumferential wave number, n_{crit}, and to obtain buckling mode shapes. If the situation shown in Fig. 41 (b) exists, then it is known that $L_1 \leq L_{cr} \leq L_2$, at least for $n_{min} \leq n \leq n_{max}$. (It may be necessary in some cases to explore another range of n to obtain a global minimum L_{cr}.) If the λ_n follow the pattern shown in Fig. 41(c), then it is known only that $L_{cr} < L_1$. It is necessary in this latter case to generate another series of values of the stability determinant $|K_1\ (n, L)|$ as in Fig. 41 (a), this time with $n=n_{crit}$ instead of $n=n_o$. The BOSOR5 program automatically performs this additional calculation and the bifurcation buckling load is identified as being in the load interval $L_1 \leq L \leq L_2$ for which $|K_1\ (n_{crit}, L)|$ first vanishes. If the analyst needs a sharper definition of L_{cr}, he may restart the case with the initial load L_1, the initial wave number n_{crit} and a smaller load increment.

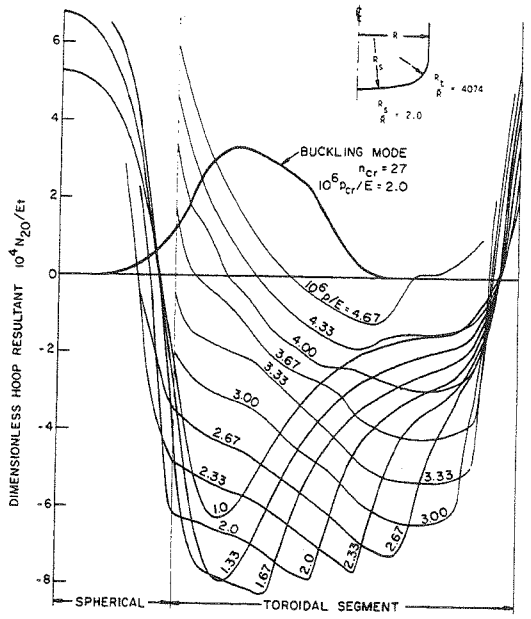

FIG. 42 PREDICTED BUCKLING MODE AND HOOP STRESS RESULTANT DISTRIBUTIONS AS FUNCTIONS OF PRESSURE FOR GALLETLY'S MILD STEEL SPECIMEN MS3 (FROM BUSHNELL AND GALLETLY [231])

The strategy just described works well if the destabilizing prebuckling stress resultants vary monotonically with increasing load. However, there are important cases, such as internally pressurized torispherical and ellipsoidal pressure vessel heads, which often exhibit more complex behavior. For example, Fig. 42 shows that the peak compressive circumferential stress resultant N_{20} in the toroidal knuckle region of a mild steel vessel head initially increases with increasing pressure. Shortly after yielding $|N_{20}|$ begins to decrease and it continues to decrease as the pressure is further increased. In this case bifurcation buckling occurs at a pressure for which the plastic region is spreading but the destabilizing hoop resultant $|N_{20}|$ is decreasing. The strategy described in the previous paragraph will yield erroneous values for n_{crit} if this situation exists. This problem is solved by calculation of $K_2\ (n)$ from L_2 alone, rather than from the difference $L_2 - L_1$. (Notice, however, that this change in strategy is not appropriate for cases involving a combination of loads, some of which are eigenvalue parameters and others of which are not).

The program user may select either the incremental flow theory or the deformation theory as a basis for calculating the stability determinant. These two options were programmed for BOSOR5 because buckling loads obtained with use of deformation theory are often in better agreement with test results than are those obtained with use of flow theory. As implied earlier, the reasons for this anomaly are not yet well understood, but it is clear that the post-yield biaxial hardening and flow laws are involved. Sewell [225] suggests that the discrepancy is due to the formation of a corner on the loading surface.

EXAMPLES OF PLASTIC BUCKLING OF VARIOUS SHELLS OF REVOLUTION

The purpose of this section is to convey to the reader a physical appreciation of plastic buckling. Many examples with comparisons between results of test and theory are presented for axially compressed monocoque cylinders, externally pressurized ring-stiffened cylinders, and externally and internally pressurized shells of more complex shape. The effects on plastic buckling of creep and of fabrication processes such as welding and cold rolling are briefly examined. The conclusion gained by these numerous comparisons between test and theory, in which agreement is generally good, is that buckling loads for shells that fail plastically are not very sensitive to initial imperfections.

AXIALLY COMPRESSED MONOCOQUE CYLINDERS

Tests have been conducted on cylinders by Lee [235], Batterman [236], Sobel and Newman [237], and others referenced in Sewell's survey [4]. Tests on truncated cylinder-like (steep) conical shells have recently been conducted by Ramsey [238]. In all the tests, end displacement was controlled. End effects are ignored in early analyses of plastic buckling of axially compressed cylinders. Batterman [236] uses flow theory and Gerard [239] uses deformation theory. Murphy and Lee [240] were the first to include the effect of radial end restraint on plastic buckling load predictions. Their predictions are shown in Figs. 43 and 44, with the results of Batterman [236], Gerard [239], and Bushnell [22] superposed in Fig. 44. End effects are accounted for in the analyses of Bushnell [22], who used the BOSOR5 computer program, and Sobel and Newman [237], who used STAGSC [207]. All of the studies in which end effects are included are based on incremental flow theory and all predict that the limit load occurs before bifurcation, as shown in Fig. 1. The comparisons between BOSOR5 predictions and Lee's tests [235] are listed in Table 5 and between BOSOR5 predictions and Batterman's tests [236] are listed in Table 6.

Two important conclusions can be drawn from the results presented in Figs. 43 and 44 and Tables 5 and 6:

1. the inclusion of end radial restraint essentially eliminates the discrepancy between test and theory, and reveals that, in the case of plastic buckling of axially compressed cylinders tested in the usual way, it is not necessary to resort to the use of a bifurcation buckling analysis with deformation theory or flow theory with a singularity in the loading surface in order to bring test and theory into agreement.

2. Fairly thick metallic cylinders ($R/t < 90$) are not very sensitive to initial random imperfections if they buckle at stresses above the material proportional limit. The axisymmetric bulge which develops near an end, so evident in Fig. 1 and in Murphy and Lee's prediction shown in Fig. 43, represents a predictable "imperfection" that grows with load and is much more significant than any unknown imperfections due to fabrication or handling errors.

Gellin [241] shows that collapse loads of axially compressed cylinders buckling in the plastic range are not as sensitive to initial axisymmetric imperfections as are collapse loads of elastic cylinders. (Hutchinson [7] demonstrates the same result for externally pressurized spherical shells, as shown in Fig. 9.)

TABLE 5 COMPARISON OF TEST AND THEORY FOR AXIALLY COMPRESSED CYLINDERS

Model	R/t	Test [Lee (1962)] Load (lb)	BOSOR5 Prediction*	Highest Test / BOSOR5	Lowest Test / BOSOR5
A300	46.1	5,400	5,202	1.038	—
A110		9,090	8,923	1.019	0.884
A210	29.2	8,680			
A310		7,890			
A120		14,500			
A220	19.4	14,840	14,328	1.036	1.005
A320		14,400			
A130		35,000			
A230	9.4	36,100	33,200	1.087	1.054
A330		36,000			

*Axisymmetric collapse predicted in all cases

TABLE 6 COMPARISON OF TEST AND THEORY FOR AXIALLY COMPRESSED CYLINDERS TESTED BY BATTERMAN (1965)

Model	R/t	Test Stress (psi)	BOSOR5 Prediction* (Clamped Edges)	Test / BOSOR5
9	116.61	31,770	44,643	0.712
8	114.56	33,030		
10	113.60	35,600	43,478	0.820
17	89.33	43,950		
26	85.95	43,690	45,063	0.970
16	56.52	51,380	52,282	0.983
25	54.93	50,640		
15	44.69	55,490		
24	44.19	53,380	55,663	0.959
4	26.61	58,200		
3	26.56	58,200		
2	26.44	57,100		
1	26.18	58,600		
5	25.94	59,570		
6	25.88	58,760	57,422	1.023
14	19.71	61,580	59,175	1.041
23	19.66	61,480		
13	14.02	64,110		
22	13.93	63,790	62,886	1.014
18	9.76	70,000		
19	9.76	69,320		
20	9.76	69,840	71,225	0.980
12	9.70	69,630		
27	9.70	69,230		

*Axisymmetric collapse predicted in all cases.

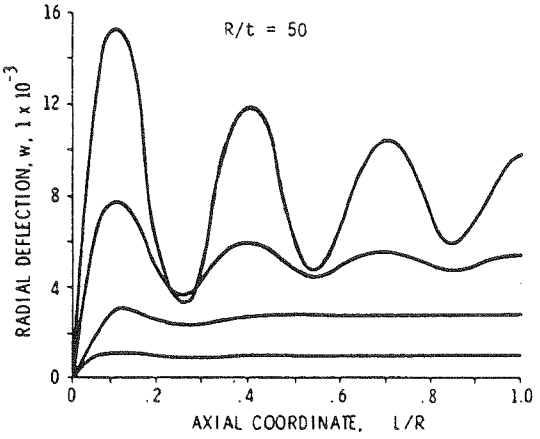

FIG. 43 RADIAL DEFLECTION PROFILES FOR CYLINDER UNDER INCREASING AXIAL LOAD (FROM MURPHY AND LEE [240])

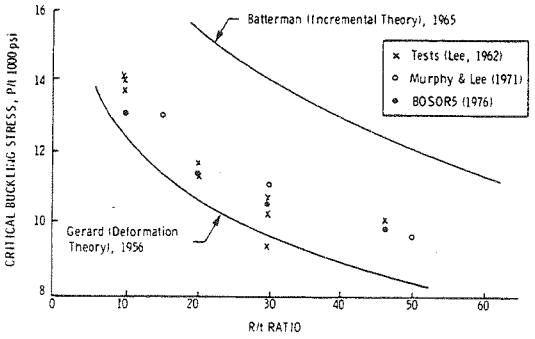

FIG. 44 COMPARISON OF TEST AND THEORY FOR PLASTIC BUCKLING OF AXIALLY COMPRESSED CYLINDERS (ADAPTED FROM MURPHY AND LEE [240])

This fact, the fact that the tangent modulus of most metals decreases by more than an order of magnitude within a stress range of 20 percent of the 0.2 percent yield stress, the fact that high quality cylinders with the relatively low radius-to-thickness ratios required for plastic buckling are easier to fabricate than those with high R/t, and the fact that significant predictable axisymmetric bulges due to radial end restraints grow as the load is increased, combine to reduce dramatically the deleterious effect of random unknown imperfections. We can therefore make fairly accurate predictions of collapse loads of axially compressed cylinders tested in the usual way. Note that this conclusion may not apply to cylinders in which the ends are locally tapered and other devices are introduced into a test to prevent failure due to bulging as shown in Figs. 1 and 43.

RING-STIFFENED CYLINDERS UNDER EXTERNAL HYDROSTATIC PRESSURE

Lee [243] calculated bifurcation buckling loads of elastic-plastic ring-stiffened cylinders with use of a Rayleigh-Ritz method. Others who have studied this problem are referenced in Sewell's survey [4]. In Ref. [228] are given comparisons between test and theory for 69 machined ring-stiffened aluminum cylinders tested by Boichot and Reynolds [242]. The geometry is given in Fig. 45. Dimensions of all the specimens are tabulated in Ref. [228].

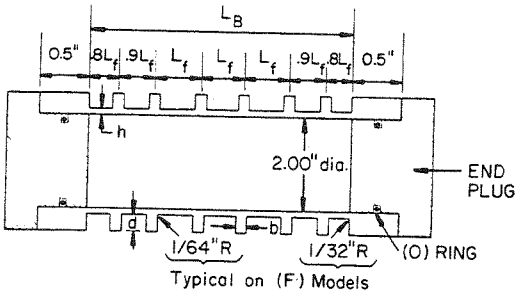

FIG. 45 ALUMINUM RING-STIFFENED CYLINDER TESTED UNDER EXTERNAL PRESSURE BY BOICHOT AND REYNOLDS AT THE NAVAL SHIP RESEARCH AND DEVELOPMENT CENTER, MARYLAND (FROM BUSHNELL [228])

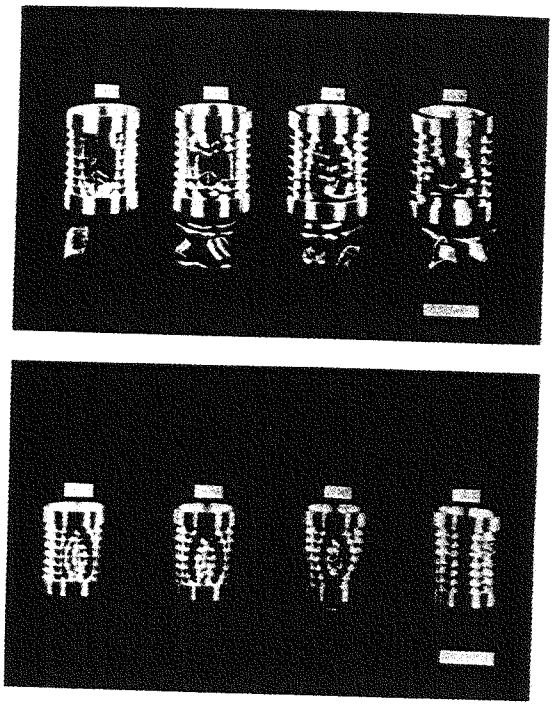

FIG. 46 SOME OF THE BUCKLED RING-STIFFENED ALUMINUM CYLINDERS TESTED UNDER HYDROSTATIC PRESSURE BY BOICHOT AND REYNOLDS (1965). TOP SPECIMENS WITHOUT FILLETS, WITH EVIDENCE OF FRACTURING; BOTTOM SPECIMENS OF SIMILAR GEOMETRY BUT WITH FILLETS (FROM BOICHOT AND REYNOLDS [242]).

Of the 69 test specimens, 24 (designated "F" in Fig. 45) had fillets near the boundaries and where the rings join the shell wall. From the photographs in [242] from which Fig. 46 is reproduced here, it appears that practically all of the specimens without fillets fractured during failure. However, it is not possible to determine from the test data alone whether fracture caused the failure or whether fracture occurred later as the shell was deforming in its buckling mode. On the other hand, there is almost no evidence of fracture occurring in the case of the 24 specimens with fillets. Therefore, it is reasonable to predict that better agreement between test and theory will be obtained for the specimens with fillets than for those without.

Furthermore, analytical predictions that are too high for the specimens without fillets would lead one to favor the hypothesis that failure was caused by fracture rather than buckling in these tests, since the analytical model (BOSOR5) is incapable of predicting fracture. This would be particularly true if the too high predictions correspond to the thicker specimens for which imperfections are less significant.

There are three different nominal radius/thickness ratios involved in the test series: $R/t \cong 12$, 20, and 50. Buckling pressures for the $R/t \cong 50$ specimens are somewhat sensitive to imperfections because buckling, especially of the models in this class with small ring stiffeners, occurs at average stresses that are barely in the plastic range. Indeed, the test results for the thinnest specimens exhibit the most scatter, as indicated in Fig. 47.

Figure 47 gives the comparison between test and theory. The generally upward sloping trend results primarily from the fact that the analytical model becomes increasingly conservative with increasing $b/\sqrt{(Rt)}$. The discrete rings are assumed to be attached to the shell at a single point with the shell free to bend in the axial direction in the immediate neighborhood of this point. The neglected effect on the shell meridional bending stiffness of the finite thicknesses of the rings leads often to predictions of axisymmetric collapse with relatively short axial wavelengths when the test specimens actually fail nonsymmetrically. The short-wavelength axisymmetric mode of failure is hindered by the increased local meridional bending stiffness afforded by the finite axial intersection lengths of shell and rings more than is the relatively long wavelength general instability mode of failure. Bushnell [228] includes modifications in the discretized BOSOR5 model to account for this

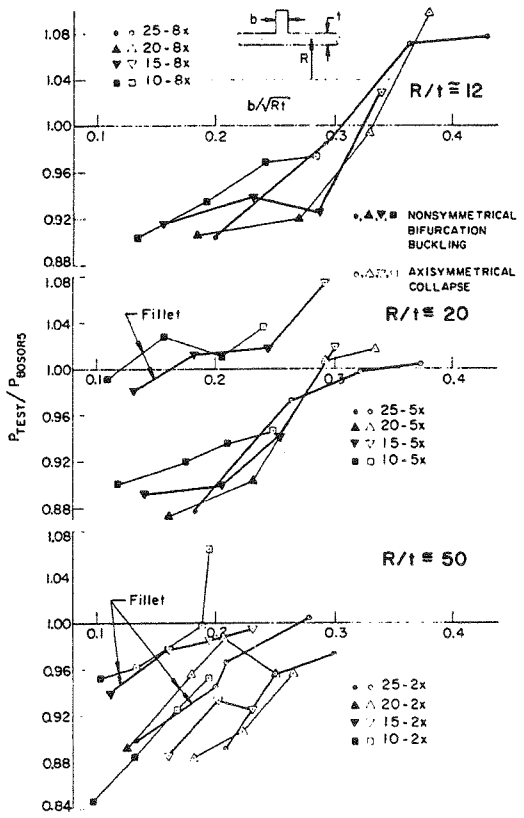

FIG. 47 COMPARISON OF TEST AND THEORY (BOSOR5) FOR BUCKLING OF EXTERNALLY PRESSURIZED RING-STIFFENED CYLINDERS PLOTTED AS FUNCTION OF RING THICKNESS PARAMETER $b/\sqrt{(Rt)}$ (FROM BUSHNELL [228])

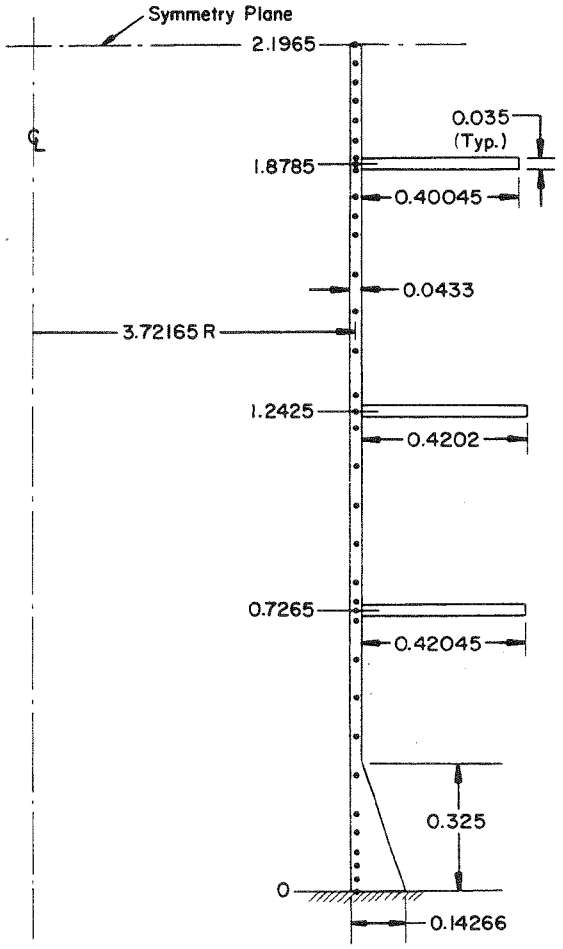

FIG. 48 RING-STIFFENED TITANIUM CYLINDER UNDER EXTERNAL HYDROSTATIC PRESSURE WITH NODAL POINTS USED IN THE BOSOR5 ANALYSIS INDICATED (FROM BUSHNELL [22])

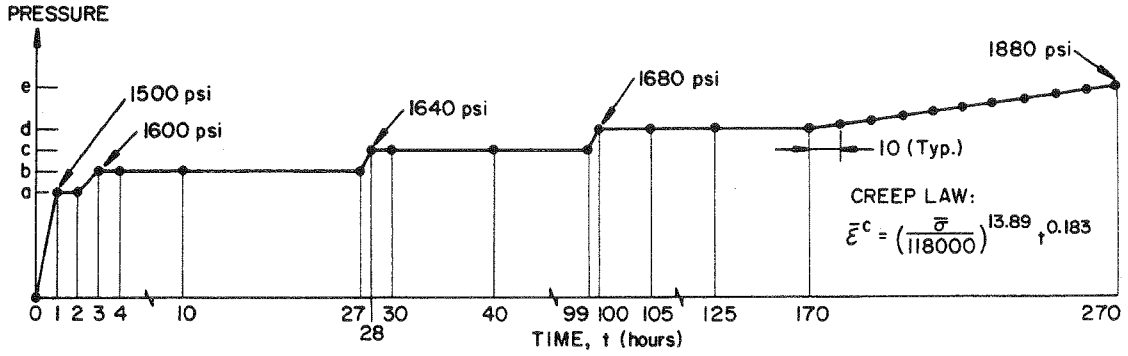

FIG. 49 LOADING SCHEDULE FOR RING-STIFFENED CYLINDER (FROM BUSHNELL [22])

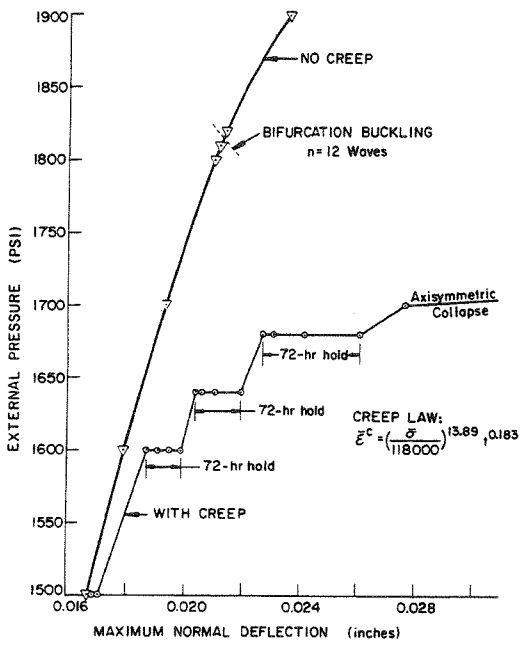

FIG. 50 LOAD-DEFLECTION CURVES FOR EXTERNALLY PRESSURIZED RING-STIFFENED CYLINDER WITH AND WITHOUT PRIMARY CREEP INCLUDED IN THE ANALYSIS (FROM BUSHNELL [22])

increased local meridional bending stiffness and thereby obtains agreement between test and theory for models with large $b/\sqrt{Rt}$.

ELASTIC-PLASTIC CREEP BUCKLING OF AN EXTERNALLY PRESSURIZED RING-STIFFENED TITANIUM CYLINDER

The BOSOR5 program [22] was used for the analysis, and the configuration and locations of nodal points in the discretized model are shown in Fig. 48. Symmetry conditions are applied at the symmetry plane. Figure 49 shows the loading schedule and gives the creep law. Solutions were obtained for each time indicated by a dot. Figure 50 gives load-deflection curves for computer runs in which the creep is neglected and

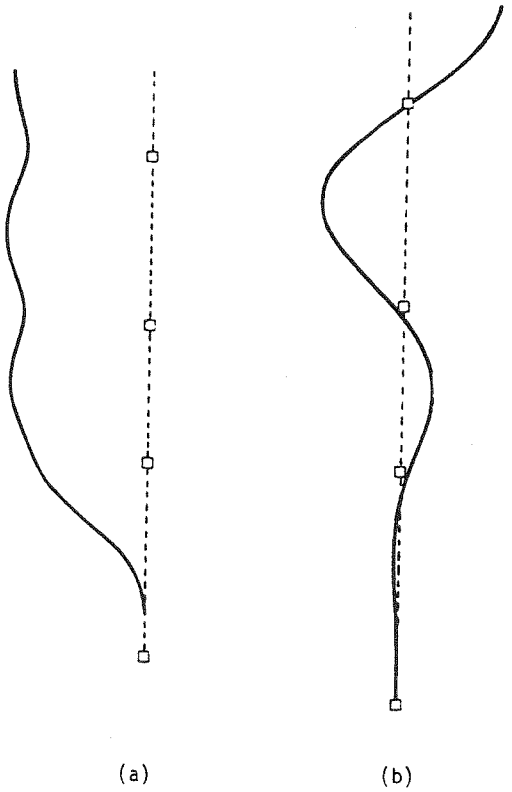

FIG. 51 (A) PREBUCKLING DEFLECTED SHAPE AND (B) (B) BIFURCATION BUCKLING MODE FOR RING-STIFFENED CYLINDER WITH CREEP NEGLECTED IN THE ANALYSIS (FROM BUSHNELL [22])

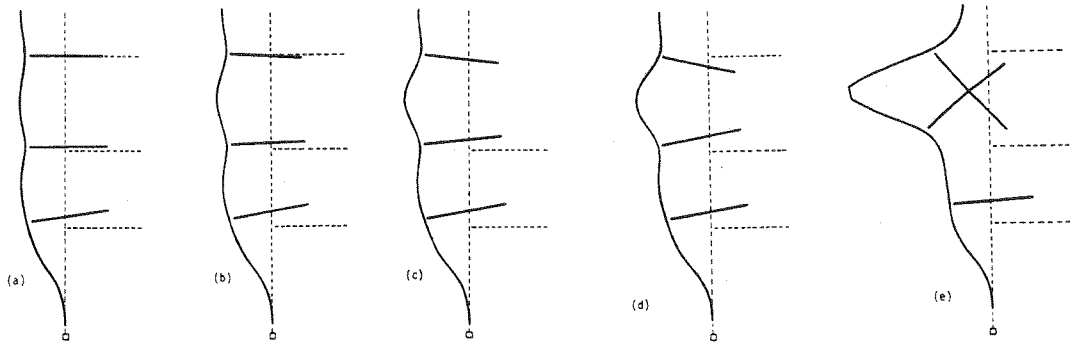

FIG. 52 AXISYMMETRIC COLLAPSE OF RING-STIFFENED CYLINDER WITH CREEP INCLUDED IN THE ANALYSIS (FROM BUSHNELL [22])

included. If creep is neglected the predicted failure mode is nonaxisymmetric bifurcation buckling with 12 circumferential waves at a pressure of about 1810 psi. The prebuckling deflected shape (exaggerated) and the bifurcation buckling mode are shown in Fig. 51. With creep included, the predicted failure mode is axisymmetric collapse at a pressure of about 1700 psi. The growth of the axisymmetric buckle is shown in Fig. 52.

SHELLS OF REVOLUTION WITH COMPLEX SHAPES UNDER EXTERNAL PRESSURE

During the past several years Galletly and his coworkers at the University of Liverpool have been performing tests on shells of revolution of various shapes under external and internal pressure. The method of testing and some BOSOR5 predictions are described in Ref. [227]. Some of these predictions are presented in Figs. 53-60.

Cone-Cylinder Combination

For the externally pressurized cone cylinder shells shown in Fig. 53 prebuckling plastic flow is confined to narrow axisymmetric bands including the junctures. Accordingly, the BOSOR5 model is set up as shown in Fig. 54, with the plasticity analysis being performed only in segments 2 and 3 in order to save computer time. Figure 55 gives the nonsymmetric bifurcation buckling pressures, mode shapes, and critical numbers of circumferential waves. In this case, the effect of plasticity is to produce a hinge at the juncture. (In an elastic analysis of these configurations the hinge would be introduced only in the stability equations, not in the prebuckling equations.) A buckled specimen is shown in Fig. 56.

Pierced Torispherical Head

For externally pressurized torispherical shells pierced by cylindrical nozzles, an example of which is shown in Fig. 57, prebuckling plastic flow is confined to a narrow axisymmetric band including the juncture between the cylindrical nozzle and spherical head. Some plastic flow also occurs near the juncture between the spherical and toroidal portions. Figure 58 shows the BOSOR5 model and predicted prebuckling deflected shape (exaggerated). The critical bifurcation pressures and mode shapes are given in Fig. 59. The buckling mode has one cir-

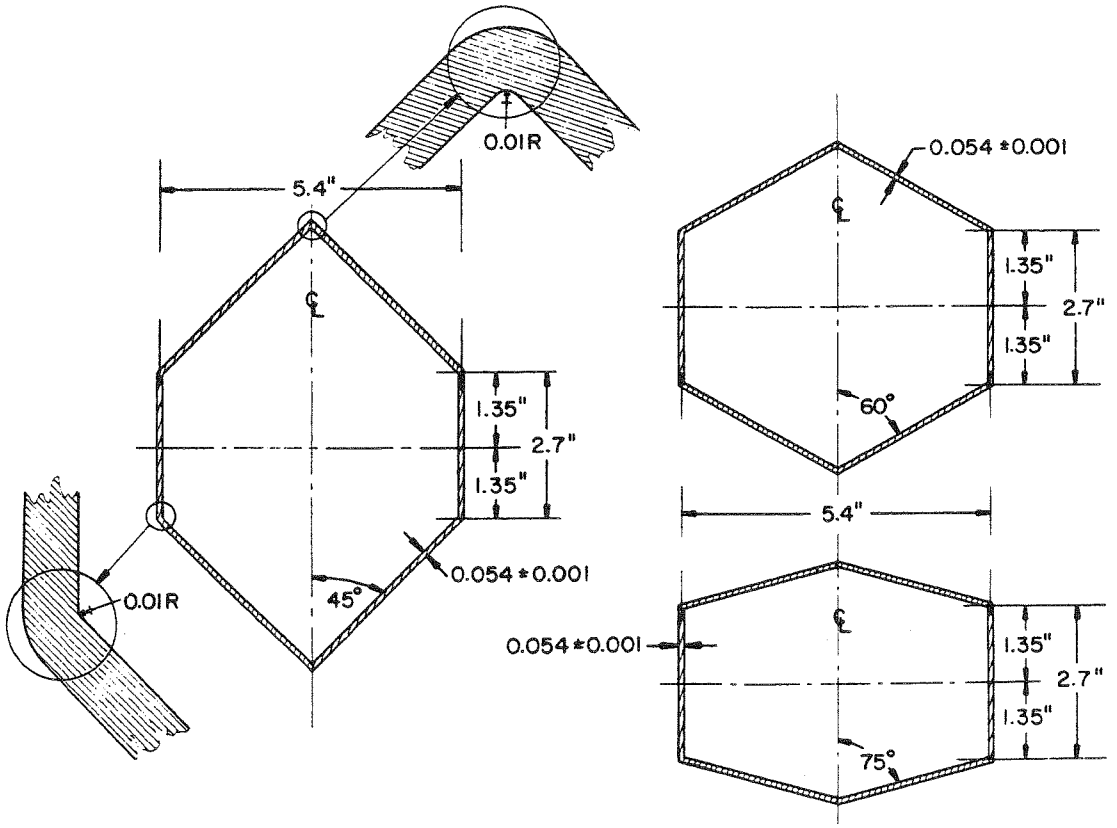

FIG. 53 ALUMINUM CONE-CYLINDER SPECIMENS TESTED UNDER EXTERNAL PRESSURE BY GALLETLY AT THE UNIVERSITY OF LIVERPOOL (FROM BUSHNELL AND GALLETLY [227])

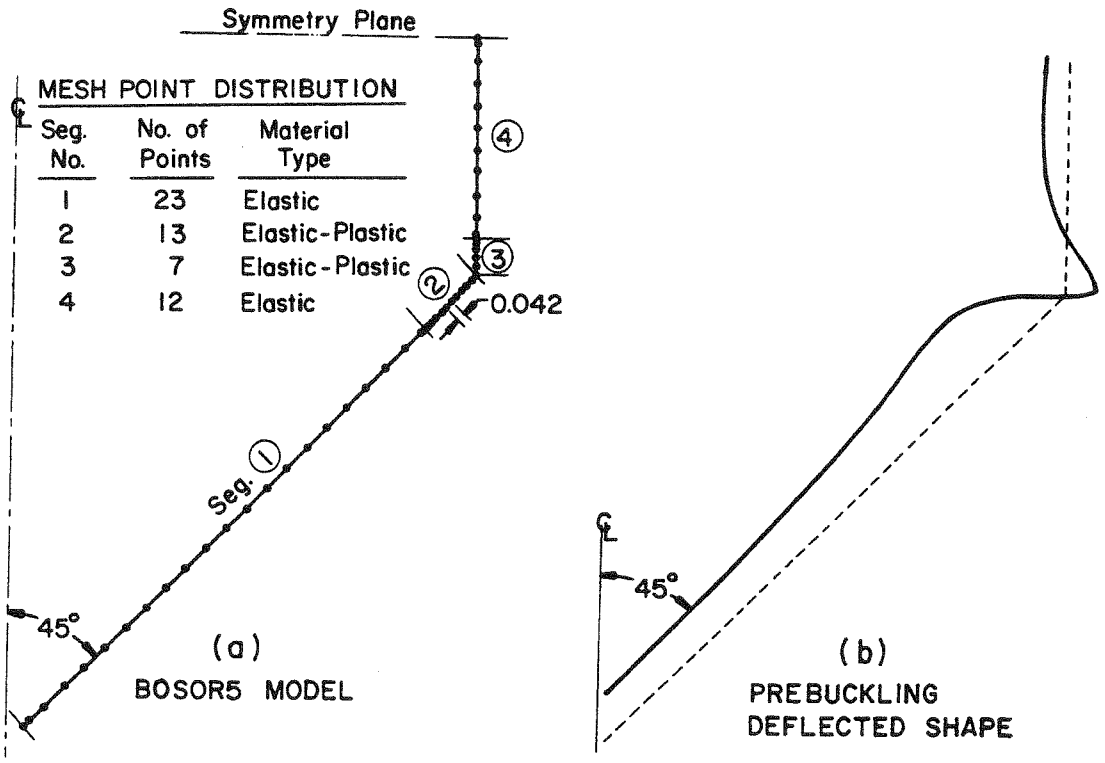

FIG. 54 DISCRETE MODEL OF THE 45 DEG. CONE-CYLINDER SPECIMEN AND EXAGGERATED VIEW OF THE PREBUCKLING DEFLECTED SHAPE AT THE BUCKLING PRESSURE (FROM BUSHNELL AND GALLETLY [227])

cumferential wave, that is, the normal displacement varies around the circumference as $\cos n\theta$ with $n = 1$. Tilting of the nozzle was also observed in the tests, as shown in Fig. 60.

More details of these tests and analysis are given in Ref. [227].

In the two classes of plastic buckling problems shown in Figs. 53-60 the prebuckling plasticity is confined to local axisymmetric stress concentrations near slope discontinuities between shell segments. It is shown in Ref. [227] that problems of this type can be solved fairly accurately with an elastic model in which the assumption is made, only in the stability part of the analysis, that a hinge exists between the two segments where the slope discontinuity occurs. This hinge cannot transmit any incremental buckling modal meridional moment resultants. The use of deformation theory rather than flow theory has a very slight effect on the predicted bifurcation loads. From the excellent agreement between experimental and theoretical results, it can be inferred that the critical elastic-plastic buckling pressures of these shells are not sensitive to initial imperfections.

ELASTIC-PLASTIC BUCKLING OF INTERNALLY PRESSURIZED TORISPHERICAL VESSEL HEADS

Summary of Past Work

Interest in internally pressurized torispherical heads was stimulated by the failure of a large fluid coker undergoing a hydrostatic proof test at Avon, California, in 1956. Galletly [244, 245] determined from an elastic, small-deflection analysis that the stresses exceeded the yield point of the material by considerable margins over substantial portions of the vessel. Galletly's work [244] stimulated Drucker and Shield [246, 247] to perform limit analyses of shells of revolution using simplified yield surfaces for a Tresca material. Other elastic-plastic analyses of torispherical shells were published by Gerdeen and Hutula [248], Crisp and Townley [249], and Simonen and Hunter [250]. Calladine [251] presented a novel analysis of the limit pressure of torispherical heads which gives results similar to those obtained by Shield and Drucker [247].

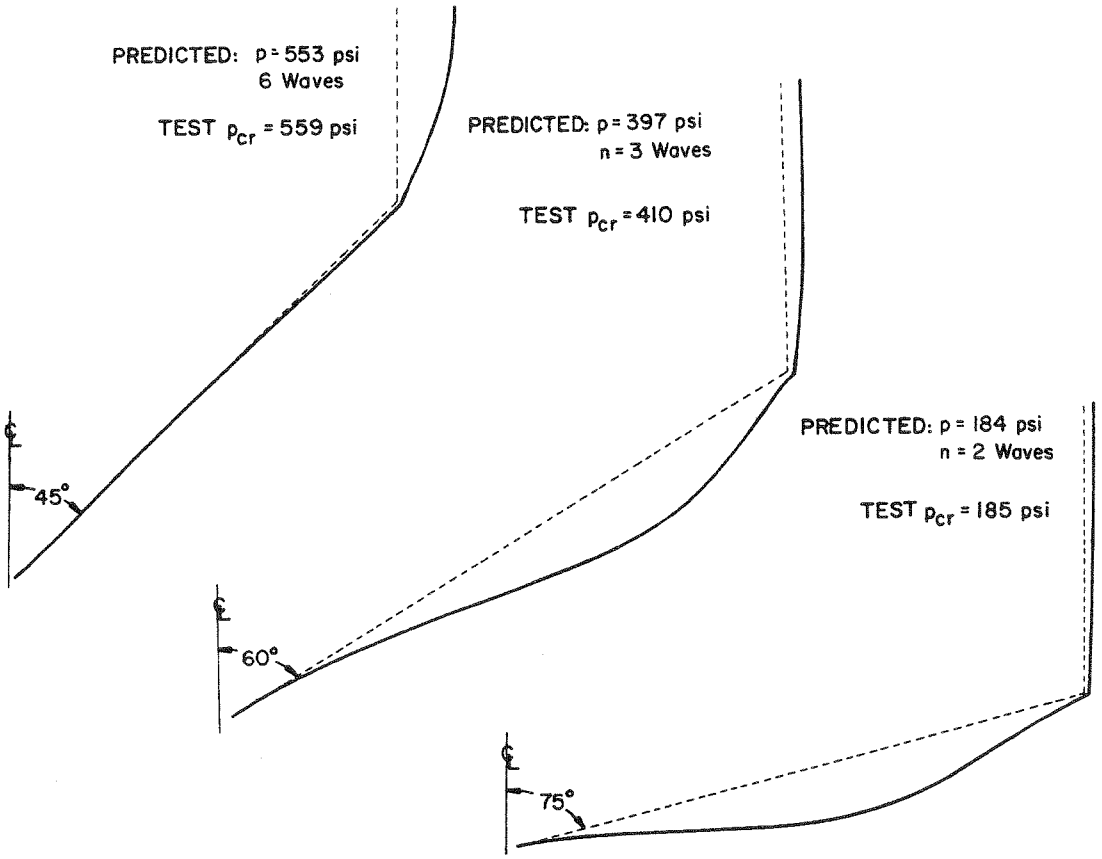

FIG. 55 BIFURCATION BUCKLING MODES AND COMPARISON WITH TEST RESULTS (FROM BUSHNELL AND GALLETLY [227])

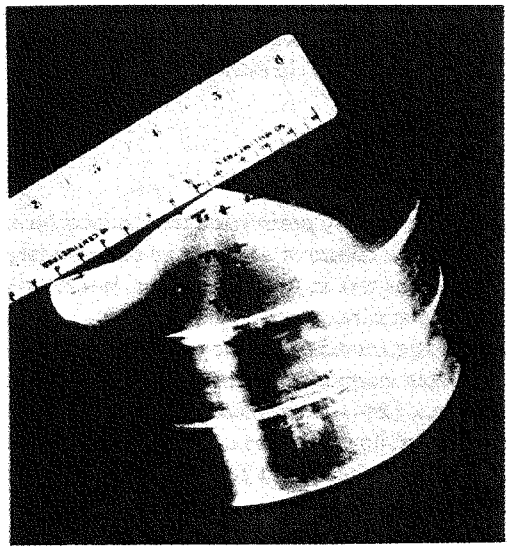

FIG. 56 75 DEG. SPECIMEN (COURTESY G. D. GALLETLY)

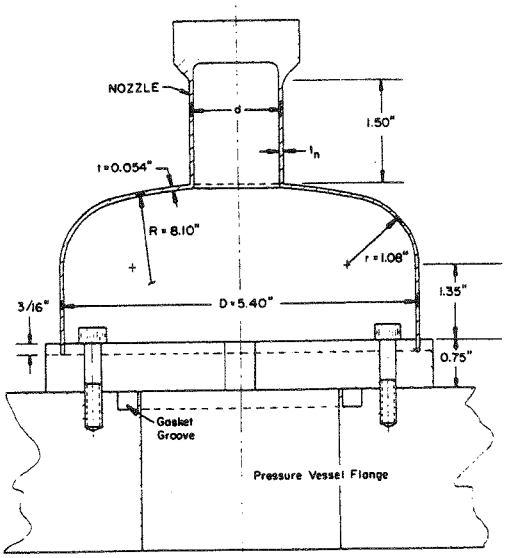

FIG. 57 ALUMINUM TORISPHERICAL HEAD WITH AXISYMMETRIC NOZZLE TESTED UNDER EXTERNAL PRESSURE BY GALLETLY AT THE UNIVERSITY OF LIVERPOOL (FROM BUSHNELL AND GALLETLY [227])

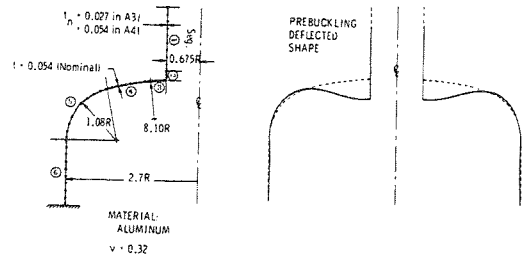

FIG. 58 DISCRETE MODEL OF ONE OF THE TORISPHERICAL SPECIMENS WITH EXAGGERATED VIEW OF THE PREBUCKLING DEFLECTED SHAPE AT THE BUCKLING PRESSURE (ADAPTED FROM BUSHNELL AND GALLETLY [227])

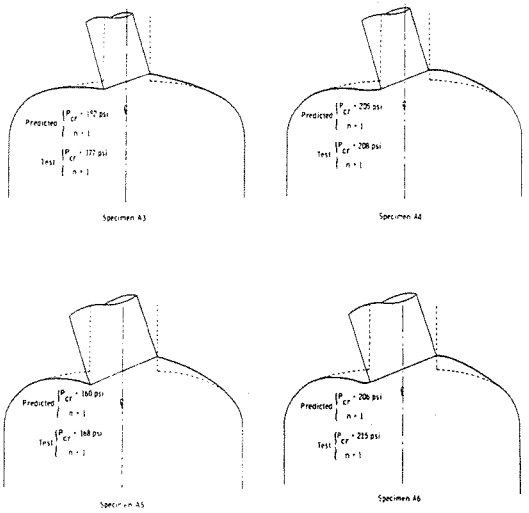

FIG. 59 BIFURCATION BUCKLING MODES AND COMPARISON WITH GALLETLY'S TEST RESULTS (ADOPTED FROM BUSHNELL AND GALLETLY [227])

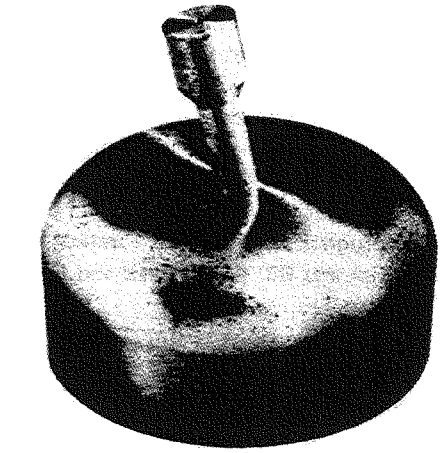

(a)

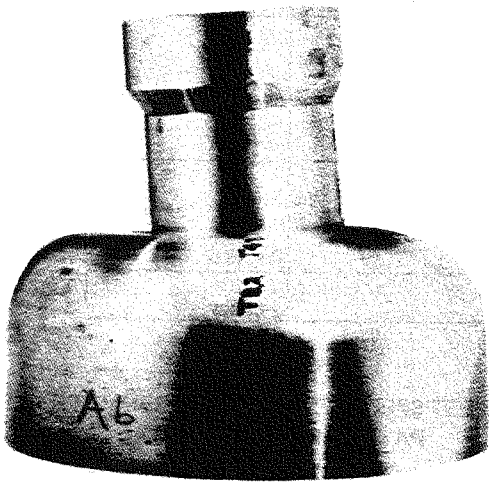

(b)

FIG. 60 GALLETLY'S BUCKLED SPECIMENS:
(A) SPECIMEN A3
(B) SPECIMEN A6
(COURTESY G. D. GALLETLY)

Savé [252] conducted a series of tests on torispherical, toriconical, and flat heads. Several papers on the elastic-plastic analysis of pressure vessel heads may be found in Ref. [253], including contributions by Gerdeen [254], Mescall [255], and Marcal [256]. Other references to work in this area are given by Esztergar [257].

The possibility of nonaxisymmetric buckling of internally pressurized torispherical heads was first predicted by Galletly [245]. Fino and Schneider [258] reported such buckling in a head designed according to the ASME Code, but at a pressure slightly below the design pressure. It is likely that the unexpectedly low buckling pressure resulted from nonaxisymmetric imperfections generated when spherical and toroidal gores were welded together to form the very large head. Mescall [259] was the first to present a solution of the nonaxisymmetric stability analysis. He used elastic small deflection theory. Adachi and Benicek [260] conducted a series of buckling tests on torispherical heads made of polyvinyl chloride (PVC), chosen primarily because of the high ratio of yield stress to Young's modulus, which ensures that buckling occurs before large scale yielding. The correlation of elastic analysis with these tests was much improved by inclusion of nonlinear geometric effects. Thurston and Holston [261] were the first to account for moderately large axisymmetric prebuckling meridional rotations in the stability analysis of these heads. Since publication of Ref. [261] many computer programs have been written which calculate nonsymmetric buckling loads of arbitrary elastic shells of revolution including geometric nonlinearity in the prebuckling analysis and prebuckling shape changes in the stability analysis [262-266].

Recently, several papers have appeared on nonsymmetric buckling of elastic-plastic pressure vessel heads: Brown and Kraus [267] calculated critical pressures for internally pressurized ellipsoidal heads with use of small deflection theory, Bushnell and Galletly [227] found buckling loads for externally pressurized torispherical heads pierced by nozzles and for conical heads with use of large deflection theory in the prebuckling analysis, and Bushnell and Galletly [231], Lagae and Bushnell [229], and Galletly [268, 269] used the BOSOR5 computer program to compare theoretical predictions with tests by Kirk and Gill [270], Patel and Gill [271], and Galletly [268, 269] for buckling of internally pressurized torispherical and ellipsoidal heads.

The work presented in Refs. [229-231] is summarized here. Figures 61-72 and Table 7 are from these sources.

Figure 61 shows the configuration of Kirk and Gill's [270] and Patel and Gill's [271] torispherical specimens, and Fig. 62 shows the discretized models analyzed with BOSOR5. Figure 63 shows the configuration of Galletly's specimens with an exaggerated view of a deformed meridian at the bifurcation buckling pressure.

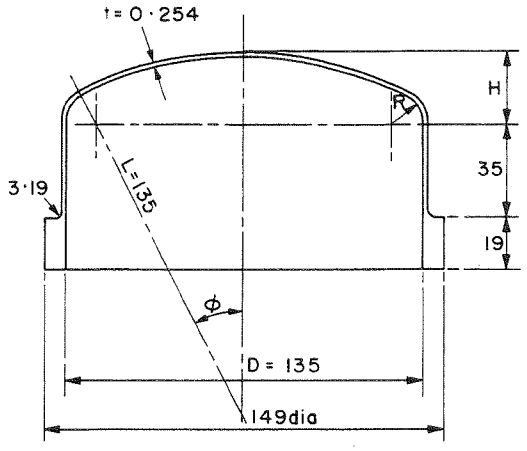

(Dimensions in mm)

FIG. 61 TEST SPECIMEN NOMINAL GEOMETRY (FROM PATEL AND GILL [271])

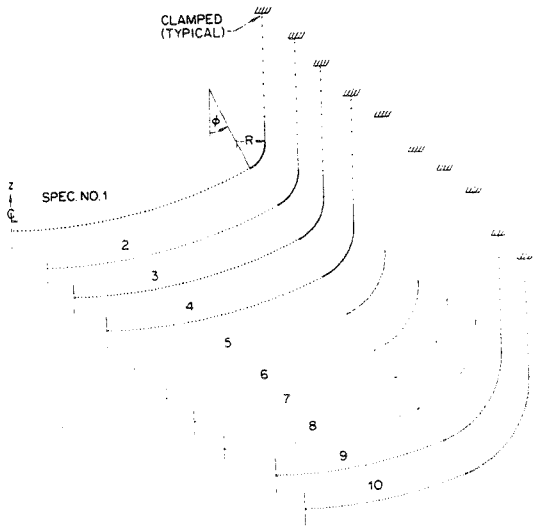

FIG. 62 DISCRETIZED MODELS FOR THE BOSOR5 ANALYSIS (FROM LAGAE AND BUSHNELL [229])

Bifurcation and Post-Bifurcation Behavior

Circumferential (hoop) compression develops wherever the radius r is diminished from that in the undeformed state. It is this hoop compression that causes nonsymmetric bifurcation buckling. The value of the buckling pressure p_{cr} depends most strongly on the value and meridional distribution on the hoop stress resultant N_{20}, on the curvature of the deformed meridian in the region where N_{20} is compressive, on the material properties, and of course on the thickness of the shell. The circumferential bending rigidity, C_{55}, is probably the most important component of stiffness in the calculation of the stability determinant because the critical circumferential wave number n_{cr} is usually very high for buckling under internal pressure and the strain energy associated with the buckling mode thus varies approximately as $C_{55}n^4{}_{cr}$. (Plots showing how C_{55} changes after yielding are given in Fig. 73.)

The development of visible buckles in these cases is a process and not the single event predicted by a bifurcation (eigenvalue) buckling analysis. As the pressure in a test specimen is increased above some critical value, a very localized, isolated incipient buckle forms in the knuckle region, invisible to the naked eye but detectable by a sensitive probe or a strain gage. The buckle grows slowly at first, and then more rapidly, and suddenly becomes visible. This visible buckle generally covers most of the knuckle region in the meridional direction but has a very short circumferential wavelength. After formation of the first buckle, the pressure can be further increased substantially, causing the formation of other visible buckles in the knuckle region, each one isolated circumferentially from its neighbors. An isolated buckle, generated by circumferential compression in the knuckle region, apparently causes the relief of this compression within a sector surrounding the buckle, thereby preventing the formation of the uniform buckle pattern typical of buckled axially compressed cylindrical or externally pressurized spherical shells. Figure 64 shows two of Patel and Gill's buckled specimens. Figure 65 shows the growth of a minute incipient buckle pattern in one of Patel and Gill's specimens over a pressure range $0.402 \leq p \leq 0.612$ MN/m^2.

The theoretical results displayed here are derived from an analysis which is founded on the assumption that one is especially interested in the pressure at which the first incipient

TABLE 7 INTERNALLY PRESSURIZED TORISPHERICAL HEADS

Specimen	Tested By	Material	Geometry					Buckling Test Results	BOSOR5 Buckling Predictions			
									Elastic-Plastic		Elastic	
			t_n(mm)	R_c/t_n	R_t/t_n	R_s/t_n	L_c/R_c	$(p_{cr}/E)\times10^6$	Flow Theory	Deformation Theory	Linear	Nonlinear
A1	Galletly	Aluminum	0.127	540	220	1080	0.6	8.25	8.93 (45)*	8.93 (45)	5.7 (50)	13.7 (50)
A2	Galletly	Aluminum	0.254	270	110	540	0.6	20.87	21.36 (21)	20.90 (25)		
A3	Galletly	Aluminum	0.254	270	110	540	0.6	21.84	22.91 (25)	21.34 (29)	24.0 (37)	No buckling
MS1	Galletly	Mild Steel	0.127	540	220	1080	0.6	4.23	1.47 (30-40)		4.0 (55)	6.9 (55)
MS2	Galletly	Mild Steel	0.127	540	220	1080	0.6	2.60	1.17 (30-40)		1.67 (65)	4.3 (55)
MS3	Galletly	Mild Steel	0.127	540	220	1080	0.6	2.73	2.00 (27)	1.73 (27)	5.01 (50)	10.77 (50)
MS4	Galletly	Mild Steel	0.127	540	220	1080	0.6	2.50	1.77 (28)		3.4 (55)	8.3 (50)
4A	Kirk and Gill	Aluminum	0.254	266	40	531	1.0	3.44 (75)	5.13 (40)	4.28 (35)	11.4 (75)	15.3 (65)
4B	Kirk and Gill	Aluminum	0.254	266	60	531	1.0	5.40 (40)	6.85 (40)	5.70 (35)	12.8 (60)	19.7 (50)
4C	Kirk and Gill	Aluminum	0.254	266	90	531	1.0	10.81 (49)	10.48 (28)	9.41 (40)	14.3 (45)	34.8 (45)
1	Patel and Gill	Aluminum	0.254	266	30	531	1.0	4.20	4.17 (45)	3.70 (80)	–	–
2	Patel and Gill	Aluminum	0.254	266	40	531	1.0	6.20 (35)	7.56 (35)	6.01 (60)	–	–
3	Patel and Gill	Aluminum	0.254	266	50	531	1.0	6.87	6.48 (45)	5.71 (55)	–	–
4	Patel and Gill	Aluminum	0.254	266	60	531	1.0	6.34	6.94 (45)	6.48 (50)	–	–
5	Patel and Gill	Aluminum	0.254	266	70	531	1.0	9.49	9.26 (35)	8.95 (40)	–	–
6	Patel and Gill	Aluminum	0.254	266	80	531	1.0	11.06	12.65 (30)	12.04 (35)	–	–
7	Patel and Gill	Aluminum	0.254	266	90	531	1.0	12.5	11.88 (35)	11.42 (35)	–	–
8	Patel and Gill	Aluminum	0.254	266	100	531	1.0	10.56	10.03 (35)	9.72 (35)	–	–
9	Patel and Gill	Aluminum	0.254	266	110	531	1.0	No buckling	17.75 (20)	16.98 (25)	–	–
10	Patel and Gill	Aluminum	0.254	266	120	531	1.0	No buckling	No buckling	No buckling	–	–

*Numbers in parentheses indicate circumferential waves, n_{cr}.

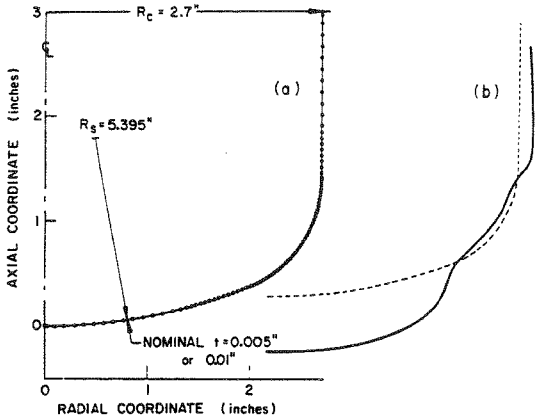

FIG. 63 ALUMINUM OR MILD STEEL TORISPHERICAL HEAD TESTED UNDER INTERNAL PRESSURE BY GALLETLY AT THE UNIVERSITY OF LIVERPOOL: (A) BOSOR5 DISCRETE MODEL; (B) EXAGGERATED VIEW OF PREBUCKLING DEFLECTED SHAPE AT THE BIFURCATION BUCKLING PRESSURE (FROM BUSHNELL AND GALLETLY [231])

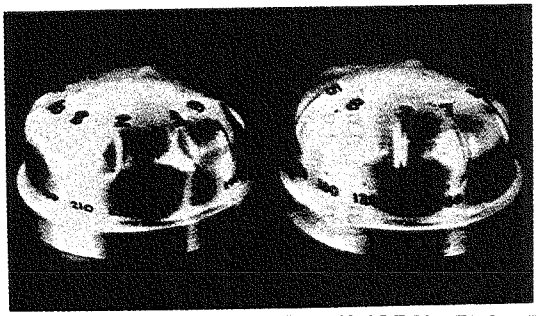

FIG. 64 TWO OF PATEL AND GILL'S SPECIMENS AFTER TESTING (FROM PATEL AND GILL [271])

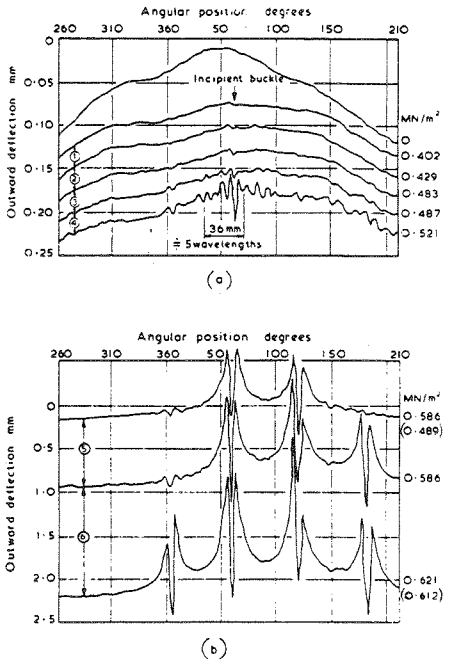

FIG. 65 DEVELOPMENT OF BUCKLES AT SPHERE/TORUS JUNCTION IN SPECIMEN 2D (FROM PATEL AND GILL [271])

buckle forms. Therefore, buckling is treated as a single event, predicted by means of the eigenvalue formulation summarized in the previous analysis section.

Figure 66 gives comparisons of predicted and measured incipient buckling pressures for the heads shown in Fig. 62. The ranges of pressures over which the buckling patterns were observed to develop are also indicated in Figure 66. In Fig. 66:

P_{ACT} = pressure at which the first buckle was fully developed

P_{CLEAR} = pressure at which the first buckle could be felt by touching the surface of the specimen

$P_{INCIPIENT}$ = pressure at which the first buckle was detected by a sensitive probe revolved around the circumference at a station in the toroidal knuckle

Table 7 lists test and predicted incipient buckling pressures for all of the internally pressurized torispherical specimens analyzed with BOSOR5. Plastic flow prior to buckling occurs in a fairly broad axisymmetric band near the junction between the spherical and toroidal portions. The thicknesses of the test specimens varied in both the circumferential and meridional directions. Typical circumferential variations of thickness in the toroidal knuckle where buckling occurs are shown in Fig. 67. BOSOR5 runs were made using the minimum thicknesses measured at each meridional station. In the BOSOR5 models as in the actual specimens the thickness varied in the meridional direction by as much as 30 percent.

Stress-strain curves for the specimens and maximum effective strains at buckling are shown in Fig. 68. Some predicted buckling mode shapes with critical numbers of circumferential waves appear in Fig. 69. The normal displacements in these buckling modes vary around the circumference as cos $n\theta$. Comparisons of axisymmetric prebuckling displacement and strains predicted from BOSOR5 and measured in one of Kirk and Gill's specimens [270] are shown in Figs. 70 and 71.

There is reasonably good agreement between test and theory for the aluminum specimens. Discrepancies may be due to the fact that the actual specimens were nonsymmetric because of circumferentially varying thickness and meridian profile, whereas the BOSOR5 models are axisymmetric. Also, the

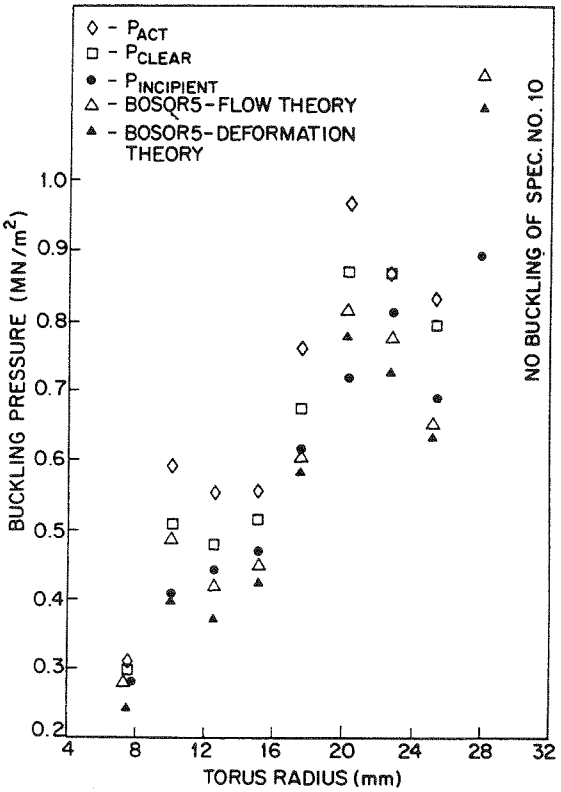

FIG. 66 VARIATION IN BUCKLING PRESSURE WITH RADIUS OF TOROIDAL KNUCKLE: COMPARISONS OF TEST RESULTS OF [271] WITH BOSOR5 PREDICTIONS FOR INCIPIENT BUCKLING (FROM LAGAE AND BUSHNELL [229])

material flow law (associated with von Mises yield surface) and hardening law (isotropic) may not be adequate to describe the actual plastic behavior. Figure 72 shows that with a small amount of strain hardening the path followed by a material point in stress space as the pressure is increased monotonically is sharply curved. We do not yet understand metal plasticity well enough to be able to predict with certainty the state of a structure that has undergone nonproportional biaxial loading.

Results given by Lagae and Bushnell [229] indicate that reasonably accurate predictions of incipient buckling can be obtained with models in which constant thickness is assumed, the model thickness being taken as the average measured thickness along the toroidal knuckle meridian for which this average is minimum. The quality of the theoretical predictions of incipient buckling as well as the behavior of the test specimens as the pressure is increased above the incipient buckling pressure indicate that these types of vessels are not particularly sensitive to initial imperfections.

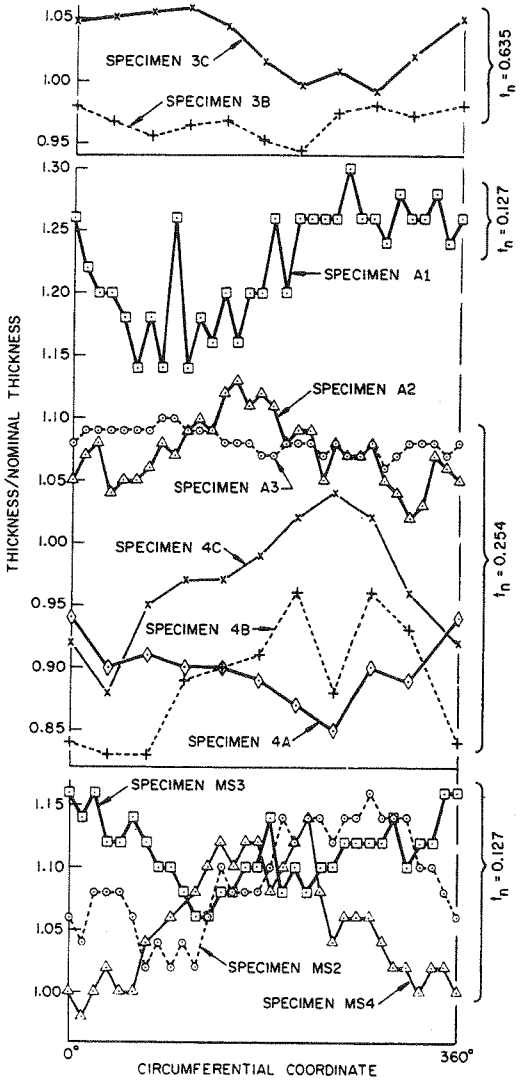

FIG. 67 MEASURED THICKNESS AROUND THE CIRCUMFERENCE AT THE LATITUDES WHERE THE MAXIMUM NORMAL BUCKLING MODAL DISPLACEMENT IS PREDICTED TO OCCUR (FROM BUSHNELL AND GALLETLY [231])

A definite explanation of the disagreement between test and theory for the mild steel specimens does not yet exist. It is possible that the buckling mode associated with the lowest predicted eigenvalue grows very little in the post-buckling regime and so this mode was therefore not observed in the tests. Possibly the use of minimum thickness everywhere explains the discrepancy, for this minimum does not actually correspond to any one meridian. However, it is felt that this is not a likely explanation.

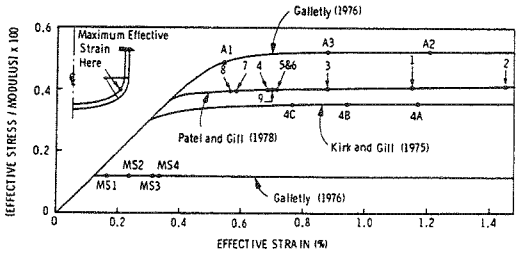

FIG. 68 MAXIMUM EFFECTIVE STRAIN AT BUCKLING FOR KIRK AND GILL'S, PATEL AND GILL'S AND GALLETLY'S SPECIMENS (ADAPTED FROM BUSHNELL AND GALLETLY [231])

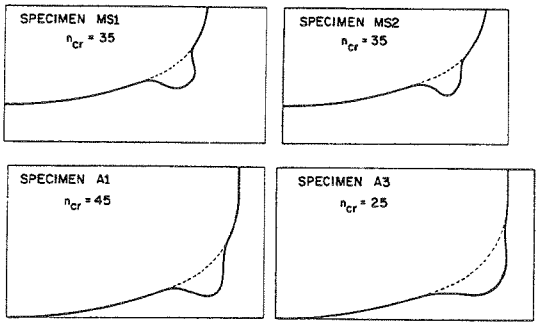

FIG. 69 PREDICTED BUCKLING MODES FOR FOUR OF GALLETLY'S SPECIMENS (FROM BUSHNELL AND GALLETLY [231])

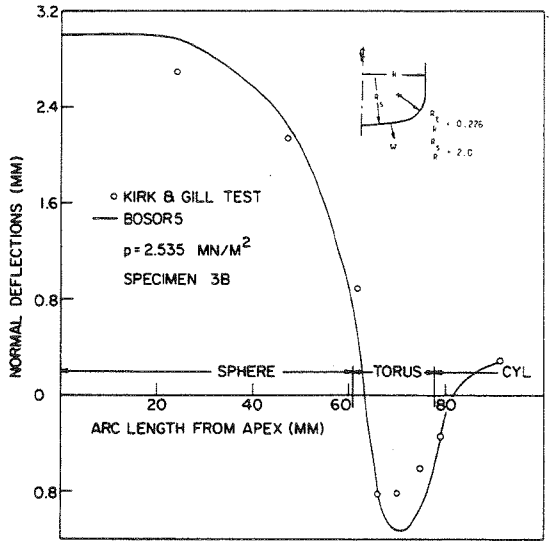

FIG. 70 MEASURED AND CALCULATED NORMAL PREBUCKLING DISPLACEMENT AT A HIGH PRESSURE (FROM BUSHNELL AND GALLETLY [231])

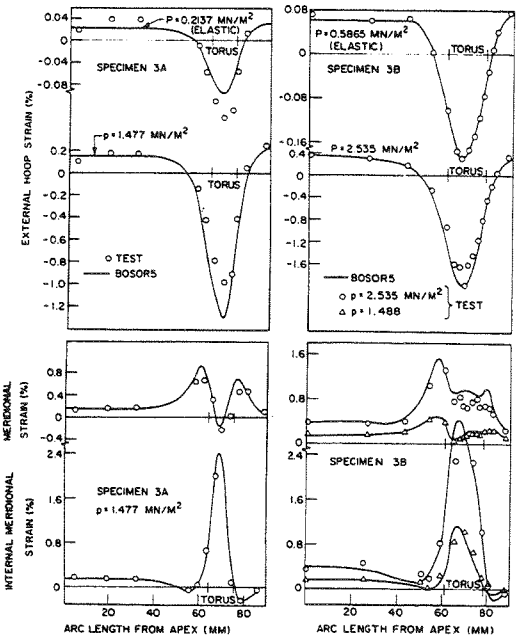

FIG. 71 COMPARISON OF TEST AND THEORY FOR PREBUCKLING STRAIN DISTRIBUTIONS IN SPECIMENS 3A AND 3B (FROM BUSHNELL AND GALLETLY [231])

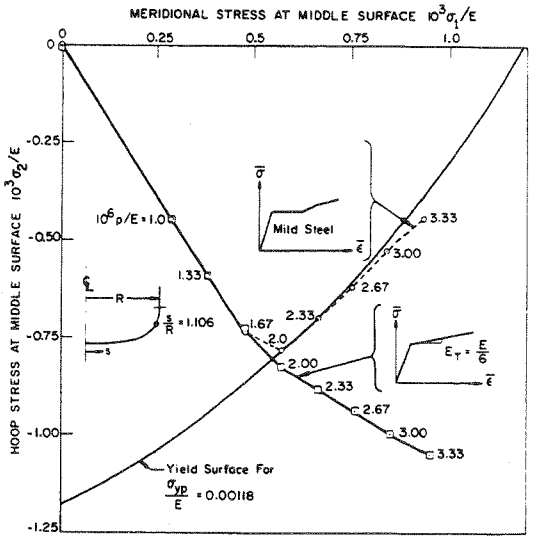

FIG. 72 COMPARISONS OF PATHS IN STRESS SPACE FOR A POINT AT s/R = 1.106 WITH USE OF TWO DIFFERENT STRESS-STRAIN CURVES (FROM BUSHNELL [230])

More likely is the fact that because circumferential nonuniformities in thickness, such as shown in Fig. 67, cause relatively large circumferential prebifurcation bending strains to develop as the pressure is increased, the compressive destabilizing circumferential stress resultant grows more slowly with increasing pressure than predicted by the axisymmetric BOSOR5 model. More details are given in [231].

Conclusions

Several conclusions are drawn in [231] based on test results and BOSOR5 calculations:

1. The major effect of moderately large axisymmetric prebuckling deformation is to cause the band of circumferential compression which occurs in the knuckle to increase more slowly than in proportion to the pressure. [See Fig. 73 (a) for example.] Thus, buckling pressures predicted with use of geometrically nonlinear prebuckling theory are higher than those predicted with use of linear prebuckling theory.

2. A smaller counteracting influence of moderately large deflections is due to the effect of the increase in meridional radius of curvature of the knuckle region during prebuckling deformations on the nonaxisymmetric stability analysis: This curvature change causes a reduction of the predicted buckling pressure from a value that would result if terms related to it were dropped from the equations governing the stability analysis.

3. For monotonically increasing pressure above that causing initial yielding, the circumferential and meridional stresses in the knuckle do not increase proportionally. The curvature of path in stress space followed by a given point depends very strongly on the amount of post-yield strain hardening exhibited by the material from which the vessel head is fabricated: The less the strain hardening, the more this path is curved, as shown in Fig. 72.

4. As might be expected, the predicted buckling pressure obtained with elastic-plastic analysis is less than that obtained with elastic analysis.

5. Use of deformation theory rather than flow theory in the stability analysis leads to lower predicted buckling pressures.

6. The distribution and magnitude of the hoop compression in the knuckle region depends very strongly on the degree of strain hardening exhibited by the material. The peak compressive hoop resultant in a vessel head fabricated from mild steel or other material with negligible strain hardening increases initially with increasing pressure, but very soon starts to decrease as the knuckle is stressed into the plastic range. [See Figs. 42 and 73 (c).] In contrast, if the material exhibits a moderate amount of strain hardening, the peak compressive hoop resultant continues to increase. [See Figs. 72 and 73 (a).] This difference in behavior of the destabilizing hoop resultant affects the strategy to be used for calculation of bifurcation buckling eigenvalues, as pointed out in the discussion associated with Fig. 42.

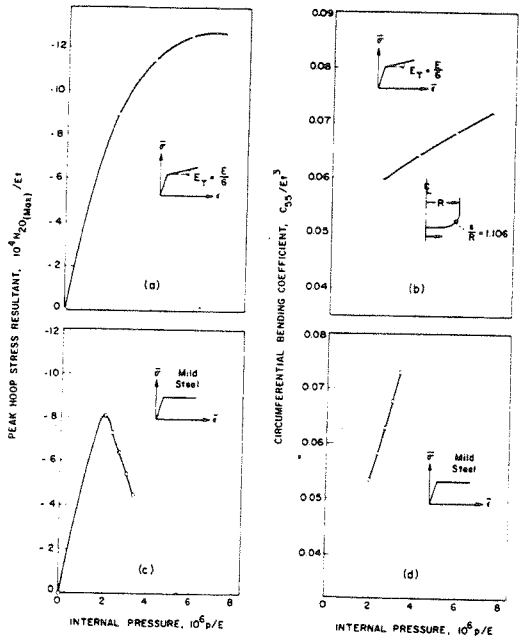

FIG. 73 COMPARISON OF PEAK COMPRESSIVE HOOP STRESS RESULTANT AND C_{55} VS PRESSURE FOR TWO DIFFERENT STRESS-STRAIN CURVES (FROM BUSHNELL [230])

7. Buckling occurs only for very thin specimens. For example, with 2:1 heads, nonsymmetric buckling occurs only if the diameter-to-thickness ratio is greater than about 500. It is not presently within the state of the art to fabricate by machining specimens of reasonable size for testing in the laboratory with thickness variations around the circumference less than 5 to 10 percent. These small nonaxisymmetric variations cause the growth of circumferential waves in the knuckle at pressure well below the buckling pressure. It is felt that the circumferential nonuniformity is responsible for rather large discrepancies between measured and predicted strains in the knuckle region of torispherical shells for pressures exceeding the proportional limit of the material.

8. The observed buckling pressure depends on how buckling is defined. In the tests on torispherical shells performed by Galletly [268], the first buckling pressure is defined as that pressure at which the first buckle becomes visible to the unaided eye. In the tests by Kirk and Gill [270], the buckling pressure is defined as that pressure at which a short-wavelength disturbance is first detected by a sensitive displacement transducer rotated around the circumference at the midpoint of the

knuckle. In one of Kirk and Gill's specimens there was more than a 50 percent increase in the pressure from that at which the transducer detected a small wave to that at which the wave grew to such a size that it become visible. (See Ref. [231] for more details.)

9. Finally, it is concluded that in order to obtain a fuller understanding of the elastic-plastic behavior of thin vessel heads under internal pressure, a better understanding of the biaxial flow of metals subjected to nonproportional loading is needed, as well as the capability to manufacture very thin test specimens in which the tolerance on axisymmetry of thickness is about an order of magnitude smaller than is possible with state-of-the-art fabrication techniques.

EFFECT OF RESIDUAL STRESSES AND DEFORMATIONS ON PLASTIC BUCKLING

In 1958 Ketter [272] identified four sources of residual stresses and deformations of fabricated metal structures: differential cooling during and after rolling sheet metal, cold bending, various erection procedures, and welding. He considered the effect of differential cooling in the fabrication process on buckling loads of axially compressed I-beams.

Cold Bending

Several authors have investigated residual stresses due to cold bending. Almen and Black [273] give the residual stress pattern through the thickness of a bar which has been bent about a circular die. Queener and De Angelis [274] derive approximate formulas for residual stresses and the ratio of die radius R_o to final radius after springback R_f for materials with stress strain curves of the form $\sigma = K\epsilon^n$. They performed tests for various materials and a wide range of R_o/R_f, obtaining good agreement between test and theory. Their treatment is based on deformation theory. Lunchik [275] determined the effect of cold bending on buckling loads of cylindrical pressure vessels. He calculated effective stress-strain curves for the prestressed material by averaging effective stresses and strains at twelve stations through the thickness of the shell wall. Such curves depend on the service loads. Lunchick's model is based on elastic-perfectly plastic material and deformation theory. It is determined in [275] that bending residual stresses have the greatest weakening effect for cylindrical shells in which the effective stress in the wall is near the material proportional limit at the buckling pressure calculated with neglect of these residual stresses. For such structures, the reduction in buckling pressure due to cold bending can be as much as 30 percent.

Shama [276] derived a simple method for calculating the magnitude and distribution of cold bending residual stresses for any beam cross section. The effects of the shape of the stress-strain curve, section characteristics, and the degree of bend are investigated. Tacey [277] has written a computer program for the calculation of the residual stress distribution and the effective stress-strain curve of cold bent beams for a wide range of practical cross section geometries. The Bauschinger effect and possible inelastic behavior on springback are accounted for. The hardening rule used in Tacey's program is a combination of isotropic and kinematic rules.

Welding

During the 1970's much work was done on the numerical modeling of multipass welding. The ASME volume, *Numerical Modeling of Manufacturing Processes*, [278], contains several papers on this subject [279-284]. Masubuchi [285] wrote a survey of the field in 1975. Three frequently referenced papers are by Hibbitt and Marcal [286], Nickell and Hibbitt [287], and Friedman [288]. The results presented in these papers are generally obtained from sophisticated computer programs for multidimensional analysis. Although the heat conduction and the thermal stress problems are uncoupled, the models include nonlinear boundary conditions for solid and liquid regions, temperature-dependent material effects, latent heat effects, and convective and radiative heat transfer boundary conditions.

It is impractical as of this date to incorporate such elaborate models of the welding process into an analysis of buckling of a ring-stiffened shell with many welds. A simple, computationally efficient model is introduced in [22], in which buckling pressures are calculated for a welded ring-stiffened ellipsoidal shell. The shell and rings are assumed to be machined and stress relieved separately and then welded together. The effects of weld shrinkage are simulated in [22] by means of the assumption that a certain amount of material in the local neighborhoods of each weld is cooled below ambient temperature to a difference approximately equal to the annealing temperature. The residual stress distribution thus generated is characterized by local tensile circumferential yielding near the welds and elastic circumferential compression over the rest of the cross sections of the shell wall and ring stiffeners. The structure prestressed in this way remains axisymmetric, of course, but the radial shrinkage varies in the meridional direction, introducing an axisymmetric imperfection with a characteristic wavelength equal to the ring spacing. The weld effect thus modeled reduces the predicted buckling pressure by about 10 percent.

Bending and Welding

Few papers exist in which residual stresses are calculated for more than one fabrication process. Chen and Ross [289] calculate residual stresses from cold bending a flat sheet into a cylindrical shape and then welding the longitudinal seam. They suggest that these residual stresses will cause early column buckling of long cylinders under axial compression. In his

computer program, Tacey [277] permits introduction of arbitrary initial stresses and then calculates residual stresses for a series of up to ten sequential bending processes. Faulkner [290] gives a survey of work done on calculation of residual stresses due to welding ring stiffeners to cylindrical shells and cold bending sheets into cylindrical shells and beams into rings. He states that when ring stiffeners are welded to a cylindrical shell of thickness t there is tensile yielding over a length of shell equal to $2\eta t$ and over a length of the ring web equal to ηt. These tensile regions are balanced by compressive residual stresses distributed over the remainder of the shell and ring cross sections. Typical values of η obtained from measurements are in the range $1.5 \leq \eta \leq 4.5$. The radial shrinkage at the welds is approximately 10 percent of the shell thickness t.

Effect of welding on the plastic buckling pressure of an ellipsoidal ring-stiffened shell

The geometry of an ellipsoidal shell with internal ring stiffeners is shown in Fig. 74. The purpose of the analysis of this structure is to determine the effect on predicted buckling pressure of axisymmetric distortions and residual stresses due to welding the rings to the shell.

Figure 75 shows the BOSOR5 model which consists of 313 degrees of freedom in the axisymmetric prebuckling analysis and 466 degrees of freedom in the nonaxisymmetric stability analysis. Symmetry conditions are imposed at the equator in both the prebuckling and bifurcation buckling analysis. (It was determined in preliminary runs on the computer that the lowest bifurcation buckling pressure corresponds to a mode symmetric rather than antisymmetric about the symmetry plane.) The locations of the discrete ring attachment points and centroids are indicated in Fig. 75 (b).

The effect of the welds shown in Fig. 76 (a) is introduced into the analytical model by means of the temperature distribution shown in Fig. 76 (b): A certain amount of the material of ring web and shell wall in the neighborhood of the welds is considered to be cooled down below room temperature. The value 1000 F corresponds approximately to the anneal temperature of the steel from which the structure is presumed to be fabricated. The anneal temperature is used as a reference value because residual stresses are relieved for higher temperatures than this. The zero-stress temperature distribution corresponds to the weld region being hot (above 1000 F) and the rest of the material being at room temperature. As the weld material cools down from 1000 F to room temperature,

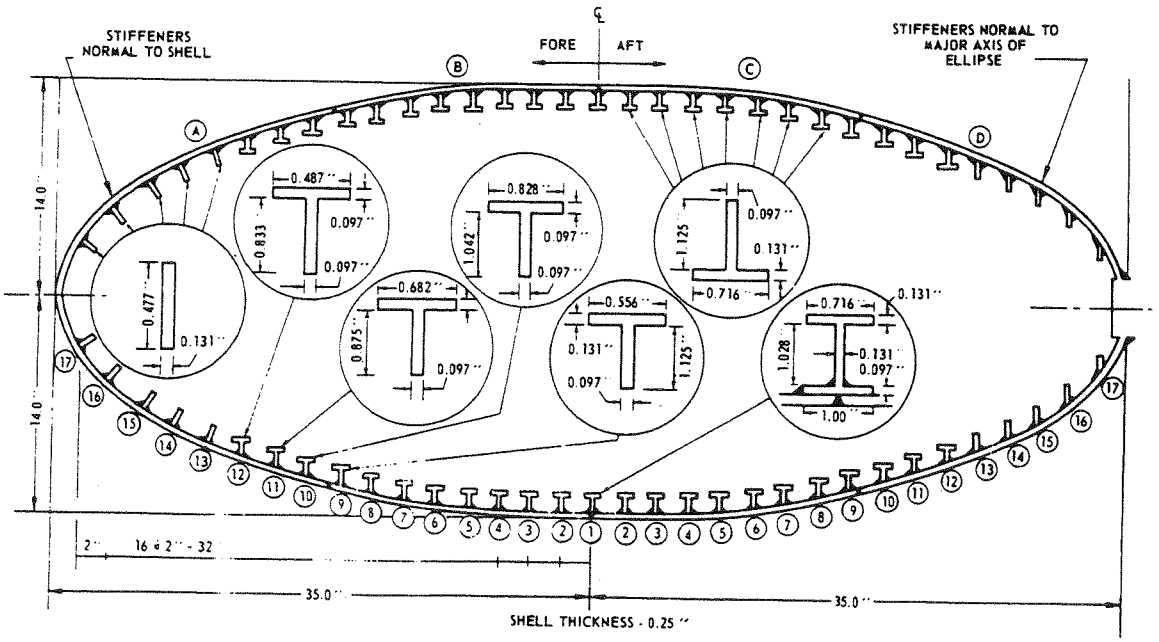

FIG. 74 STEEL ELLIPSOIDAL SHELL WITH INTERNAL RING-STIFFENERS WELDED TO IT. THIS STRUCTURE IS SUBMITTED TO EXTERNAL PRESSURE (FROM BUSHNELL [22]).

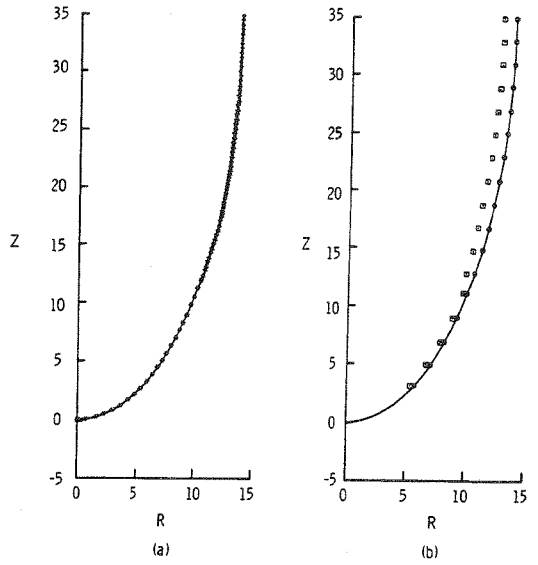

FIG. 75 BOSOR5 MODEL OF THE RING-STIFFENED ELLIPSOIDAL SHELL: (A) NODAL POINTS; (B) LOCATIONS OF DISCRETE RING ATTACHMENT POINTS AND CENTROIDS (FROM BUSHNELL [22])

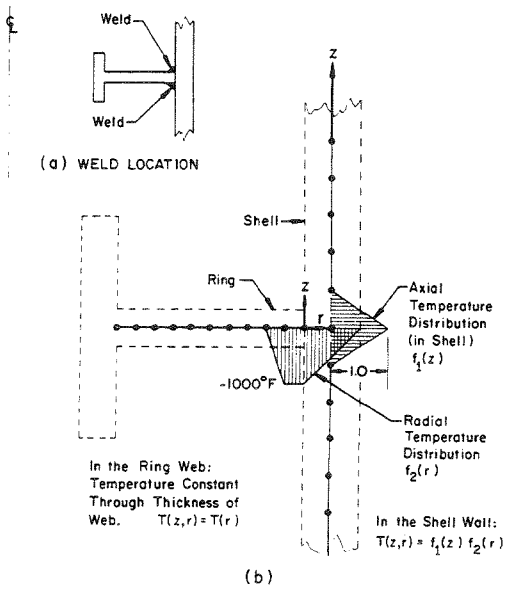

FIG. 76 WELD LOCATIONS AND SIMULATION OF WELD THERMAL EFFECT BY LOCAL COOLING (FROM BUSHNELL [22])

stresses build up in the shell and ring, tensile in the region that was originally heated above 1000 F and compressive elsewhere. Thus, the nonzero stress state corresponds to a uniform ambient temperature distribution. In BOSOR5 it is not possible to generate a nonzero initial thermal stress state with a uniform temperature distribution. Therefore, one must simulate the growth of residual stresses and deformations by treating the weld region as if it were cooled down below ambient temperature.

Figure 77 shows the prebuckling axisymmetrically deformed shape with increasing external pressure and a comparison with and without welding effects. The relatively advanced scalloping of the meridian corresponding to p = 4100 psi with the weld effect arises because of increased local plastic flow near the ring attachment points. The ring at the plane of symmetry moves inward rapidly with pressure increasing above 3500 psi because the flange yields and flows plastically, having zero tangent modulus for $p > 3500$ psi. (There is more welding required in the neighborhood of this ring than the others because the ring must first be welded to one of the halves of the shell and then the two halves of the shell must be welded together. Hence, in this area more of the material is cooled down by an amount approximately equal to the anneal temperature.)

Figure 78 shows predicted incipient buckling modes with and without the weld thermal effect. The lowest predicted

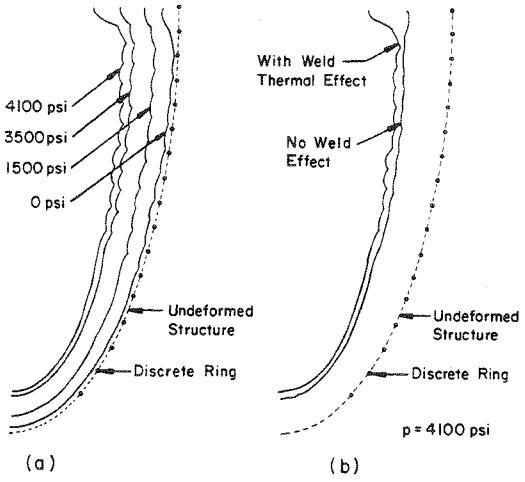

FIG. 77 PREBUCKLING DEFLECTIONS WITH INCREASING PRESSURE AND COMPARISON WITH AND WITHOUT THE WELD COOL-DOWN EFFECT (FROM BUSHNELL [22])

critical pressure corresponds in both cases to nonaxisymmetric buckling with five circumferential waves. The buckle modes are quite different in the two cases because of the increased amount of prebuckling plastic flow in the ring at the plane of symmetry predicted with the model which includes the weld effect.

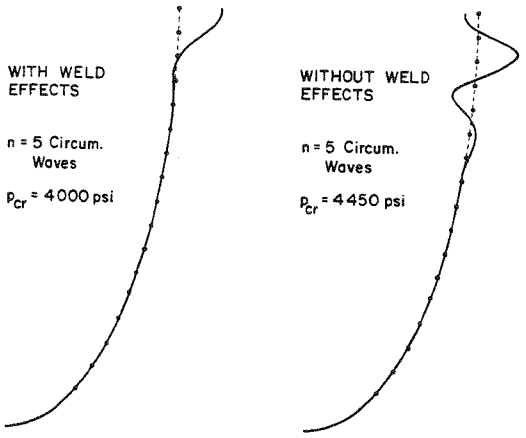

FIG. 78 PREDICTED BIFURCATION BUCKLING MODES AND PRESSURES WITH AND WITHOUT THE WELD COOL-DOWN EFFECT INCLUDED IN THE ANALYSIS (FROM BUSHNELL [22]

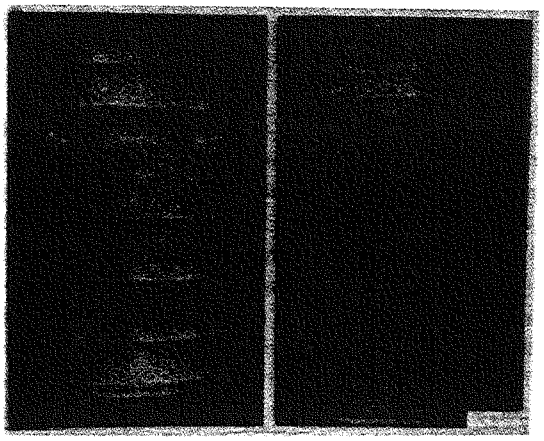

BR-4 (a) BR-4A (b)

FIG. 79 BUCKLING PATTERNS IN:
(A) THE COLD BENT AND WELDED SPECIMEN BR-4 (p_{cr} = 390 psi)
(B) THE MACHINED SPECIMEN BR-4A (p_{cr} = 540 psi)

EFFECT OF COLD BENDING AND WELDING ON BUCKLING OF RING-STIFFENED CYLINDERS

The BOSOR5 computer program can be used for calculation of bifurcation buckling of cold bent and welded ring-stiffened cylinders under external pressure. Residual stresses and deformation from cold bending and welding can be included in the model for buckling under service loads by introduction of these manufacturing processes as functions of a time-like parameter, "time," which ensures that the material in the analytical model experiences the proper sequence of loading prior to and during application of the service loads. The cold bending process is first simulated by a thermal loading cycle in which the temperature varies linearly through the shell thickness, initially increasing in "time" to simulate cold bending around a die to radius R_o and then decreasing in "time" to simulate springback to a final somewhat larger design radius R. The welding process is subsequently simulated by the assumption that the material in the immediate neighborhoods of the welds is cooled below the ambient temperature by an amount that leads to weld shrinkage amplitudes typical of those observed in tests. Buckling loads are calculated for a configuration including and neglecting the cold bending and welding processes. These predictions are compared to values obtained from tests by Kirstein and Slankard [291] and Slankard [292] on two nominally identical specimens, shown in Figs. 79 and 80. The specimen designated BR-4 was fabricated by cold bending the shell and then welding machined ring stiffeners to it, and the specimen designated BR-4A was carefully machined. Details of the analysis and predictions are given in [232].

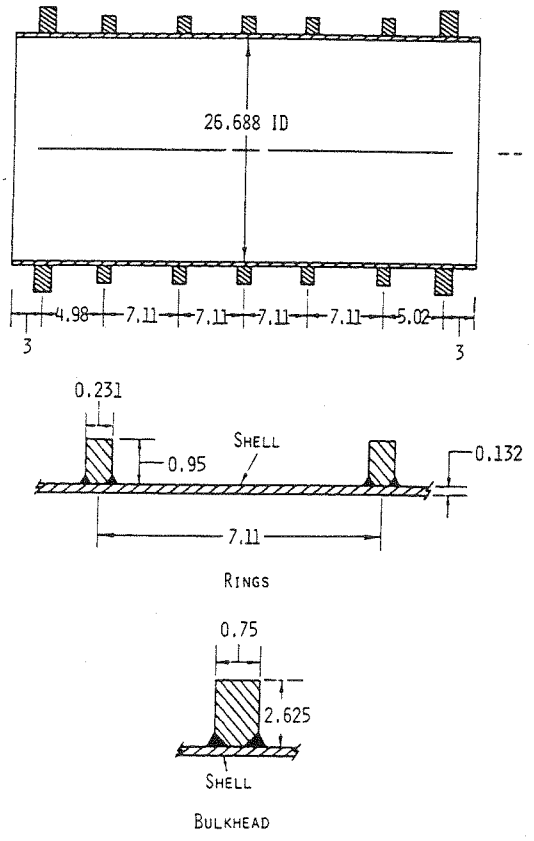

FIG. 80 DIMENSIONS OF SPECIMENS BR-4 AND BR-4A

ELASTIC-PLASTIC BENDING AND BUCKLING OF PIPES AND ELBOWS

The elastic-plastic collapse and bifurcation buckling analysis of straight and curved tubes subjected to bending is needed for design and evaluation of nuclear power plant piping components, offshore pipelines, and other structures involving tubular members. Most of the recent work on piping has been motivated by a desire to be able to predict stress, stiffness, and limit moments of piping systems in nuclear reactors. Since the most flexible and highly stressed piping components are elbows, a significant portion of the total effort has been focused on test and analysis of various elbows under in-plane and out-of-plane moments. In the offshore oil industry, the laying of underwater oil pipelines involves bending of rather large diameter straight pipes in the presence of external hydrostatic pressure. The degree of ovalization of the pipe cross section under bending is very much affected by the external pressure, as will be seen later.

ELASTIC MODELS

The bending of elastic piping components is explored in Refs. [293-301]. Brazier [293] was the first to calculate collapse moments, including in his theory the important effect of increasing ovalization (flattening) of the pipe cross section as the bending moment is increased. Clark and Reissner [294] use an asymptotic formulation in which ovalization of initially curved tubes under bending is assumed to be symmetric about a tube diameter normal to its plane of curvature. Wood [295] expanded Brazier's treatment to include pressure, and Reissner [296] further improved the theory by including higher order nonlinear terms and introducing the effect of pressure on the bending of slightly curved tubes. Aksel'rad [297] was the first to predict bifurcation buckling of straight pipes under bending, including the effect of flattening of the cross section in the prebuckling analysis. In all of the analyses just cited, end effects are ignored; the pipes are assumed to be infinitely long. Stephens, *et al.* [298], used the STAGS computer program [207] to calculate collapse and bifurcation buckling of initially straight tubes of finite length. For tubes with radius-to-thickness R/t=100 they carried out a parameter study, predicting limit and bifurcation bending moments for length-to-radius ratios $3.4 \leq L/R \leq 20$. They included internal and external pressure in their analysis.

Elastic analyses of piping elbows have been performed by Dodge and Moore [299] who wrote a computer program, ELBOW, based on a model similar to Clark and Reissner's [294] and Hibbitt, *et al.* [300], who introduced a curved piping finite element into the MARC computer program [171]. This element, called no. 17 in the MARC element library, is based on neglect of elbow end effects. Discretization is in the circumferential coordinate only. Sobel [301] used the MARC no. 17 element in a convergence study with mesh size. He referred to Clark and Reissner's asymptotic formulas to establish optimal finite element nodal point density in the hoop direction as a function of elbow geometry. Rodabaugh, *et al.* [302] performed a study of 45, 90, and 180 deg. elbows, determining the stiffening effects of straight pipes attached to the ends of the elbows. They used the EPACA computer program [170] for their analysis in which end effects are included. Although EPACA includes the capability to treat structures made of elastic-plastic material, the work described in Ref. [302] is restricted to elastic behavior.

BENDING TESTS ON ELASTIC-PLASTIC STRAIGHT PIPES AND ELBOWS

Several test programs on bending of elastic-plastic straight pipes and elbows have been carried out in the past decade. Bolt and Greenstreet [303] give load-deflection curves for 14 commercial 6-in. diameter carbon steel elbows and one 6-in. diameter stainless steel elbow with and without internal pressure. Vrillon, *et al.* [304] compare test and theory for the in-plane bending of a 180 deg. elbow subjected to both opening and closing moments. They used the TRICO program [205] for their analysis. Sherman [305] tested several straight pipes, noting formation of relatively short axial wavelength buckles just before collapse. A comparison between one of Sherman's experiments and theoretical results obtained with a modified version of the BOSOR5 computer program [22, 306] is given later. Sobel and Newman [307] describe a test on a 90 deg. elbow carried out on the multiload test facility (MLTF) at the Westinghouse Advanced Reactors Division. Bung, *et al.* [308], ran tests at elevated and room temperature on 304 stainless steel elbows. Comparisons between the test results of Sobel and Newman [307] and Bung, *et al.* [308], and theoretical predictions obtained with the modified version of BOSOR5 referred to above are presented in a following section.

ELASTIC-PLASTIC PIPING ANALYSIS

There are basically three types of elastic-plastic piping analysis for the prediction of stress, stiffness, and buckling failure of straight and curved tubes and combinations thereof:

1. A "brute force" method in which the tubes are divided into a two-dimensional field of finite elements.
2. A simplified model in which tube end effects are ignored and discretization is in the circumferential coordinate only.
3. A further simplified model in which resultant forces and moments integrated over the tube cross section are related to strains and changes in curvature of the tube axis.

The STAGSC computer program [207], the EPACA code [170], and the TRICO code [205] have been used for the "brute force" analysis of elastic-plastic elbows attached to straight pipes. Vrillon, *et al.* [304], Roche and Hoffman

[309], and Skogh and Brogan [310] used these general purpose shell analysis computer programs to calculate moment-deflection curves for combinations of straight pipes and elbows, including elastic-plastic material behavior and moderately large deflections. Remseth, *et al.* [311], calculate elastic-plastic collapse of straight tubes subjected to combined bending and external pressure in a two-dimensionally discretized model in which arbitrarily large rotations are permitted. These nonlinear analyses require large amounts of computer time. The more economical but less rigorous one-dimensionally discretized model has been employed by Mello and Griffin [312] and Sobel and Newman [313], who used the MARC computer program [171] element no. 17 [300], and by Bushnell [306], who modified BOSOR5 [22] to obtain predictions for the bending and buckling of straight pipes and elbows. The most economical and more approximate beam-type models have been used by Roche, *et al.* [314], Spence and Findlay [315, 316] and Calladine [317]. Popov, *et al.* [318], used a beam bending model combined with a rigorous axisymmetric large deflection elastic-plastic analysis to predict axial wrinkling of pipes under combined internal pressure, axial loading and flexure. However, they neglected the important effect of ovalization of the pipe cross section during bending.

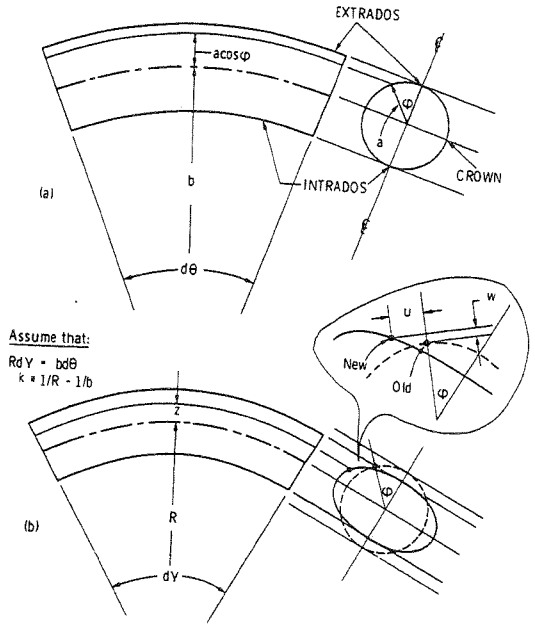

FIG. 81 IN-PLANE BENDING OF CURVED PIPE:
(A) INITIAL CONFIGURATION
(B) UNIFORMLY BENT CONFIGURATION

AXISYMMETRIC MODEL OF PIPE OR ELBOW BENDING PROBLEM

In the following section results from an approximate analysis of the second type (one-dimensional discretization) are given for various configurations. The theoretical results were obtained with a modified version of BOSOR5 [22, 306]. In [306] a uniformly curved pipe is treated as if it were part of a toroidal shell. The model is similar to that described in Ref. [319]. Bending in the plane of the curvature of the pipe centerline is applied by means of an appropriate temperature distribution over the pipe cross section, as is described in [306] and summarized here. Every cross section of the uniformly curved pipe is assumed to deform identically. Therefore, the structure can be treated as a shell of revolution, a torus. Figure 81a shows the undeformed curved pipe reference surface with centerline radius of curvature b and meridional radius of curvature a. The centerline radius of curvature of the deformed pipe reference surface (Fig. 81b) is R and the cross section has ovalized such that a generator that was originally at a radius

$$r = b + a\cos\phi$$

is now at a radius $R + z$, where z is given by

$$z = (a + w)\cos\phi - u\sin\phi \qquad (52)$$

If we assume that the centerline remains inextensional, the reference surface axial strain is

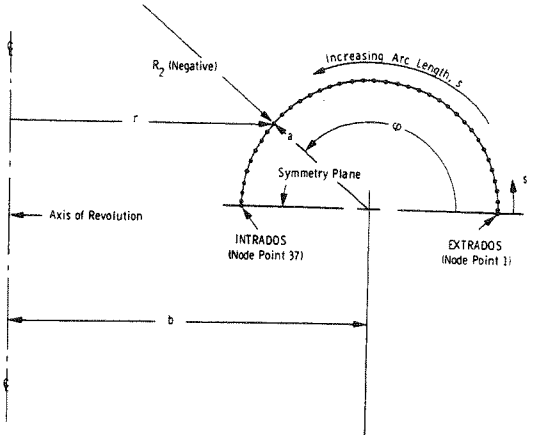

FIG. 82 DISCRETIZATION OF PIPE MODELED AS TOROIDAL SEGMENT

$$\epsilon = \frac{(R + z)\dfrac{b}{R} - (b + a\cos\phi)}{b + a\cos\phi} \qquad (53)$$

Rearrangement of Eq. (53) and use of the relationships

$$\cos\phi = r/R_2;\ \sin\phi = -r' \equiv -dr/ds \qquad (54)$$

leads to the expression

$$\epsilon = \frac{b}{R}(w/R_2 + ur'/r) + \frac{a(\frac{1}{R} - \frac{1}{b})\cos\phi}{1 + \frac{a}{b}\cos\phi} \qquad (55)$$

in which R_2 is normal circumferential radius of curvature of the reference surface of the undeformed torus, r is the radius to a point on the torus reference surface, and r' is the derivative of r with respect to meridional arc length s. Figure 82 shows these quantities.

Simulation of the Pipe Bending Problem by Thermal Loading of a Torus

In order to use BOSOR5 to treat the problem of elastic-plastic bending and bifurcation buckling of a curved pipe, it is necessary to write the axial strain given by Eq. (55) as a stress-producing prebuckling hoop strain for the shell-of-revolution (torus) analysis. This is easily done by definition of the prebuckling stress-producing hoop strain as

$$\epsilon = \epsilon_2 - \alpha_2 \Delta T \qquad (56)$$

in which, from Eq. (55), it is seen that

$$\epsilon_2 = \frac{b}{R}(w/R_2 + ur'/r) \qquad (57)$$

$$\alpha_2 \Delta T = -a(\frac{1}{R} - \frac{1}{b})\left[\frac{\cos\phi}{1 + \frac{a}{b}\cos\phi}\right] \qquad (58)$$

In this way, the problem of bending of a curved pipe is simulated by a problem of a nonuniformly heated torus. Further details of the analysis are given in [306].

BENDING, LIMIT MOMENT, AND BIFURCATION BUCKLING MOMENT OF A STRAIGHT PIPE

Figures 83-86 pertain to the elastic-plastic bending, collapse, and bifurcation buckling of straight pipes tested by Sherman [305]. (In Sherman's test there was no pressure, however.)

Figure 83 shows test results and the results of two BOSOR5 runs, one in which the pressure is zero and the other in which the pressure is one-half the external pressure p_{cr} that would cause buckling in the absence of an applied bending moment, M. The pipe material is elastic perfectly plastic with a yield strength of 421 N/mm^2. The quantity k is the curvature change of the pipe axis (Fig. 81). With zero external pressure, bifurcation buckling is predicted to occur at an applied moment slightly below that corresponding to nonlinear collapse due to flattening of the cross-section. Thus, in a test of such a pipe one would expect to see relatively short axial-

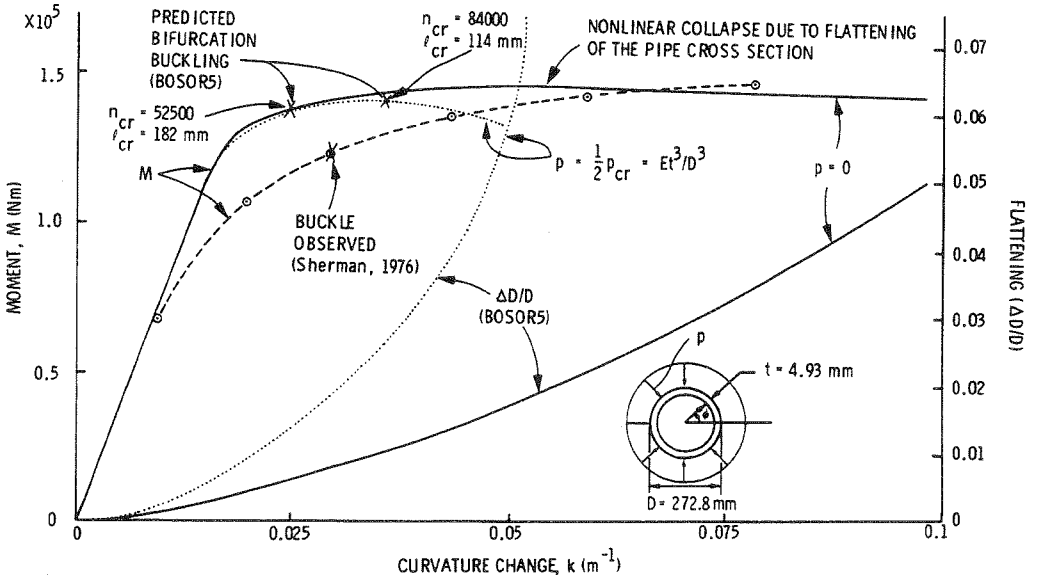

FIG. 83 BENDING OF STRAIGHT PIPE WITH AND WITHOUT EXTERNAL PRESSURE

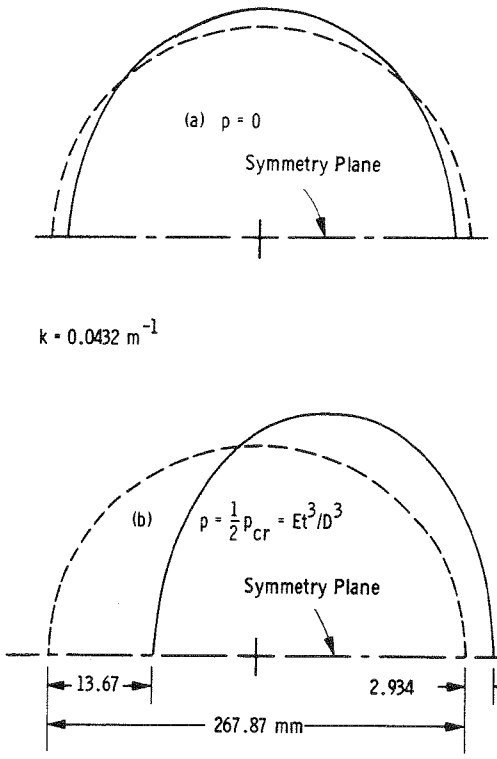

FIG. 84 OVALIZATION OF STRAIGHT PIPE WITH AND WITHOUT EXTERNAL PRESSURE UNDER IMPOSED CURVATURE k = 0.0432 m^{-1}

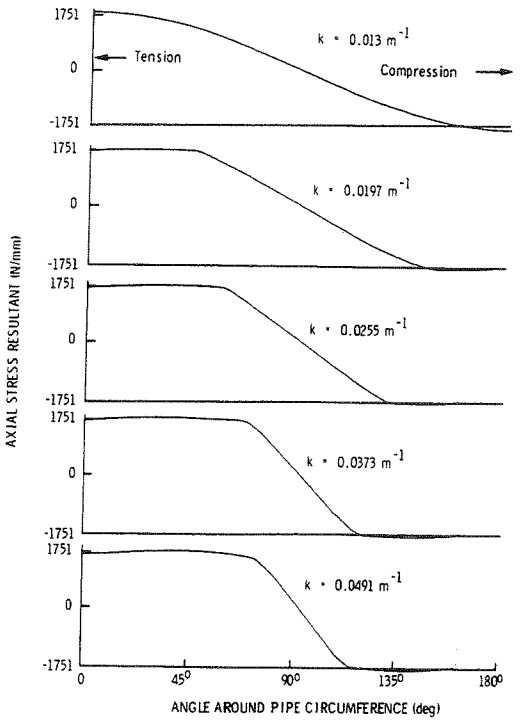

FIG. 85 GROWTH OF PLASTIC REGION IN STRAIGHT PIPE AS IMPOSED CURVATURE, k, IS INCREASED

wavelength wrinkles or a single wrinkle appear just before failure. Indeed Sherman observed the formation of such buckles in his tests.

With external pressure, ovalization or flattening of the pipe cross section is predicted to occur more precipitously with increasing applied curvature change $k = (1/R - 1/b)$. Note, however, that the maximum moment-carrying capability of the pipe is not much less than that of the pipe without external pressure. In the case treated here, bifurcation buckling occurs with a somewhat shorter axial wavelength at a value of k slightly greater than that corresponding to collapse due to flattening of the cross section. Hence, if the moment M is applied rather than the curvature change k, axial wrinkles might not appear before failure. Figure 84 shows the predicted deformations of the pipe cross sections with and without external pressure at $k = 0.0432\ m^{-1}$. The deformations are exaggerated but plotted to the same scale in Figs. 84 (a) and 84 (b).

Figure 85 shows the axial stress resultant at several values of applied curvature change k for the case with external pressure $p = 1/2\ p_{cr} = ET^3/D^3$. The plots clearly show the growth of the plastic regions as the applied curvature is increased. Yielding begins when the applied moment is about 10^5 Nm,

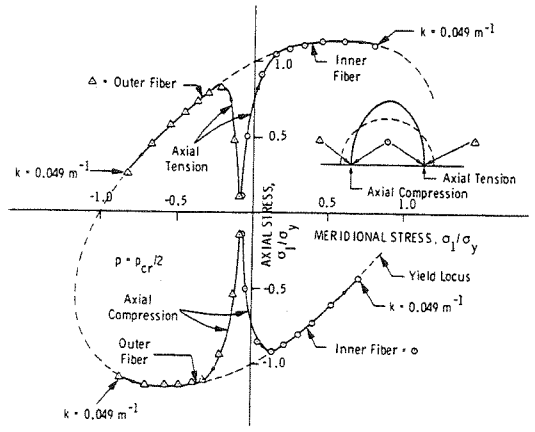

FIG. 86 PATHS IN STRESS SPACE FOLLOWED BY INNER AND OUTER FIBER POINTS ON THE PLANE OF SYMMETRY AS EXTERNALLY PRESSURIZED STRAIGHT PIPE IS BENT ($p = p_{cr}/2 = Et^3/D^3$)

well below the maximum moment. The development of extreme fiber stresses at the equator are shown in Fig. 86 for the case $p = 1/2\ p_{cr}$. The plastic biaxial loading of this elastic-perfectly plastic material is far from being radial (radial = proportional loading) as the centerline curvature k is monotonically increased.

BENDING AND LIMIT MOMENT OF ELASTIC-PLASTIC ELBOWS

Figures 87-90 show results from application of the BOSOR5 analysis [306] to in-plane bending of 90 and 180 deg. piping elbows. The BOSOR5 predictions are compared to tests and to other analyses.

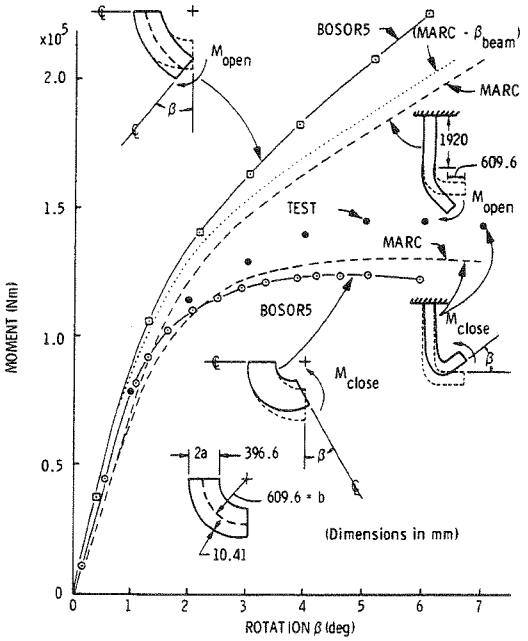

FIG. 87 COMPARISON OF TEST AND THEORY FOR BENDING OF 90 DEG. ELBOW. TEST BY WESTINGHOUSE ADVANCED REACTOR DIVISION, 1978.

Figure 87 gives a comparison of BOSOR5 results with a test of a 90 deg. elbow by Sobel and Newman [307] and an analysis in which the MARC element no. 17 is used for the elbow. The test was for a closing moment. Analytical predictions are shown for both opening and closing moments. The quantity β_{beam} is the part of the end cross-section rotation attributable to beam-type bending, which is not included in the BOSOR5 model.

Figure 88 shows a comparison of test and theory for a 180 deg. elbow tested by Bung, *et al.* [308]. The theoretical results labled "TRICO" and "TEDEL" were obtained, respectively, by Roche and Hoffmann [309] and Roche, *et al.* [314]. TRICO is a general nonlinear computerized shell analyzer [205] and TEDEL is a program based on a simplified nonlinear beam model. The axial and hoop strains plotted in Figs. 89 and 90 correspond to an increase in d of 76 mm. There is reasonably good agreement between the BOSOR5 predictions

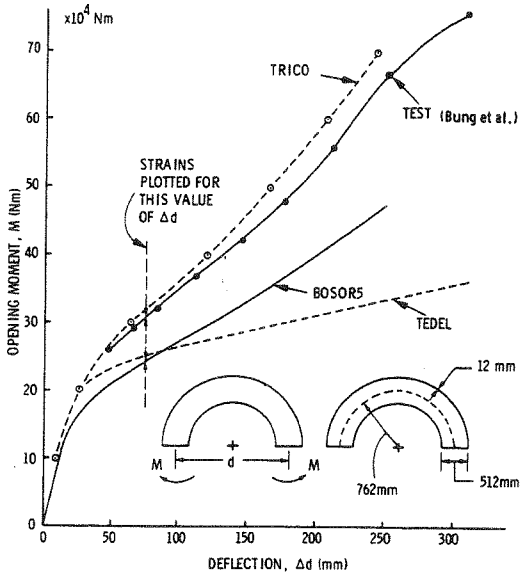

FIG. 88 MOMENT-DEFLECTION CURVES FROM TEST AND THEORY FOR 180 DEG. ELBOW WITH OPENING MOMENT

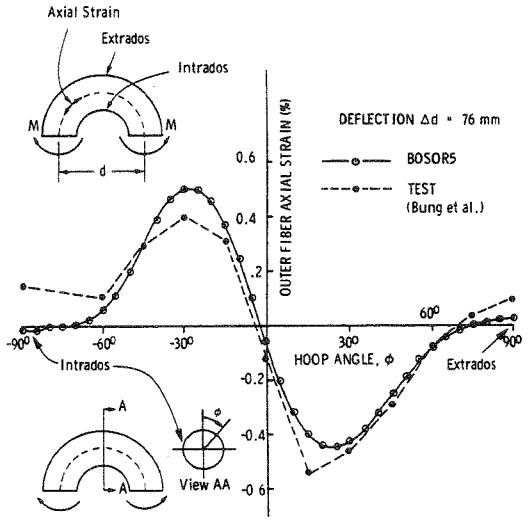

FIG. 89 OUTER FIBER AXIAL STRAIN AT SYMMETRY PLANE IN 180 DEG. ELBOW WITH OPENING MOMENT

and measured strains. (Note that the definition of hoop angle ϕ differs from that in Fig. 82)

SUMMARY AND SUGGESTIONS FOR FURTHER WORK

SUMMARY

In the introduction, plastic buckling is illustrated by an example of a rather thick cylindrical shell under axial

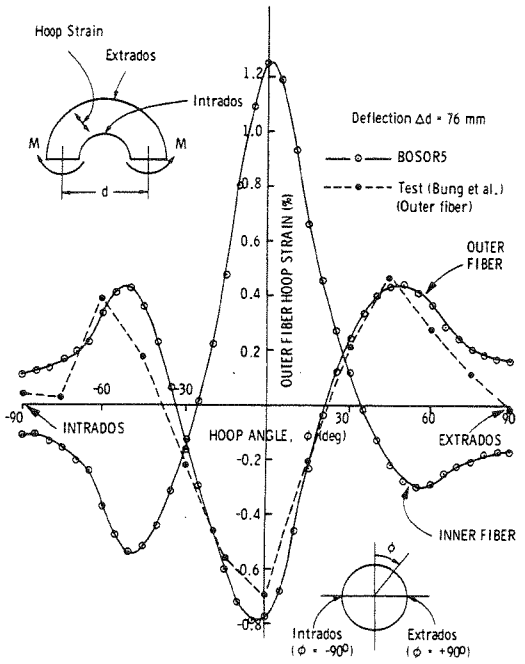

FIG. 90 HOOP STRAIN AT SYMMETRY PLANE IN 180 DEG. ELBOW WITH AN OPENING MOMENT

compression. Two types of buckling, limit load collapse and bifurcation, occur in the case of the cylindrical shell shown in Fig. 1. The limit load collapse demonstrates the need for general nonlinear analysis in which both moderately large deflections and elastic-plastic material behavior are accounted for. The bifurcation of the equilibrium path after considerable bulging near the boundaries has occurred and after yielding of the material demonstrates the need for a theoretical test of uniqueness of equilibrium which includes moderately large prebifurcation deflections and post-yield plastic flow. A capsule of recent improvements in analysis techniques and in our understanding of the plastic buckling process is then given. The introduction concludes with a chart (Fig. 3) showing how plastic buckling, as described here, fits into the overall picture of static and dynamic structural analysis.

Certain conceptual difficulties with regard to plastic bifurcation buckling are next discussed, with particular emphasis being given to the rationale leading to Shanley's model of elastic-plastic column buckling and the paradoxical discrepancy between buckling predictions from flow theory and deformation theory.

An important goal of the following sections is to bring together under one roof, so to speak, three major areas of activity in plastic buckling research: asymptotic post-bifurcation analysis, general nonlinear analysis, and analysis of shells of revolution.

In the section on asymptotic post-bifurcation analysis the recent work of Hutchinson, Tvergaard, Needleman, and their coworkers is summarized.

The main contribution of their work is to give us an improved physical understanding of the stability of structures loaded into the plastic range and of the effect of initial imperfections on the load-carrying capacity of these structures.

In the sections on general nonlinear analysis, the development of general-purpose computer programs by Marcal, Bathe, and others is described with particular emphasis being given to formulation of the equations, elastic-plastic material models, and strategies for solving large systems of nonlinear equations. The main contribution of the many workers in this field has been to provide us with greatly improved analytical tools for the analysis of complex structures which undergo large deflections and nonlinear material behavior.

In the sections on plastic buckling of axisymmetric shells, the basic equations are given followed by numerous examples in which plastic collapse and bifurcation buckling predictions for shells of various shapes are compared with tests by Lee, Batterman, Galletly, Gill, and others. The main contributions of this theoretical and experimental work are to provide a greater physical understanding of limit load collapse and bifurcation buckling for a class of structures of particular significance to the pressure vessel and piping industry, to illustrate the application of a computerized analysis method to these axisymmetric shell problems, and to reveal that critical loads for these structures are not very sensitive to initial imperfections when the material has been stressed beyond its proportional limit.

This work closes with a discussion of elastic-plastic bending and buckling of pipes and elbows. Comparisons between test and theory are given for collapse and bifurcation buckling of straight pipes and elbows of various geometries.

IMPORTANT AREAS NOT COVERED HERE

The important area of dynamic plastic buckling has not been covered here. References [320-334] deal with this problem, which is shown in Fig. 3 as a special case of nonlinear dynamic response. Other areas not explored here include crashworthiness, a name sometimes given to large deflection, elastic-plastic dynamic response analysis when it is applied to stiffened vehicular structures [335-337]; and fluid-structure or solid-structure interaction, which is important for predicting the response of submarine structures to hydrodynamic shock waves and the response of nuclear structures such as containment vessels and piping to earthquakes [338, 339]. Also, buckling of structures made of composite material that behaves nonlinearly and irreversibly is not covered. An example is a nuclear containment vessel made of reinforced concrete, which displays rather complex behavior under biaxial loading, as described by Murray and his coworkers [340-341].

Various finite elements used for shell analysis are not described; only the Ahmad element [154] as modified by Zienkiewicz, *et al.* [155], and Pawsey and Clough [156] is briefly mentioned because of its great popularity. Various adaptive finite element mesh refinement schemes, such as that discussed by Babuska and Rheinbolt [342], are not enlarged upon here. Creep buckling is only discussed for situations in which there is combined creep and plasticity; the important work of Samuelson [343] is omitted.

Finally, the important area of simple formulas for plastic buckling is neglected. Griffin [344] presents inelastic and creep buckling formulas for axial compression, bending, and twisting of cylindrical shells, and Neale [345] describes a method for estimation of plastic buckling loads. Gerdeen [346] has written a survey of limit analysis and Nickel [347] has written a survey of simplified analytical methods involving plasticity and creep.

SUGGESTIONS FOR FURTHER WORK

Plastic buckling is a difficult field for the engineer or designer to understand. The simultaneous presence of moderately large deflections and nonlinear path-dependent material behavior leads to a multitude of possibilities for misusing sophisticated state-of-the-art computer programs created to explore plastic buckling. If the load increment is too large the solution may fail to converge. It may converge to the wrong answer because of an inadequate model of the path-dependent material behavior in the plastic range, because the discretization is too coarse, or because of drift from the equilibrium path. If the load increment is too small, excessive computer time will be used. A discretization which is optimal for a prebifurcation analysis of a structure is not necessarily adequate for the bifurcation phase. Boundary conditions may differ in the prebuckling and bifurcation buckling phases. Load-deflection paths for structures under destabilizing loads, especially thin shell structures, often appear to be almost linear until they abruptly change direction near the critical load. This abrupt change in stiffness requires the use of variable load or time increments.

Most computer programs for plastic buckling analysis require decisions by the user that he or she, through lack of general knowledge about the phenomenon of plastic buckling or mistaken intuition with regard to the specific case at hand, may not be adequately prepared to make. This frequent mismatch between the computer program and the user can be diminished by the introduction of strategy parameters into the program that cause some of the decisions about load or time step discretization and method of solution of the nonlinear equations to be made automatically. The mismatch can be further diminished by education of the user in two ways: education about plastic buckling in general, gained for example by a reading of survey papers such as this one and by analyzing many structures over a period of time; and education about the specific case being treated, gained perhaps by plots, comments, and advice provided by the computer program and its documentation. Almroth, *et al.* [348, 349] offer many suggestions regarding automated selection of strategy parameters and solution techniques based on computerized evaluation of data obtained during a series of previous load steps.

In addition to our expending future effort to develop automated adaptive computerized modeling and solution strategies and user education, we need a better understanding of the time-independent and time-dependent, nonlinear, irreversible behavior of metals and composite materials under multiaxial stress fields. We need better ways to handle the effect of fabrication processes on buckling of assembled structures—processes which include hot and cold rolling plate, cutting plate, cold bending to a prescribed radius, and welding. We need ways to avoid errors associated with poor numerical conditioning near limit points and bifurcation points along equilibrium paths. After all these years and articles devoted to finite element analysis of shell structures, the best method of discretization of a curved surface with finite bending stiffness is still an open question. Finally, we need simple design formulas for structurally simple but phenomenologically complex problems such as plastic buckling of internally pressurized torispherical or ellipsoidal pressure vessel heads and collapse of pipes and elbows under combined bending and internal or external pressure.

ACKNOWLEDGMENTS

This work was performed for the Air Force Office of Scientific Research under Contract F49620-77-C-0122. Lt. Col. Joseph Morgan was contract monitor. The author is grateful for permission to use many figures from various papers on plastic buckling by eminent researchers.

The author very much appreciates the contributions of the following experts in plastic buckling: Oscar Hoffman and Bo Almroth, Lockheed Palo Alto Research Laboratory, California; Larry Sobel, Advanced Reactors Division of Westinghouse Electric Corp., Madison, Pennsylvania; Klaus-Jürgen Bathe, Dept. of Mechanical Engineering, Massachusetts Institute of Technology, Cambridge, Mass.; Pål G. Bergan, University of Trondheim, Norway; Viggo Tvergaard, Dept. of Solid Mechanics, Technical University of Denmark, Lyngby; and Jon Hagstrom, Chicago Bridge & Iron. These scientists took time from their busy schedules to read the manuscript and offer numerous helpful comments for its improvement. Colleen Miller drew many of the figures.

REFERENCES

[1] Brush, D. O. and Almroth, B. O., *Buckling of Bars, Plates and Shells,* McGraw-Hill, New York, (1975).

[2] Hutchinson, J. W., and Koiter, W. T., "Postbuckling Theory," *Appl. Mech. Rev.,* Vol. 23, pp. 1353-1365 (1970).

[3] Hutchinson, J. W., "Plastic Buckling" *Advances in Applied Mechanics* (C. S. Yih, Ed.), Vol. 14, Academic Press, New York, pp. 67-144 (1974).

[4] Sewell, M. J., "A Survey of Plastic Buckling," in *Stability* (H. Leipholz, Ed.), Chap. 5, pp. 85-197, Univ. of Waterloo Press, Ontario (1972).

[5] Tvergaard, V., "Buckling Behavior of Plate and Shell Structures," *Proc. 14th Int. Congr. Theor. and Appl. Mech.* (W. T. Koiter, Ed.) pp. 233-247, North-Holland Publishing Co. (1976).

[6] Tvergaard, V., "On the Numerical Analysis of Necking Instabilities and of Structural Buckling in the Plastic Range," in *Proc. Int. Conf. on Finite Elements in Nonlinear Solid and Structural Mechanics,* Norway, Aug. (1977).

[7] Hutchinson, J. W., "On the Postbuckling Behavior of Imperfection-Sensitive Structures in the Plastic Range," *J. Appl. Mech.* Vol. 39, pp. 155-162 (1972).

[8] Hutchinson, J. W., "Post-Bifurcation Behavior in the Plastic Range," *J. Mech. Phys. Solids,* Vol. 21, pp. 163-190 (1973).

[9] Hutchinson, J. W., "Imperfection Sensitivity in the Plastic Range," *J. Mech. Phys. Solids,* Vol. 21, pp. 191-204 (1973).

[10] Needleman, A., "Post-Bifurcation Behavior and Imperfection Sensitivity of Elastic-Plastic Circular Plates, *Int. J. Mech. Sci.,* Vol. 17. No. 1, pp. 1-14 (1975).

[11] Tvergaard, V. and Needleman, A., "On the Buckling of Elastic-Plastic Columns with Asymmetric Cross-sections," *Int. J. Mec. Sci.,* Vol. 17 pp. 419-424 (1975).

[12] Tvergaard, V. and Needleman, A., "Buckling of Eccentrically Stiffened Elastic-Plastic Panels on Two Simple Supports or Multiply Supported," *Int. J. Solids Structures,* Vol. 11, pp. 647-663 (1975).

[13] Tvergaard, V. and Needleman A., "Mode Interaction in a Eccentrically Stiffened Elastic-Plastic Panel Under Compression," *Buckling of Structures* (B. Budiansky, Ed.), Springer-Verlag, pp. 160-171 (1976).

[14] Needleman, A. and Tvergaard, V., "An Analysis of the Imperfection-Sensitivity of Square Elastic-Plastic Plates Under Axial Compression, *Int. J. Solids Structures,* Vol. 12, pp. 185-201 (1976).

[15] Tvergaard, V., "Buckling of Elastic-Plastic Cylindrical Panel Under Axial Compression," *Int. J. Solids Structures,* Vol. 13, pp. 957-970 (1977).

[16] Tvergaard, V., "Buckling of Elastic-Plastic Oval Cylindrical Shells Under Axial Compression," *Int. J. Solids Structures,* Vol. 12, pp. 683-691 (1976) (see also Errata, *ibid.,* Vol. 14, p. 329 (1978).

[17] Hutchinson, J. W. and Budiansky, B., "Analytical and Numerical Study of the Effects of Initial Imperfections on the Inelastic Buckling of a Cruciform Column," *Buckling of Structures,* (B. Budiansky, Ed.), Springer-Verlag, pp. 98-105 (1976).

[18] Budiansky, B. and Hutchinson, J.W., "Buckling: Progress and Challenge," *Trends in Solid Mechanics,* Dalft Univ. Press, The Netherlands, (1979).

[19] Pilkey, W., Saczalski , K., and Schaeffer, H. (Eds.), *Structural Mechanics Computer Programs: Surveys, Assessments, and Availability,* Univ. Press of Virginia, Charlottesville, Virginia (1974).

[20] Bushnell, D., "A Computerized Information Retrieval Systems," pp. 735-804 in [19] (1974).

[21] Yamada, Y., "Verification and Qualification Activities in Japan of Inelastic Analysis Computer Programs," ASME Paper 76-PVP-44, presented at Joint Petroleum Mechanical Eng. and Pressure Vessels & Piping Conf., Mexico City, Sept. 19-24, 1976.

[22] Bushnell, D., "BOSOR5—Program for Buckling of Elastic-Plastic Complex Shells of Revolution Including Large Deflections and Creep," *Computers & Structures,* Vol. 6, pp. 221-239 (1976).

[23] Bushnell, D., "Stress, Buckling and Vibration of Hybrid Bodies of Revolution," *Computers & Structures,* Vol. 7, pp. 517-537 (1977).

[24] Hill, R., "On the Problem of Uniqueness in the Theory of a Rigid/Plastic Solid," *J. Mech. Phys. Solids,* Vol. 4, pp. 247-255 (1956).

[25] Hill, R., "A General Theory of Uniqueness and Stability in Elastic/Plastic Solids," *J. Mech. Phys. Solids,* Vol. 6, pp 236-249 (1958)

[26] Hill, R., "Some Basic Principles in the Mechanics of Solids Without a Natural Time," *J. Mech. Phys. Solids,* Vol. 7, pp. 209-225 (1959).

[27] Hill, R. "Bifurcation and Uniqueness in Nonlinear Mechanics of Continua," pp. 155-164 (Muskhelishvili Volume), Soc. Ind. Appl. Meth., Philadelphia, Pennsylvania (1961).

[28] Koiter, W.T., "Over de stabiliteit van het elastisch evenwicht," Delft thesis, H. J. Paris, Amsterdam; (England transl.) Nat. Aeronaut. Space Admin. Rep. TTF-10, 1967 (1945).

[29] Koiter, W. T., "Stress-Strain Relations, Uniqueness, and Variational Theorems for Elastic-Plastic Materials with a Singular Yield Surface," *Quart. Appl. Math.,* Vol. 11, pp. 350-354 (1953).

[30] Biot, M. H., *Mechanics of Incremental Deformation,* J. Wiley, New York (1965).

[31] Fung, Y.C., *Foundations of Solid Mechanics,* Prentice-Hall, Englewood Cliffs, New Jersey (1965).

[32] Washizu, K., *Variational Methods in Elasticity and Plasticity,* Pergamon Press, New York (1968).

[33] Green, A. E. and Zerna, W., *Theoretical Elasticity,* 2nd Ed. Oxford Univ. Press, London and New York (1968).

[34] Malvern, L. E., *Introduction to the Mechanics of a Continuous Medium,* Prentice-Hall, Englewood Cliffs, New Jersey (1969).

[35] Oden, J. T., *Finite Elements of Nonlinear Continua,* McGraw-Hill, New York (1972).

[36] Przemieniecki, J. S., *Theory of Matrix Structural Analysis,* McGraw-Hill, New York (1968).

[37] Zienkiewicz, O. C., The Finite Element Method in Engineering Science, McGraw-Hill, London (1971).

[38] Desai, C. S. and Abel, J. F., *Introduction to the Finite Element Method,* Van Nostrand Reinhold Co., New York (1972).

[39] Martin, H. C. and Carey, G. F., *Introduction to Finite Element Analysis: Theory and Applications,* McGraw-Hill, New York (1973).

[40] Gallagher, R. H., *Finite Element Analysis: Fundamentals,* Prentice-Hall, Englewood Cliffs, New Jersey (1975).

[41] Ralston, A., *A First Course in Numerical Methods,* McGraw-Hill, New York (1965).

[42] Byrne, G. D. and Hall, C. A. (Eds.) *Numerical Solution of Systems of Nonlinear Algebraic Equations,* Academic Press, New York (1973).

[43] Hildebrand, F. B., *Introduction to Numerical Analysis,* McGraw-Hill, New York (1974).

[44] Dahlquist, G. and Björk, Å., *Numerical Methods,* Prentice-Hall, Englewood Cliffs, New Jersey (1974).

[45] Bathe, K. J. and Wilson, E. L., *Numerical Methods in Finite Element Analysis,* Prentice-Hall, Englewood Cliffs, New Jersey (1976).

[46] Hartung, R. F. (Ed.), *Numerical Solution of Nonlinear Structural Problems,* AMD Vol. 6, ASME, New York (1973).

[47] Oden, J. T., *et al.* (Eds.), *Computational Methods in Nonlinear Mechanics,* Proc. Int. Conf. on Computational Methods in Nonlinear Mechanics (Austin, Texas, Sept. 1974), TICOM, Univ. of Texas, Austin, Texas (1974).

[48] *Belytschko, T.,* Osias, J. R., and Marcal, P. V. (Eds.), *Finite Element Analysis of Transient Nonlinear Structural Behavior,* AMD Vol. 10, ASME, New York (1975).

[49] Bathe, K. J., Ramm, E., and Wilson, E. L., "Finite Element

Formulations for Large Deformation Dynamic Analysis," *Int. J. Numerical Methods,* Vol. 9, pp. 353-386 (1975).

[50] Bathe, K. J. and Ozdemir, H., "Elastic-Plastic and Dynamic Analysis," *Computers & Structures,* Vol. 6, No. 2, pp. 81-92 (1976).

[51] Bathe, K. J., "An Assessment of Current Finite Element Analysis of Nonlinear Problems in Solid Mechanics," *Proc. SYNSPADE 1975,* Academic Press, New York (1976).

[52] Stricklin, J. A., Haisler, W. E., and von Riesemann, W. A., "Evaluation of Solution Procedures for Material and/or Geometrically Nonlinear Structural Analysis," *AIAA J.,* Vol. 11, No. 3, pp. 292-299, March 1973.

[53] Stricklin, J. A., Von Riesemann, W. A., Tillerson, J. R. and Haisler, W. E., "Static Geometric and Material Nonlinear Analysis," pp. 301-324 of [85] (1972).

[54] Tillerson, J. R., Stricklin, J. A., and Haisler, W. E., "Numerical Methods for the Solution of Nonlinear Problems in Structural Analysis," pp. 67-101 of [46] (1973).

[55] Felippa, C. A., "Procedures for Computer Analysis of Large Nonlinear Structural Systems," *Large Engineering Systems,* (A. Wexler, Ed.), pp. 60-101, Pergamon Press (1977).

[56] Felippa, C. A. and Park, K. C., "Direct Time Integration Methods in Nonlinear Structural Dynamics," Proc. Int. Conf. on Finite Elements in Nonlinear Mechanics (FENOMECH 1978), Univ. of Stuttgart, West Germany, Aug. 1978, to appear, *Computer Meth. in Appl. Mech. & Engng.,* Vol. 17 (1979).

[57] Nickell, R. E., "Direct Integration Methods in Structural Dynamics," *ASCE J. Engng. Mech. Div.,* Vol. 99, pp. 303-317 (1973).

[58] Belytschko, T., "*Transient* Analysis," pp. 255-276 of [19] (1974).

[59] Zudans, Z., "Implicit and Explicit Computational Schemes in Dynamic Plasticity," *J. of Pressure Vessel Technology,* ASME, (1976) (ASME Paper 76-PVP-B).

[60] Haisler, W. E., Stricklin, J. A., and Key, J. E., "Displacement Incremention in Nonlinear Structural Analysis by the Self-correcting Method," *Int. J. Num. Meth. Engng.,* Vol. 11, pp. 3-10 (1977).

[61] Bergan, P.G. and Søreide, T. H., "A Comparative Study of Different Solution Techniques as Applied to a Nonlinear Structural Problem," *Computer Meth. Appl. Mech. Engng.,* Vol. 2, pp. 185-201 (1973).

[62] Bergan, P. G., Horrigmoe, G., Kråkeland, B., and Søreide, T. H., "Solution techniques for nonlinear finite element problems," *Int. J. Num. Meth. Engng.,* Vol. 12, pp. 1677-1696 (1978).

[63] Bergan, P. G., Holand, I., and Søreide, T. H., "Use of the Current Stiffness Parameter in Solution of Nonlinear Problems," in *Energy Methods in Finite Element Analysis,* R. Glowinski, E. Y. Rodin, and O. C., Zienkiewicz (Eds.) J. Wiley & Sons, New York pp. 265-282 (1979).

[64] Mondkar, D. P. and Powell, G. H., "Finite Element Analysis of Nonlinear Static and Dynamic Response," *Int. J. Num. Meth. Engng.,* Vol. 11, pp. 499-520 (1977).

[65] Riks, E., "The Application of Newton's Method to the Problem of Elastic Stability, *J. Appl. Mech.,* Vol. 39, pp. 1060-1065 (1972).

[66] Riks, E., "The Solution of Snapping and Buckling Problems," *Proc. of the 14th Int. Cong. of Theor. and Appl. Mech* (IUTAM), Delft, the Netherlands (1976).

[67] Haftka, R. T., Mallett, R. H., and Nachbar, W., "Adaptation of Koiter's Method to Finite Element Analysis of Snap-through Buckling Behavior," *Int. J. Solids Structures,* Vol. 7, pp. 1427-1445 (1971).

[68] Cohen, G. A. and Haftka, R. T., "Feasibility Study of Shell Buckling Analysis Using the Modified Structure Method," NASA CR-2008, March, 1972.

[68a] Nickell, R. E., "Nonlinear Dynamics by Mode Superposition," *Proc. 15th AIAA/ASME Structures, Structural Dynamics and Material Conf.,* paper 74-341 (1974).

[68b] Nagy, D. A., "Modal Representation of Geometrically Nonlinear Behavior by the Finite Element Method," paper presented at 4th SMiRT Conf., San Francisco (August 1977).

[69] Almroth, B. O., Stern, P., and Brogan, F. A., "Automatic Choice of Global Shape Functions in Structural Analysis, "*AIAA J.,* Vol. 16, No. 5, pp. 525-528 (May, 1978).

[70] Noor, A. K. and Peters, J. M., "Reduced Basis Technique for Nonlinear Analysis of Structures," *Proc. 20th AIAA/ASME Structures Meeting,* St. Louis, MO, pp. 116-126, AIAA Paper No. 79-0747, April, 1979.

[71] Hajela, P. and Sobiezczanski-Sobieski, J., "Accuracy of an Approximate Static Structural Analysis Technique Based on Stiffness Matrix Eigenmodes," *Ibid.,* pp. 127-136.

[72] Hoffman, O. and Sachs, G., *Introduction to the Theory of Plasticity for Engineers,* McGraw-Hill, New York (1953).

[73] Prager, W., *An Introduction to Plasticity,* Addison-Wesley, Reading, Massachusetts (1959).

[74] Hodge, P. G., *Plastic Analysis of Structures,* McGraw-Hill, New York (1959).

[75] Mendelson, A., *Plasticity: Theory and Applications,* Macmillan, New York (1968).

[76] Hill, R., *The Mathematical Theory of Plasticity,* (6th Ed.) Clarendon Press, Oxford (1971).

[77] Saczalski, K. J., Stricklin, J. A., *The Office of Naval Research Plasticity Workshop,* Texas A&M Univ., Rept. 75-51, June, 1975.

[78] Stricklin, J. A. and Saczalski, K. J. (Eds.), *Constitutive Equations in Viscoplasticity: Computational and Engineering Aspects,* ASME AMD Vol. 20 (1976).

[79] Hunsaker, B., Vaughan, D. K., and Stricklin, J. A., "A Comparison of the Capability of Four Hardening Rules to Predict a Material's Plastic Behavior," *J. Pressure Vessel Tech.,* Vol. 98, pp. 66-74 (Feb., 1976).

[80] Armen, H., Jr., "Assumptions, Models, and Computational Methods for Plasticity, *Computers & Structures,* Vol. 10, pp. 161-174 (1979).

[81] Knets, I. V., *Fundamental Modern Direction in the Mathematical Theory of Plasticity* (in Russian), Zinatne Press, Riga USSR, 1971; translated to English by Morris Friedmann, Lockheed MSC, Palo Alto, California (Available through National Translation Center, Chicago, ILL.).

[82] Almroth, B. O., "Evaluation of Available Technology for Prediction of Plastic Strain," pp. 201-211 of [78] (1976).

[83] Gallagher, R. H., Yamada, Y., and Oden, J. T. (Eds.) *Proc. 1st U.S.-Japan Seminar on Matrix Methods in Structural Mechanics and Design,* Tokyo, August 1969, UAH Press, University of Alabama, Alabama (1970).

[84] *Proc. Symposium of Applications of Finite Element Methods in Civil Engineering* (Nashville, Tennessee, Nov. 1969), Vanderbilt Univ., Nashville, Tenn. (1970).

[85] Oden, J. T., Clough, R. W., and Yamamoto, Y. (Eds.) *Proc. 2nd U.S.-Japan Seminar on Advances in Computational Methods in Structural Mechanics and Design* (Berkeley, California, August 1972), UAH Press, Univ. of Alabama, Huntsville, Alabama (1972).

[86] Fenves, S. J., Perrone, N., Robinson, A. R., and Schnobrich, W. C. (Eds.), *Numerical and Computer Methods in Structural Mechanics,* Academic Press, New York (1973).

[87] Bathe, L. J., Oden, J. T., and Wunderlich, W., *Formulations and Computational Algorithms in Finite Element Analysis,* U.S.-Germany Symposium, Massachusetts Institute of Technology, Aug., 1976 (1977).

[88] Engesser, F. "Ueber die knickfestigkeit geradu stråbe," *Z. Architek Ing.,* Vol. 35, p. 455 (1889).

[89] Considère, A., "Resistance des Pieces Comprimees, "*Congress*

Inst. Procedes de Construction, p. 371, Annexe, Librairie Polytechnique, Paris (1981).

[90] von Kármán, Th., "Untensuchungen uder Knickfestigkeit, , Mitteilungen uder Forschungsarbeiten," *Verein Deutsc. Ing.,* Vol. 81 (1910).

[91] Shanley, F. R., "Inelastic Column Theory," *J. Aeronaut. Sci.,* Vol. 14, pp. 261-267 (1947).

[92] Duberg, J. E. and Wilder, T. W., III, "Column Behavior in the Plastic Stress Range," *J. Aero Sci.,* Vol. 17, p. 323 (1950).

[93] Handelman, G. H. and Prager, W., "Plastic Buckling of a Rectangular Plate Under Edge Thrusts," NACA TN 1530, August 1948.

[94] Stowell, E. Z., "A unified Theory of Plastic Buckling of Columns and Plates," NACA TN 1556, April, 1948.

[95] Bijlaard, P. P., "Theory and Tests on the Plastic Stability of Plates and Shells," *J. Aero. Sci.* Vol. 16, pp. 529-541 (1949).

[96] Batdorf, S. B., "Theories of Plastic Buckling," *J. Aero. Sci.,* Vol. 16, pp. 405-408 (1949).

[97] Onat, E. T. and Drucker, E. T., "Inelastic Instability and Incremental Theories of Plasticity," *J. Aero. Sci.,* Vol. 20, pp. 181-186 (1953).

[98] Pride, R. A. and Helmerl, G. J., "Plastic Buckling of Simply-Supported Compressed Plates," NACA TN 1817, April, 1949.

[99] Jones, R. M., "Plastic Buckling of Eccentrically Stiffened Circular Cylindrical Shells," *AIAA Journal,* Vol. 5, pp. 1147-1152 (1967).

[100] Batterman, S. C., "Tangent Modulus Theory for Cylindrical Shells: buckling under increasing load," *Int. J. Solids Struct.,* Vol. 3, p. 501 (1967).

[101] Batterman, S. C., "Plastic Stability of Spherical Shells," *J. Engng Mech. ASCE,* Vol. EM2, pp. 433-446 (1969).

[102] Gerard, G. and Becker, H., "Handbook of Structural Stability: Part I — Buckling of Flat Plates," *Nat. Adv. Comm. Aeronaut. Tech. Note,* p. 3781 (1957).

[103] Smith, S. and Almroth, B. O., "An Experimental Investigation of Plastic Flow Under Biaxial Stress, *Exp. Mech.* (June, 1970).

[104] Michno, M. J., Jr. and Findley, W. N., "An Historical Perspective of Yield Surface Investigations for Metals," *Int. J. Nonlinear Mechanics,* Vol. 11, pp. 59-82 (1976).

[105] Hecker, S. S., "Experimental Studies of Yield Phenomena in Biaxially Loaded Metals," pp. 1-34 of [78] (1976).

[106] Drucker, D. C., "A Discussion of Theories of Plasticity," *J. Aero. Sci.,* Vol. 16, pp. 567-568 (1949).

[107] Cicala, P., "On the Plastic Buckling of a Compressed Strip," *J. Aero Sci.,* Vol. 17, pp. 378-379 (1950).

[108] Bijlaard, P. P., "On the Plastic Buckling of Plates," *J. Aero. Sci.,* Vol. 17, pp. 742-743 (1950).

[109] Koga, T. and Hoff, N. J., "The Axisymmetric Snap-Through Buckling of Thin-Walled Spherical Shells," *Int. J. Solids Structures,* Vol. 5, p. 169 (1969).

[110] Turner, J. L., Clough, R. W., Martin, H. C., and Topp, L. J., "Stiffness and Deflection Analysis of Complex Structures," *J. Aero Sci.,* Vol. 23, pp. 805-825 (1956).

[111] Turner, M. J., Dill, E. H., Martin, H. C., and Melosh, R. J., "Large Deflection Analysis of Complex Structures Subjected to Heating and External Loads," *J. Aero. Space Sci.,* Vol. 27, pp. 97-106 (1960).

[112] Argyris, J. H., "Recent Advances in Matrix Methods of Structural Analysis," *Progress in Aeronautical Sciences,* Vol. 4, Pergamon Press, Oxford and London (1963).

[113] Gallagher, R. H., and Padlog, J., "Discrete element approach to structural instability analysis," *AIAA J.,* Vol. 1, No. 6, pp. 1437-1439 (1963).

[114] Argyris, J. H., Kelsey, S., and Kamel, H., "Matrix Methods of Structural Analysis—a Precis of Recent Developments," *Matrix Methods in Structural Analysis*-AGARDograph 72 (B. Fraeijs de Veubeke, Ed.), Pergamon Press, Oxford, pp. 1-164 (1964).

[115] Argyris, J. H., "Matrix Analysis of Three-Dimensional Elastic Media, Small and Large Displacements," *AIAA J.,* Vol. 3, pp. 45-51 (1965).

[116] Martin, H. C., "Derivation of Stiffness Matrices for the Analysis of Large Deflection and Stability Problems," *Proc. 1st Conf. on Matrix Methods in Struct. Mech.,* AFFDL-TR-66-80, pp. 697-716 (1966).

[117] Gallagher, R. H., Gellatly, R.A., Padlog, J., and Mallett, R. H., "Discrete Element Procedure for Thin-shell Instability Analysis," *AIAA J.,* Vol. 5, No. 1, pp. 138-144 (1967).

[118] Mallett, R. H., and Marcal, P. V., "Finite-Element Analysis of Nonlinear Structures," *J. Struct. Div.,* ASCE, Vol. 94, ST9, pp. 2081-2105 (1968).

[119] Murray, D. W. and Wilson, E. L., "Finite-Element Postbuckling Analysis of Thin Elastic Plates," *AIAA J.,* Vol. 7, No. 10, pp. 1915-1920 (Oct., 1969).

[120] Oden, J. T., "Numerical Formulation of Nonlinear Elasticity Problems," *J. Struct. Div.,* ASCE, Vol. 93, ST3, pp. 235-255 (1967).

[121] Oden, J. T. and Key, J. E., "Numerical Analysis of Finite Axisymmetric Deformation of Incompressible Elastic Solids of Revolution," *Int. J. Solids and Struct.,* Vol. 6, pp. 497-518 (1970).

[122] Stricklin, J. A., Haisler, W. E., and Von Riesemann, W. A., "Self-Correcting Initial Value Formulations in Nonlinear Structural Mechanics," *AIAA Journal,* Vol. 9, No. 10, pp. 2066-2067 (Oct. 1971).

[123] Martin, H. C., "Finite Element Formulation of Geometrically Nonlinear Problems," Paper US 2-2, *Proceedings of Japan-U.S. Seminar on Matrix Methods in Structural Analysis and Design,* Tokyo, pp. 1-53 (1969).

[124] Oden, J. T., "Finite Element Applications in Nonlinear Structural Analysis," pp. 419-457 in [84] (1970).

[125] Haisler, W. E., Stricklin, J. A., and Stebbins, F. J., "Development and Evaluation of Solution Procedures for Geometrically Nonlinear Structural Analysis," *AIAA J.,* Vol. 10, pp. 264-272 (1972).

[126] Gallagher, R. H., Padlog, J., and Bijlaard, P. P., "Stress Analysis of Heated Complex Shapes," *J. American Rocket Society,* Vol. 32, pp. 700-707, (May, 1962).

[127] Argyris, J. H., "Elasto-Plastic Matrix Displacement Analysis of Three-Dimensional Continua," *J. of the Royal Aeronautical Society,* Vol. 69, pp. 633-636 (1965).

[128] Swedlow, J. L. and Yang, W. H., "Stiffness Analysis of Elastic Plastic Plates," Graduate Aero. Lab, C.I.T., SM65-10 (1965).

[129] Pope, G. G., "The Application of the Matrix Displacement Method in Plane Elasto-Plastic Problems," *Proc. of Conf. on Matrix Methods in Structural Mech.,* AFFDL-TR-66-80, pp. 635-654 (Oct., 1966).

[130] Marcal, P. V., "A Stiffness Method for Elastic-Plastic Problem," *Int. J. Mech. Sci.,* Vol. 7, pp. 229-238 (1965).

[131] Marcal, P. V. and Pilgrim, W. R., "Stiffness Method for Elastic-Plastic Shells of Revolution," *J. of Strain Anal.,* Vol. 1, pp. 339-350 (1966).

[132] Marcal, P. V. and King, I. P., "Elastic-Plastic Analysis of Two-Dimensional Stress Systems by the Finite Element Method," *Int. J. Mech. Sci.,* Vol. 9, No. 3, pp. 143-155 (1967).

[133] Marcal, P. V., "A Comparative Study of Numerical Methods of Elastic-Plastic Analysis," *AIAA J.,* Vol. 6, No. 1, pp. 157-158 (June, 1968).

[134] Witmer, E. A. and Kotanchik, J. J., "Progress Report on Discrete-Element Elastic and Elastic-Plastic Analysis of Shells of Revolution Subjected to Axisymmetric and Asymmetric Loading," *Proc. of the 2nd Conf. on Matrix Methods in Structural Mechanics,* AFFDL-TR-

68-150, pp. 1,341-1,453 (Dec., 1969).

[135] Zienkiewicz, O. C., Valliappan, S., and King, I. P., "Elasto-Plastic Solutions of Engineering Problems: 'Initial Stress,' Finite-Element Approach," *Int. J. Numerical Methods Engng.,* Vol. 1, pp. 75-100 (1969).

[136] Yamada, Y., Yoshimura, N., and Sakurai, T., "Plastic Stress-Strain Matrix and Its Application for the Solution of Elastic-Plastic Problems by the Finite Element Method," *Int. J. Mech. Sci.,* Vol. 10, pp. 343-354 (1969).

[137] Khojasteh-Bakht, M., and Popov, E. P., "Analysis of Elastic-Plastic Shells of Revolution," *J. of Eng. Mech. Div.,* ASCE, Vol. 96, No. EM3, pp. 327-340 (June, 1970).

[138] Marcal, P. V., "Finite Element Analysis with Material Nonlinearities—Theory and Practice, pp. 257-282 of [85] (1972).

[139] Yamada, Y., "Recent Japanese Developments in Matrix Displacement method for Elastic-Plastic Problems," in [83] (1970).

[140] Felippa, C. A., "Refined Finite Element Analysis of Linear and Nonlinear Two-Dimensional Structures," Ph.D Thesis, University of California, Berkeley (1966).

[141] Armen, H., Jr., Pifko, A., and Levine, H. S., "Finite Element Method for the Plastic Bending Analysis of Structures," *Proc. 2nd Conf. on Matrix Methods in Structural Mechanics,* AFFDL-TR-150, pp. 1,301-1,339 (Oct., 1968).

[142] Pifko, A. and Isakson, G., "A Finite Element Method for the Plastic Buckling of Plates," *AIAA J.,* Vol. 7, No. 10 (1969).

[143] Hibbitt, H. D., Marcal, P. V., and Rice, J. R., "Finite Element Formulation for Problems of Large Strain and Large Displacements," *Int. J. Solids Struct.,* Vol. 6, pp. 1,069-1,086 (1970).

[144] Marcal, P. V., "Large Deflection Analysis of Elastic-Plastic Shells of Revolution," *AIAA J.,* Vol. 8, No. 9, pp. 1627-1634 (Sept., 1970).

[145] Zudans, Z., "Finite Element Incremental Elastic-plastic Analysis of Pressure Vessels," *J. Engng. Industry,* ASME, Vol. pp. 293-302 (1970).

[146] Dupuis, G. A., Hibbitt, H. D., McNamara, S. F., and Marcal, P. V., "Nonlinear Material and Geometric Behavior of Shell Structures," *Computers & Structures,* Vol. 1, pp. 223-239 (1971).

[147] Maier, G., "Incremental Plastic Analysis in the Presence of Large Displacements and Physical Instabilizing Effects," *Int. J. Solids Structures,* Vol. 7, pp. 345-372 (1971).

[148] Yagmai, S., and Popov, E. P., "Incremental Analysis of Large Deflections of Shells of Revolution," *Int. J. Solids Struct.,* Vol. 7, pp. 1,375-1,393 (1971).

[149] Hofmeister, L. D., Greenbaum, G. A., and Evensen, D. A., "Large Strain, Elasto-Plastic Finite Element Analysis," *AIAA J.,* Vol. 9, No. 7, pp. 1,248-1,254 (July 1971).

[150] Zienkiewicz, O. C., and Nayak, G. C., "A General Approach to Problems of Large Deformation and Plasticity Using Isoparametric Elements," *Proc. 3rd Conf. of Matrix Methods in Structural Mechanics,* AFFDL-TR-71-160, pp. 881-928 (Dec. 1971).

[151] Nayak, G. C. and Zienkiewicz, O. C., "Elasto-Plastic Stress Analysis: a Generalization for Various Constitutive Relations Including Strain Softening," *Int. J. Num. Meth. Engng.,* Vol. 5, pp. 113-135 (1972).

[152] Levine, H. S., Armen, H., Jr., Winter, R., and Pifko, A., "Nonlinear Behavior of Shells of Revolution under Cyclic Loading," *Computers & Structures,* Vol. 3, pp. 589-617 (May, 1973).

[153] Levine, H. S. and Svalbonas, V., "Inelastic Nonlinear Analysis of Stiffened Shells of Revolution by Numerical Integration," *ASME J. Press. Ves. Tech.,* Vol. 96, No. 2, pp. (May, 1974).

[154] Ahmad, S., Irons, B. M., and Zienkiewicz, O. C., "Analysis of Thick and Thin Shell Structures by Curved Finite Elements," *Int. J. Num. Meth. Engng.,* Vol. 2, pp. 419-451 (1970).

[155] Zienkiewicz, O. C., Taylor, R. L., and Too, J. A., "Reduced Integration Technique in General Analysis of Plates and Shells," *Int. J. Num. Meth. Engng.,* Vol. 3, pp. 275-290 (1971).

[156] Pawsey, S. F. and Clough, R. W., "Improved Numerical Integration of Thick Shell Finite Elements," *Int. J. Num. Meth. Engng.,* Vol. 3, pp. 575-586 (1971).

[157] Prager, W., "A New Method of Analyzing Stress and Strains in Work-hardening Plastic Solids," *J. Appl. Mech.* Vol. 23, pp. 493-(1956).

[158] Ziegler, H., "A Modification of Prager's Hardening Rule," *Quart. Appl. Math.,* Vol. 17, No. 1, pp. 55-65 (1959).

[159] Besseling, J. F., "A Theory of Elastic, Plastic, and Creep Deformation of an Initially Isotropic Material Showing Strain Hardening, Creep Recovery, and Secondary Creep," *J. Appl. Mech.,* Vol. 25, No. 4, pp. 529-536 (1958).

[160] Mroz, Z., "An Attempt to Describe the Behavior of Metals Under Cyclic Loads Using a More General Workhardening Model," *Acta Mechanica,* Vol. 7, pp. 199-212 (1969).

[161] Eisenberg, M. A. and Phillips, A., "A Theory with non-coincident Yield and Loading Surfaces," *Acta Mech.,* Vol. 11, pp. 247-260 (1971).

[162] Batdorf, S. B. and Budiansky, B., "A Mathematical Theory of Plasticity Based on the Concept of Slip," NACA TN NO. 1871 (1949).

[163] Hodge, P. G. and Berman, I., "Piecewise Linear Strain Hardening Plasticity," *ASME AMD* Vol. 20, pp. 57-77 (1976).

[164] Pugh, C. E., Corum, J. M., Liu, K. C., and Greenstreet, W. L., "Currently Recommended Constitutive Equations for Inelastic Design Analysis of FFTF Components," Oak Ridge National Laboratory, Oak Ridge, Tennessee, Rept. ORNL-TM-3602, Sept., 1972.

[165] Armen, H., Jr., "Plastic Analysis," pp. 37-79 of [19] (1974).

[166] De Salvo, G. J. and Swanson, J. A., "ANSYS Engineering Analysis Systems Manual," Swanson Analysis Systems, Inc., Elizabeth, Pennsylvania (Oct., 1972).

[167] ASAS (Atkins Stress Analysis System), Atkins Research and Development, Ashley Road, Epsom, Surrey, U.K.

[168] Schrem, E., Roy, J. R., "An Automated System for Kinematic Analysis," Institut für Statik und Dynamik der Luft und Raumfahrtkonstructionen, University of Stuttgart, ISD Report No. 98 (1971).

[169] Hellen, T. K., and Protheroe, S. J., "The BERSAFE Finite Element System," *Computer Aided Design* (Jan., 1974).

[170] Zudans, Z., *et al.,* "Theory and User's Manual for EPACA," *Franklin Institute* Report F-C-3038, (June 1972).

[171] "MARC-CDC Nonlinear Finite Element Analysis Program," *User Information Manual,* Vol. 1, Control Data Corp. (1971).

[172] Sharifi, P. and Yates, D. N., "Nonlinear Thermo-Elastic-Plastic and Creep Analysis by the Finite Element Method," *AIAA J.,* Vol. 12, pp. 1,210-1,215 (1974).

[173] Henshell, R. D., "PAFEC 70+ Users Manual," Mechanical Engineering Department, Nottingham University, Nottingham, England (1972).

[174] Pifko, A., Levine, H., and Armen, H., Jr., "PLANS – A Finite Element Program for Nonlinear Analysis of Structures," NASA-CR-2568 (Nov., 1975).

[175] Green, A. E., and Naghdi, P. M., "A General Theory of an Elastic-Plastic Continuum," *Archive for Rational Mechanics and Analysis,* Vol. 18, pp. 251-281 (1965).

[176] Budiansky, B., "Remarks on Theories of Solid and Structural Mechanics," *Problems of Hydrodynamics and Continuum Mechanics,* SIAM, Philadelphia, pp. 77-83 (1969).

[177] Budiansky, B., unpublished notes referred to in Ref. [180].

[178] Lee, E. H., "Elastic-Plastic Deformation at Finite Strains,"

J. Mech. Phys., Vol. 36, pp. 1-6 (March 1969).

[179] Willis, J. R., "Some Constitutive Equations Applicable to Problems of Large Dynamic Plastic Deformation," *J. Mech. Phys. Solids,* Vol. 17, p. 359 (1969).

[180] Hutchinson, J. W., "Finite Strain Analysis of Elastic-Plastic Solids and Structures," AMD-Vol. 6, *Numerical Solution of Nonlinear Structural Problems* (R. F. Hartung, Ed.) ASME, New York, pp. 17-30 (1973).

[181] McMeeking, R. M. and Rice, J. R., "Finite Element Formulations for Problems of Large Elastic-Plastic Deformations," *Int. J. Solids, Struct.,* Vol. 11, pp. 601-616 (1975).

[182] Miles, J. P., "Bifurcation in Plastic Flow Under Uniaxial Tension," *J. Math. Phys. Solids,* Vol. 19, pp. 89-102 (1971).

[183] Chen, W. H., "Necking of a bar," *Int. J. Solids Structures,* Vol. 7, pp. 685-717 (1971).

[184] Needleman, A., "A Numerical Study of Necking in Circular Cylindrical Bars," *J. Mech. Phys. Solids,* Vol. 20, pp. 111-127 (1972).

[185] Hutchinson, J. W. and Miles, J. P., "Bifurcation Analysis of the Onset of Necking in an Elastic-plastic Cylinder Under Uniaxial Tension," *J. Mech. Phys. Solids,* Vol. 22, pp. 61-71 (1974).

[186] Needleman, A., "Void Growth in an Elastic-Plastic Medium," *J. Appl. Mech.,* Vol. 39, pp. 964-970 (1972).

[187] Hill, R. and Hutchinson, J. W., "Bifurcation Phenomena in the Plane Tension Test," *J. Mech. Phys. Solids,* Vol. 23, pp. 239-264 (1975).

[188] Needleman, A., "Bifurcation of Elastic-Plastic Spherical Shells Subject to Internal Pressure," *J. Meth. Phys. Solids,* Vol. 23, pp. 357-367 (1975).

[189] Stören, S. and Rice, J. R., "Localized Necking in Thin Sheets," *J. Mech. Phys. Solids,* Vol. 23, pp. 421-441 (1975).

[190] Tvergaard, V., "Effect of Thickness Inhomogeneities in Internally Pressurized Elastic-Plastic Spherical Shells," *J. Mech. Phys. Solids,* Vol. 24, pp. 291-304 (1976).

[191] Needleman, A. and Tvergaard, V., "Necking of Biaxially Stretched Elastic-Plastic Circular Plates," *J. Mech. Phys. Solids,* Vol. 25, pp. 159-183 (1977).

[192] Tvergaard, V., "On the Burst Strength and Necking Behavior of Rotating Disks," *Int. J. Mech. Sci.,* Vol. 20, pp. 109-120 (1978).

[193] Cyr, N. A. and Teter, R. D., "Finite Element Elastic-Plastic Creep Analysis of Two-Dimensional Continuum with Temperature Dependent Material Properties," *Computers & Structures,* Vol. 3, pp. 849-863 (1973).

[194] Bushnell, D., "Large Deflection Elastic-Plastic Creep Analysis of Axisymmetric Shells," *Numerical Solution of Nonlinear Structural Problems* (R. F. Hartung, Ed.), *AMD* Vol. 6, ASME, New York, 103-138 (1973).

[195] Bushnell, D., "Bifurcation Buckling of Shells of Revolution Including Large Deflections, Plasticity and Creep," *Int. J. Solids Structures,* Vol. 10, pp. 1287-1305 (1974).

[196] Bushnell, D., "A Strategy for the Solution of Problems Involving Large Deflections, Plasticity and Creep," *Int. J. Num. Meth. Engng.,* Vol. 11, pp. 683-708 (1977).

[197] Zienkiewicz, O. C. and Cormeau, I., "Viscoplasticity, Plasticity and Creep in Elastic Solids—a Unified Numerical Solution Approach," *Int. J. Num. Meth. Engng.,* Vol. 8, pp. 821-845 (1974).

[198] Nagarajan, S. and Popov, E. P., "Plastic and Viscoplastic Analysis of Axisymmetric Shells," *Int. J. Solids Structures,* Vol. 11, pp. 1-19 (1975).

[199] Kanchi, M. B., Zienkiewicz, O. C., and Owen, D. R. J., "The Visco-Plastic Approach to Problems of Plasticity and Creep Involving Geometric Nonlinear Effects," *Int. J. Num. Meth. Engng.,* Vol. 12, pp. 169-181 (1978).

[200] Krieg, R. D., "Numerical Integration of Some New Unified Plasticity-Creep Formulations," *Proc. 4th SMiRT Conf.,* Paper M6/4, San Francisco, California (1977).

[201] Hughes, T. J. R. and Taylor, R. L., "Viscoplastic Finite Element Analysis by Unconditionally Stable Implicit Methods," 4th SMiRT Conf., Paper No. M5/5, San Francisco, California (1977).

[202] Rashid, Y. R. and Tang, H. T., "A Numerical Scheme for Treating Strain-Rate-Dependent Plasticity in Piece-Wise-Linear Incremental Analysis," 4th SMiRT Conf, Paper M6/3, San Francisco, California (1977).

[203] Bathe, K-J., "ADINA—a Finite Element Program for Automatic Dynamic Incremental Nonlinear Analysis", Acoustics and Vibration Lab., Dept. of Mech. Eng., M.I.T., Cambridge, Mass. Rept 82448-1 Sept. 1975 (Revised Dec. 1978).

[204] Haisler, W. E. and Sanders, D. R., "Elastic-Plastic-Creep-Large Strain Analysis at Elevated Temperature by the Finite Element Method, *Computers & Structures,* Vol. 10, pp. 375-381 (1979).

[205] Hoffman, A., Livolant, M., and Roche, R., "Plastic Analysis of Shell by Finite Element Method: Global Plasticity Model for Any Shapes of Shells," 2nd SMiRT Conf., Berlin, Paper L6/2 (1973).

[206] Argyris, J. H., Szimmat, J., Willam, K. J., and Pister, K. S., "Finite Element Analysis of Inelastic Structural Behavior," 4th SMiRT Conf. Paper M5/1*, San Francisco, California (1977).

[207] Almroth, B. O., Brogan, F. A., and Stanley, G. M., "Structural Analysis of General Shells, Vol. II: User Instructions for STAGSC," Lockheed Missiles & Space Co., Rept. LMSC-D633873, Jan. 1979.

[208] Mondkar, D. P. and Powell, G. H., "ANSR — A General Purpose Computer Program for Analysis of Nonlinear Structural Response," 4th SMiRT Conf., Paper M 1/4, San Francisco, California (1977).

[209] Callabresi, M. L. and Young, R. C., "Large Strain Elastic-Plastic Analysis of Two-Dimensional Quasi-Static Structures," 4th SMiRT Conf., Paper M7/5, San Francisco, California (1977).

[210] Clinard, J. A., Corum, J. M., and Sartory, W. K., "Comparison of Typical Inelastic Analysis Predictions with Benchmark Problem Experimental Results," *Pressure Vessels and Piping: Verification and Qualification of Inelastic Analysis Computer Programs,* pp. 79-98, ASME Publication G00088 (1975).

[211] Krieg, R. D., "A Practical Two Surface Plasticity Theory, *J. Appl. Mech.,* Vol. 31, pp. 641-644 (1975).

[212] Dafalias, Y.F. and Popov, E. P., "Plastic Internal Variables Formalism of Cyclic Plasticity," *J. Appl. Mech.,* Vol. 43, pp. 645-651 (1976).

[213] Petersson, H. and Popov, E. P., "Constitutive Relations for Generalized Loading," ASCE *J. Eng. Mech. Div.,* EM4, pp. 611-627 (1977). Also see ASCE J. Eng. Mech. Div., EM6, pp. 1371-1388 (1978)

[214] Krieg, R. D. and Key, S. W., "Implementation of a Time-Independent Plasticity Theory into Structural Computer Programs," pp. 125-137 of [78] (1976).

[215] Gallagher, R.H., "Finite Element Analysis of Geometrically Nonlinear Problems," in *Theory and Practice in Finite Element Structural Analysis* (Y. Yamada, R. H. Gallagher, Eds.), University of Tokyo Seminar on Finite Element Analysis, (1973).

[215a] Gallagher, R. H., "Perturbation procedures in Nonlinear finite Element Structural Analysis," *Computational Mechanics Lecture Notes in Mathematics,* No. 461, Springer-Verlag, Berlin, pp. 75-90 (1975).

[216] Yokoo, Y., Nakamura, T., and Uetani, K., "The Incremental Perturbation Method for Large Displacement Analysis of Elastic-Plastic Structures," *Int. J. Num. Meth. Engng.,* Vol. 10, pp. 503-525 (1976).

[217] Sabir, A. B. and Lock, A. C., "The Application of Finite Elements to the Large Deflection Geometrically Nonlinear Behavior of Cylindrical Shells," in *Variational Methods in Engineering* (C. A.

Brebbia and H. Tottenham, Eds.), Southampton University Press, pp. 7/66-7/75 (1973).

[218] Almroth, B. O. and Felippa, C. A., "Structural Stability," pp. 499-539 of [19] (1974).

[219] Bieniek, M. P. and Funaro, J. R., "Elasto-Plastic Behavior of Plates and Shells," Weidlinger Assoc., New York, Report DNA 001-76-C-0125 (March 1976).

[220] Holden, J. T., "On the Finite Deflections of Thin Beams," *Int. J. Solids Struct.*, Vol. 8, pp. 1051-1055 (1972).

[221] Hodge, P. G., Jr., "A New Method of Analysing Stress and Strains in Work Hardening Solids," *J. Appl. Mech.* Vol. 23, pp. 482-483 (1957).

[222] Brandzaeg, A., "Failure of a Material Composed of Non-isotropic Elements," The Royal Norwegian Society of Science, Publication No. 2, Trondheim, Norway (1927).

[223] Christman, D. R., Michaels, T. E., Isbell, W. M., and Babcock, S. G., "Measurements of Dynamic Properties of Materials," Vol. IV, Alpha Titanium, DASA 2501-4, Defense Nuclear Agency, Washington, D.C. (Nov. 1971).

[224] Marin, J., and Hu, L. W., "Biaxial Plastic Stress-Strain Relations of a Mild Steel for Variable Stress Ratios," *Trans. ASME,* Vol. 78, No. 3, pp. 499-509 (April, 1956).

[225] Sewell, M. J., "A Yield Surface Corner Lowers the Buckling Stress of an Elastic-Plastic Plate Under Compression," *J. Mech. Phys. Solids,* Vol. 21, pp. 19-45 (1973).

[226] Hodge, P. G., Jr., "Piecewise Linear Plasticity," *Proc. 9th Int. Cong. Appl. Mech.,* Vol. 8, p. 65 (1957).

[227] Bushnell, D., and Galletly, G. D., "Comparisons of Test and Theory for Nonsymmetric Elastic-Plastic Buckling of Shells of Revolution," *Int. J. Solids Struct.,* Vol. 10, pp. 1,271-1,286 (1974).

[228] Bushnell, D., "Buckling of Elastic-Plastic Shells of Revolution with Discrete Elastic-Plastic Ring Stiffeners," *Int. J. Solids Structures,* Vol. 12, pp. 51-66 (1976).

[229] Lagae, G. and Bushnell, D., "Elastic-Plastic Buckling of Internally Pressurized Torispherical Vessel Heads," *Nuclear Engineering and Design,* Vol. 48, pp. 405-414 (1978).

[230] Bushnell, D., "Nonsymmetric Buckling of Internally Pressurized Ellipsoidal and Torispherical Elastic-Plastic Pressure Vessel Heads," *ASME J. of Pressure Vessel Technology,* Vol. 99, pp. 54-63 (Feb. 1977).

[231] Bushnell, D. and Galletly, G. D., "Stress and Buckling of Internally Pressurized Elastic-Plastic Torispherical Vessel Heads—Comparisons of Test and Theory," *ASME J. Pressure Vessel Technology,* Vol. 99, pp. 39-53 (Feb. 1977).

[232] Bushnell, D., "Effect of Cold Bending and Welding on Buckling of Ring-Stiffened Cylinders," *Computers and Structures,* Vol. 12, pp. 291-307 (1980).

[233] Bushnell, D., Holmes, A. M. C., and Loss, E. J., "Failure of Axially Compressed Frangible Joints in Cylindrical Shells," presented at 20th AIAA/ASME Structures, Structural Dynamics and Materials Meeting, St. Louis, Missouri, pp. 145-157 of *Volume on Structures* (April, 1979), *Computers and Structures,* Vol. 12, pp. 193-210 (1980).

[234] Roark, R. J., *Formula for Stress and Strain,* 3rd ed., Chap. 10, Art. 55, Case #2, 194, McGraw-Hill, NY (1954).

[235] Lee, L. H. N., "Inelastic Buckling of Initially Imperfect Cylindrical Shells Subject to Axial Compression," *J. Aero. Sci.,* Vol. 29, pp. 87-95 (1962).

[236] Batterman, S. C., "Plastic Buckling of Axially Compressed Cylindrical Shells," *AIAA J.,* Vol. 3, No. 2, pp. 316-325 (Feb., 1965).

[237] Sobel, L. H. and Newman, S. Z., "Plastic Buckling of Cylindrical Shells Under Axial Compression," Third U. S. Congress on Pressure Vessels and Piping, San Francisco, California, June 25-29 Paper #79-PVP-99.

[238] Ramsey, H., "Plastic Buckling of Conical Shells Under Axial Compression," *Int. J. of Mech. Sci.,* Vol. 19, pp. 252-272 (1977).

[239] Gerard, G., "Compressive and Torsional Buckling of Thin Walled Cylinders in the Yield Region," NACA TN 3726 (Aug., 1956).

[240] Murphy, L. M. and Lee, L. H. N., "Inelastic Buckling Process of Axially Compressed Cylindrical Shells Subject to Edge Constraints," *Int. J. Solids Struct.,* Vol. 7, pp. 1,153-1,170 (Sept., 1971).

[241] Gellin, S., "Effect of an Axisymmetric Imperfection on the Plastic Buckling of an Axially Compressed Cylindrical Shell," *J. Appl. Mech.,* Vol. 46, pp. 125-131 (1979).

[242] Boichot, L. and Reynolds, T. E., "Inelastic Buckling Tests of Ring-Stiffened Cylinders under Hydrostatic Pressure," *David Taylor Model Basin Rep.* 1992, Washington, D.C. (May 1965).

[243] Lee, L. H. N., "Inelastic Asymmetric Buckling of Ring-Stiffened Cylindrical Shells Under External Pressure," *AIAA J.,* Vol. 12, No. 8, pp. 1,051-1,056 (1974).

[244] Galletly, G. D., "Stress Failure of Large Pressure Vessels—Recommendations Resulting from Studies of the Collapse of a 68 ft High x 45 ft dia. Pressure Vessel," Tech. Rept. No. 45-57, Shell Development Corp., Emeryville, California (Mar 1957).

[245] Galletly, G. D., "Torispherical Shells — A Caution to Designers," *Trans. ASME,* Vol. 81, Series B, No. 1 (Feb. 1959); also published in *Pressure Vessel and Piping Design — Collected Papers 1927-1959,* ASME, New York (1960).

[246] Drucker, D. C. and Shield, R. J., "Limit Analysis of Symmetrically Loaded Thin Shells of Revolution," *Journal of Applied Mechanics,* Vol. 26, No. 1, pp. 61-68 (March 1959).

[247] Shield, R. J. and Drucker, D. C., "Design of Thin-Walled Torispherical and Toriconical Pressure Vessel Heads," *Journal of Applied Mechanics,* Vol. 28, No. 2, pp. 292-297 (June, 1961).

[248] Gerdeen, J. C. and Hutula, D. N., "Plastic Limit Analysis of Hemispherical and Toriconical Head Pressure Vessels," *Welding Research Council Bulletin* No. 163 (1971).

[249] Crisp, R. J. and Townley, C. H. A., "The Application of Elastic and Elastic-Plastic Analysis to the Design of Torispherical Heads," *First International Conference on Pressure Vessel Technology,* Delft, pp. 345-354 (1969).

[250] Simonen, F. A. and Hunter, D. T., "Elastic-Plastic Deformations in Pressure Vessel Heads," *Welding Research Council Bulletin,* No. 163 (1971).

[251] Calladine, C. R., "Lower-Bound Analysis of Symmetrically Loaded Shells of Revolution," *First International Conference on Pressure Vessel Technology,* Delft., pp. 335-344 (1969).

[252] Savé, M., "Verification Experimentale de l'Analyse Limite Plastique des Plaques et des Coques en Acier Doux," Centre de Recherches Scientifiques et Techniques de L'Industrie des Fabrications Metalliques, Brussels, Belgium (Feb. 1966).

[253] *Use of Computer in Pressure Vessel Analysis, ASME,* 1969 (Papers and Discussion from ASME Computer Seminar, Dallas, Texas (Sept. 26,1968).

[254] Gerdeen, J. C., "Use of the Computer in the Plastic Limit Analysis of Pressure Vessels," *ibid.,* pp. 37-49.

[255] Mescall, J. F., "Large Deflections and Stability of Shells of Revolution," *ibid.,* pp. 1-25.

[256] Marcal, P. V., "Elastic-Plastic Analysis of Pressure Vessel Components," *Ibid.,* pp. 71-81.

[257] Esztergar, E., "Development of Design Rules for Dished Pressure Vessel Heads," *Welding Research Council Bulletin,* 215, April, 1976.

[258] Fino, A. and Schneider, R. W., "Wrinkling of a Large, Thin Code Head Under Internal Pressure," *Welding Research Council Bulletin,* No. 69, June, 1961.

[259] Mescall, J., "Stability of Thin Torispherical Shells Under Uniform Internal Pressure," NASA TN D-1510, *Collected Papers on Instability of Shell Structures,* pp. 671-692, Dec., 1962.

[260] Adachi, J. and Benicek, M., "Buckling of Torispherical Shells

Under Internal Pressure," *Experimental Mechanics,* Vol. 4, No. 8, pp. 217-222 (Aug., 1964).

[261] Thurston, G. and Holston, A. A., Jr., "Buckling of Cylindrical Shell End Closures by Internal Pressure," NASA CR-540 (July, 1966).

[262] Bushnell, D., "Stress, Stability and Vibration of Complex, Branched Shells of Revolution," *Computers & Structures,* Vol. 4, pp. 399-435 (1974).

[263] Cohen, G. A., "Computer Analysis of Ring-Stiffened Shells of Revolution," NASA CR 2085 (Sept., 1972).

[264] Anderson, M., Fulton, R., Heard, W., and Walz, J., "Stress, Buckling and Vibration Analysis of Shells of Revolution," *Computers & Structures,* Vol. 1, pp. 157-192 (1971).

[265] Svalbonas, V. and Key, J., "Static, Stability and Dynamic Analysis of Shells of Revolution by Numerical Integration—A Comparison," *Nuclear Engineering and Design,* Vol. 27, pp. 30-45 (1974).

[266] Kalnins, A., "Analysis of Shells of Revolution Subjected to Symmetrical and Nonsymmetrical Loads," *Journal of Applied Mechanics,* Vol. 31, pp. 467-476 (1964).

[267] Brown, K. W. and Kraus, H., "Stability of Internally Pressurized Vessels with Ellipsoidal Heads," presented at 2nd National Congress on Pressure Vessels and Piping Technology, San Francisco, June 23-27, 1975.

[268] Galletly, G. D., "Internal Pressure Buckling of Very Thin Torispherical Shells—A Comparison of Experiment and Theory," 3rd SMiRT Conf., London, paper G2/3 (1975).

[269] Galletly, G.D., "Elastic and Elastic-Plastic Buckling of Internally Pressurized 2:1 Ellipsoidal Shells," *J. Pressure Vessel Technology,* Vol. 100, pp. 335-343 (1978).

[270] Kirk, A. and Gill, S. S., "The Failure of Torispherical Ends of Pressure Vessels Due to Instability and Plastic Deformation—An Experimental Investigation," *Int. J. Mech. Sci.,* Vol. 17, pp. 525-544 (1975).

[271] Patel, P. R. and Gill, S. S., "Experiments on the Buckling Under Internal Pressure of Thin Torispherical Ends of Cylindrical Pressure Vessels," *Int. J. Mech. Sci.,* Vol. 20, pp. 159-175 (1978).

[272] Ketter, R. L., "The Influence of Residual Stresses on the Strength of Structural Members," *Welding Research Council Bulletin* No. 44, (Nov., 1958).

[273] Almen, J. O. and Black, P. H., *Residual Stresses and Fatigue In Metals,* McGraw Hill, Ch. 5, pp. 46-47 (1963).

[274] Queener, C. A. and De Angelis, R. J., "Elastic Springback and Residual Stresses in Sheet Metal Formed by Bending," *ASM Transactions Quarterly,* Vol. 61, pp. 757-768, (Dec., 1968).

[275] Lunchick, M. E., "Influence of Residual Rolling Stresses on the Strength of Cylindrical Pressure Vessels Under external Loading," *J. Eng. Ind., Trans ASME,* Vol. 92, pp. 275-280 (May, 1970).

[276] Shama, M. A., "Cold Forming Residual Stresses and Their Effect on the Accuracy of Post-Forming Operations," *European Shipbuilding,* Vol. 19 No. 2, pp. 23-26 (1970).

[277] Tacey, R. K., "A Computer Program for Calculation of the Residual Stress Distribution and the Effective Stress-Strain Curve of Cold-Formed Structural Members," David W. Taylor Naval Ship Research and Development Center, Bethesda, Maryland, Report 76-0141, November, 1976.

[278] *Numerical Modeling of Manufacturing Processes,* PVP-PB-025, ASME, New York (R. F. Jones, Jr., H. Armen, and J. T. Fong, Ed.) presented at ASME Winter Annual Meetings Atlanta, Georgia, 1977.

[279] Masubuchi, K., "Numerical Modeling of Thermal Stresses and Metal Movement During Welding," pp. 1-17 of Ref. [278] (1977).

[280] Friedman, E., "Numerical Simulation of the Gas Tungsten-Arc Welding Process," pp. 35-47 of Ref. [278] (1977).

[281] Lobitz, D. W., McClure, J. D., and Nickell, R. E., "Residual Stresses and Distortions in Multi-pass Welding," pp. 81-88 of Ref. [278] (1977).

[282] Hsu, M. B., "Analysis of Welds by the Finite Element Method," pp. 97-115 of Ref. [278] (1977).

[283] Rybicki, E. F., Schmueser, D. W., Stonesifer, R. B., Greom, J. J., and Mishler, H. W., "A Finite Element Model for Residual Stresses in Girth-Butt Welded Pipes," pp. 131-142 of Ref. [278] (1977).

[284] DeYoung, R. M., and Chin, S. S., "Some Applications of Numerical Methods to Practical Welding Problems," pp. 143-156 of Ref. [278] (1977).

[285] Masubuchi, K., "Report on Current Knowledge of Numerical Analysis of Stresses, Strains, and Other Effects Produced by Welding," *Welding in the World,* Vol. 13, No. 11/12, pp. 271-288 (1975).

[286] Hibbitt, H. D., and Marcal, P. V., "A Numerical Thermo-mechanical Model for the Welding and Subsequent Loading of a Fabricated Structure," *Computers & Structures,* Vol. 3, pp. 1145-1174 (1973).

[287] Nickell, R. E. and Hibbitt, H. D., "Thermal and Mechanical Analysis of Welded Structures," *Nuclear Engineering and Design,* Vol. 32, No. 1, pp. 110-120 (April, 1975).

[288] Friedman, E., "Thermomechanical Analysis of the Welding Process Using the Finite Element Methods," *ASME J. of Pressure Vessel Technology,* pp. 206-213 (August, 1975).

[289] Chen, W. F. and Ross, D. A., "Axial Strength and Behavior of Cylindrical Columns," *Proc. 8th Annual Offshore Technology Conference,* Houston, Texas, Vol. 3, pp. 741-754 (May, 1976).

[290] Faulkner, D., "Effects of Residual Stresses on the Ductile Strength of Plane Welded Grillages and of Ring-Stiffened Cylinders," *J. Strain Anal. & Eng. Design,* Vol. 12, pp. 130-139 (April 1977).

[291] Kirstein, A. F. and Slankard, R. C., "An Experimental Investigation of the Shell-Instability Strength of a Machined, Ring-Stiffened Cylindrical Shell Under Hydrostatic Pressure (Model BR-4A)," David Taylor Model Basin, Washington, D.C., Report 997 (April, 1956).

[292] Slankard, R. C., "Tests of the Elastic Stability of a Ring-Stiffened Cylindrical Shell, Model BR-4 Subjected to Hydrostatic Pressure," David Taylor Model Basin, Washington, D.C., Report 876 (Feb., 1955).

[293] Brazier, L. G., "On the Flexure of Thin Cylindrical Shells and Other 'Thin' Sections," *Proc. of the Royal Soc.,* Series A, Vol. 116 pp. 104-114 (1927).

[294] Clark, R. A. and Reissner, E., "Bending of Curved Tubes," *Advances in Applied Mechanics* Vol. 2, pp. 93-122 (1951).

[295] Wood, J. D., "The Flexure of a Uniformly Pressurized Circular Cylindrical Shell," *J. Appl. Mech.,* Vol. 25, pp. 453-458 (1958).

[296] Reissner, E., "On Finite Bending of Pressurized Tubes," *J. Appl. Mech.,* Vol. 26, pp. 386-392 (1959).

[297] Aksel'rad, E. L., "Refinement of the Upper Critical Loading of Pipe Bending Taking Account of the Geometric Nonlinearity," *Izv. An. SSSR, OTN, Mekhanika,* No. 4, pp. 133-139 (1965).

[298] Stephens, W. B., Starnes, J. H., Jr., and Almroth, B. O., "Collapse of Long Cylindrical Shells Under Combined Bending and Pressure Loads," *AIAA J.,* Vol. 13 pp. 20-24 (1975).

[299] Dodge, W. G. and Moore, S. E., "ELBOW: a FORTRAN Program for the Calculation of Stresses, Stress Indices, and Flexibility Factors for Elbows and Curved Pipes," ORNL-TM-4098 (April, 1973).

[300] Hibbitt, H. D., Sorensen, E. P., and Marcal, P. V., "The Elastic-Plastic and Creep Analysis of Pipelines by Finite Elements," *Second International Conference on Pressure Vessel Technology,* ASME, San Antonio, TX, Part 1, pp. 239-251 (Oct. 1973).

[301] Sobel, L. H., "In-plane Bending of Elbows," *Computers & Structures,* Vol. 7, pp. 701-715 (1977).

[302] Rodabaugh, E. C., Iskander, S. K., and Moore, S. E., "End Effects on Elbows Subjected to Moment Loadings," Battelle Columbus

Laboratories, OH, Rept. ORNL/Sub-2913/7 (March, 1978).

[303] Bolt, S. E. and Greenstreet, W. L., "Experimental Determination of Plastic Collapse Loads for Pipe Elbows," ASME Paper 71-PVP-37.

[304] Vrillon, B., Montfort, C., and Befre, J., "Experimental Analysis of Piping Components of Fast Breeder Reactors," *Third Int. Conf. on Structural Mechanics in Reactor Technology* Vol. 2, Part F, Paper F3/4, American Elsevier, New York (1975).

[305] Sherman, D. R., "Tests of Circular Steel Tubes in Bending," *ASCE J. of Structural Div.,* Vol. 102, ST11, pp. 2,181-2,195 (1976).

[306] Bushnell, D., "Use of BOSOR5 for the Elastic-Plastic Bending and Buckling Analysis of Pipes and Elbows," to be published in *Computers and Structures* (1981).

[307] Sobel, L. H. and Newman, S. Z., "Plastic In-Plane Bending and Buckling of an Elbow: Comparison of Experimental and Simplified Analysis Results," Westinghouse Advanced Reactors Div. Report-WARD-HT-94000-2, (Aug., 1979); Available from US-DOE Tech. Inf. Ctr.

[308] Bung, H., Clement, G., Hoffman, A., and Jakubowicz, "Piping Bench-mark Problems Computer Analysis with the CEASEMT Finite Element System," CEASEMT Report EMT/78/61, (Oct., 1978).

[309] Roche, R. and Hoffmann, A., "Global Plastic Models for Computerized Structural Analysis," 4th SMiRT, San Francisco, Paper, L5/5 (1977).

[310] Skogh, J. and Brogan, F., "Collapse Analysis of Finite-Length Pipe Bends," Lockheed Missiles & Space Co. Rept., Dec., 1978.

[311] Remseth, S. N., Holthe, K., Bergan, P. G., and Holand, I., "Tube Collapse Analysis Using Finite Elements," *Computers & Structures,* Vol. 8, pp. 383-390 (1978).

[312] Mello, R. M. and Griffin, D. S., "Plastic Collapse Loads for Pipe Elbows Using Inelastic Analysis," *J. Pressure Vessel Technology,* pp. 177-183 (Aug., 1974).

[313] Sobel, L. H., and Newman, S. Z., "Instability Analysis of Elbows in the Plastic Range," *4th Int. Conf. on Structural Mechanics in Reactor Technology, Vol. L, Inelastic Analysis of Metal Structures,* San Francisco, Paper *L3/2* (1977).

[314] Roche, R., Hoffmann, A., and Vrillon, B., "Piping Systems, Inelastic Analysis-A Simplified Numerical Method," *3rd Int. Conf. on Pressure Vessel Technology,* Tokyo, Japan, ASME, New York, pp. 133-142 (1977).

[315] Spence, J. and Findlay, G., "Limit Load for Pipe Bend Under Plane Bending," *Proc. 2nd Int. Conf. on Pressure Vessel Technology,* Vol. 1, ASME, New York, pp. 393-399 (1973).

[316] Spence J. and Findlay, G.E., "Limit Moments for Non-circular Cross-section (elliptical)) pipe bends," 4th SMiRT Conf., San Francisco, Vol. F, Paper F 1/6(1977).

[317] Calladine, C. I., "Limit Analysis of Curved Tubes," *J. of Mech. Eng. Sci.,* Vol. 16, No. 2, pp. 85-87 (1974).

[318] Popov, E. P., Sharifi, P., and Nagarajan, S., "Inelastic Buckling Analysis of Pipes Subjected to Internal Pressure, Flexure and Axial Loading," *Pressure Vessels and Piping: Analysis and Computers,* I. S. Tuba, R. A. Selby, and W. B. Wright, ASME Symposium Vol., pp. 11-23 (1974).

[319] Bushnell, D., "Stress, Buckling, and Vibration of Prismatic Shells," *AIAA J.,* Vol. 9, No. 10, pp. 2004-2013 (1971).

[320] Underwood, P., "Transient Response of Inelastic Shells of Revolution," *Computers & Structures,* Vol. 2, pp. 975-989 (1972).

[321] Ni, C. M. and Lee, L. H. N., "Dynamic Behavior of Inelastic Cylindrical Shells at Finite Deformation," *Int. J. Nonlinear Mech.,* Vol. 9, pp. 193-207 (1974).

[322] Lee, L. H. N., "Dynamic plasticity," *Nuclear Engng & Design,* Vol. 27, pp. 386-397 (1974).

[323] Al-Hassani, S. T. S., "The Plastic Buckling of Thin-walled Tubes Subject to Magnetomotive Forces," *J. Mech. Eng. Sci.,* Vol. 16, pp. 59-70 (1974).

[324] Jones, N. and Ahn, C. S., "Dynamic Buckling of Complete Rigid-Plastic Spherical Shells," *J. Appl. Mech.,* Vol. 41, pp. 609-614 (1974).

[325] Jones, N. and Ahn, C. S., "Dynamic Elastic and Plastic Buckling of Complete Spherical Shells," *Int. J. Solids Structs.,* Vol. 10, pp. 1357-1374 (1974).

[326] Wesenberg, D. L., "Elastic-Plastic Buckling of Aluminum Cylindrical Shells Subjected to Axisymmetric Impulse Loads," *J. Appl. Mech.,* Vol. 41, pp. 985-988 (1974).

[327] Klein, S., "The Nonlinear Dynamic Analysis of Shells of Revolution with Axisymmetric Properties by the Finite Element Method," *J. Pressure Vessel Technology,* Vol. 97, pp. 163-171 (1975).

[328] Lindberg, H. E. and Kennedy, T. C., "Dynamic Plastic Pulse Buckling Beyond Strain-rate Reversal," *J. Appl. Mech.,* Vol. 42, pp. 411-416 (1975).

[329] Nagarajan, S. and Popov, E. P., "Nonlinear Dynamic Analysis of Axisymmetric Shells," *Int. J. Num. Meth. Engng.,* Vol. 9, pp. 535-550 (1975).

[330] Wu, R. W. H. and Witmer, E. A., "Theoretical and Experimental Studies of Transient Elastic-Plastic Large Deflections of Geometrically Stiffened Rings," *J. Appl. Mech.,* Vol. 42, pp 793-799 (1975).

[331] Jones, N. and Okawa, D. M., "Dynamic Plastic Buckling of Rings and Cylindrical Shells," *Nuclear Engineering and Design,* Vol. 37, pp. 125-147 (1976).

[332] Florence, A. L. and Abrahamson, G. R., "Critical Velocity for Collapse of Viscoplastic Cylindrical Shells Without Buckling," *J. Appl. Mech.,* Vol. 44, pp. 89-94 (1977).

[333] Lee, L. H. N., "Quasi-bifurcation in Dynamics of Elastic-Plastic Continua," *J. Appl. Mech.,* Vol. 44, pp. 413-418 (1977).

[334] Taylor, J. W., Harlow, F. H., and Amsden, A. A., "Dynamic Plastic Instabilities in Stretching Plates and Shells," *J. Appl. Mech.,* Vol. 45, pp. 105-110 (1978).

[335] McIvor, I. K., Anderson, W. J., and Bijak-Zochowski, M., "An Experimental Study of the Large Deformation of Plastic Hinges," *Int. J. Solids Struct.,* Vol. 13, pp. 53-61 (1977).

[336] McIvor, I. K., Wineman, A. S., and Wang, H. C., "Plastic Collapse of General Frames," *Int. J. Solids Struct.* (1977 or 1978).

[337] Winter, R., Cronkhite, J. D., and Pifko, A. B., "Crash Simulation of Composite and Aluminum Helicopter Fuselages Using a Finite Element Program" *Proc. 20th AIAA/ASME Structures Meeting,* AIAA Paper 79-0781, pp. 233-240 (April 1979).

[338] Belytschko, T. and Geers, T. L. (Ed.), *Computational Methods for Fluid-Structure Interaction Problems,* AMD, Vol. 26, ASME, New York (1977).

[339] Desai, C. S. and Christian, J. T. (Ed.), *Numerical Methods in Geotechnical Engineering,* McGraw Hill, New York (1977).

[340] Epstein, M. and Murray, D. W., "A Biaxial Law for Concrete Incorporated in the BOSOR5 Code," *Computers and Structures,* Vol. 9 pp. 57-63 (July 1978).

[341] Murray, D. W., Chitnuyanondh, L., and Wong, C., "Computer Implementation of an Elastic-Plastic Concrete Relationship," 5th SMiRT Conf., Berlin, Paper M2/4 (Aug. 1979).

[342] Babuška, I. and Rheinbolt, W. C., "On the Reliability and Optimality of the Finite Element Method," *Computers & Structures,* Vol. 10, pp. 87-94 (1979).

[343] Samuelson, L. Å., "Creep Buckling of a Cylindrical Shell Under Nonuniform External Loads," *Int. J. Solids Structures,* Vol. 6, pp. 91-116 (1970).

[344] Griffin, D. S., "Inelastic and Creep Buckling of Circular Cylinders due to Axial Compression, Bending, and Twisting," ASME Paper 74-PVP-46 (1974).

[345] Neale, K. W., "Method for the Estimation of Plastic Buckling Loads, *Int. J. Solids Struct.,* Vol. 10, pp. 217-230 (1974).

[346] Gerdeen, J. C., "Summary and Interpretive Report on Limit Analysis, Elastic-Plastic Analysis and Experiments on Shells," submitted to task group on characterization of plastic behavior of structures, PVRC (April, 1976).

[347] Nickell, R. E., "A Survey of Simplified Inelastic Analysis Methods," Pacifica Technology, Del Mar, CA, Rept. PT-U78-0162 (Jan., 1979).

[348] Almroth, B. O., Stern, P., and Brogan, F. A., "Future Trends in Nonlinear Structural Analysis," *Computers and Structures,* Vol. 10, pp. 369-374 (1979).

[349] Almroth, B. O. and Felippa, C. A., "Problem Adaptive Programming in Structural Analysis," presented at ASCE meeting, Boston (April 2-6, 1979).

We wish to thank the following organizations for allowing us to use their material in this article.

Figures	Credits
16-18	Bergen, *et al., Int. J. Num. Meth. Engng.,* 12, 1677-1696 (1978)
19	Bathe, K-J, *et al., Int. J. Num. Meth. Engng.,* 9, 353-386 (1975)
37-40	Bushnell, D., *Int. J. Num. Meth. Engng,* 11, 683-708 (1977) John Wiley & Sons, Ltd., Sussex, England
6, 7	Tvergaard. V., *Proc. 14th IUTAM* (W. T. Koiter, Ed.), pp. 233-247 (1976)
41, 62, 66	Lagae, *et al., Nuclear Engr. & Des.,* 48, 405-414 (1978) North Holland Publishing Company, Amsterdam, The Netherlands
10-12	Tvergaard, V., *Int. J. Solids Struct.,* 13, 957-970 (1977)
53-55, 57-59	Bushnell, D. and Galletly, G. D., *Int. J. Solids Struct.,* 10, 1,271-1,286 (1974)
45-47	Bushnell, D., *Int. J. Solids Struct.,* 12, 51-66 (1976)
43-44	Murphy, L. M. and Lee, L. H. N., *Int. J. Solids Struct.,* 7, 1,153-1,170 (Sept. 1971)
61, 64, 65	Patel, P. R. and Gill, S. S., *Int. J. Mech. Sci.,* 20, 159-175 (1978)
34, 35, 48-52, 74-78	Bushnell, D., *Computers & Structures,* 6, 221-239 (1976)
20, 21	Bathe, K. J. and Ozdemir, H., *Computers & Structures,* 6, 81-92 (1976)
22, 24, 31, 32	Armen, H., Jr., *Computers & Structures,* 10, 161-174 (1979) Pergamon Press, Ltd., Oxford, England
56	Galletly, G. D., *et al., Ingenieur-Archiv.,* 43, 345-358 (1974) Springer-Verlag, New York

reprinted from

Pressure Vessels and Piping: Design Technology – 1982
A Decade of Progress
Edited by S.Y. Zamrik, and D. Dietrich
(Book No. G00213)

published by

THE AMERICAN SOCIETY OF MECHANICAL ENGINEERS
345 East 47th Street, New York, N.Y. 10017
Printed in U.S.A.